

Study to investigate the mechanism that controls cisternal stacking in Golgi apparatus

By

Bhawik Kumar Jain

(LIFE09201204008)

Tata Memorial Centre, Mumbai

A thesis submitted to the

Board of Studies in Life Sciences

In partial fulfillment of requirements

For the Degree of

DOCTOR OF PHILOSOPHY

OF

HOMI BHABHA NATIONAL INSTITUTE




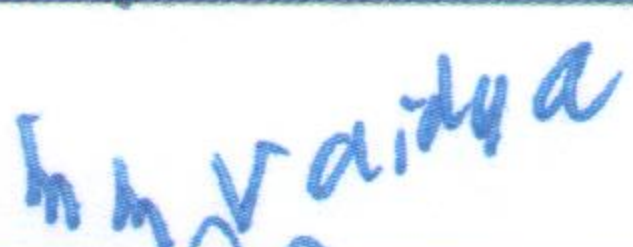
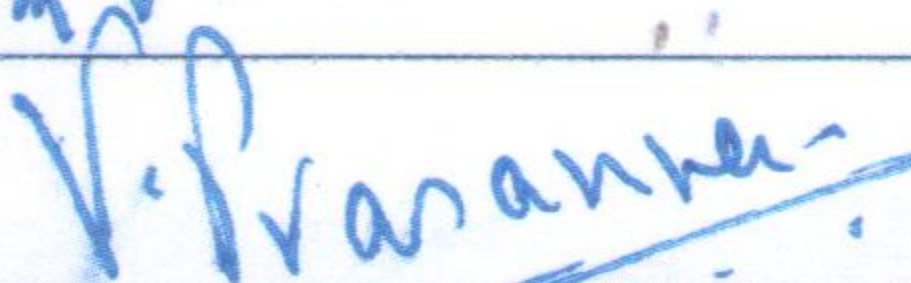


January, 2019

Homi Bhabha National Institute

Recommendations of the Viva Voce Committee

As members of the Viva Voce Committee, we certify that we have read the dissertation prepared by Mr. Bhawik Kumar Jain entitled "Study to investigate the mechanism that controls the cisternal stacking in Golgi apparatus" and recommend that it may be accepted as fulfilling the thesis requirement for the award of Degree of Doctor of Philosophy.


	17.01.2019
Chairman – Dr. Sorab N. Dalal	date
	17.01.2019
Guide / Convener – Dr. Dibyendu Bhattacharyya	date
	17.01.2019
Examiner – Dr. Jomon Joseph	date
	17.01.2019
Member 1- Dr. Milind Vaidya	date
	17.01.2019
Member 2- Dr. Prasanna Venkataraman	date
	

Final approval and acceptance of this thesis is contingent upon the candidate's submission of the final copies of the thesis to HBNI.

I hereby certify that I/we have read this thesis prepared under my/our direction and recommend that it may be accepted as fulfilling the thesis requirement.

Date: 17.01.2019

Place: Navi Mumbai


Dr. Dibyendu Bhattacharyya
Guide

STATEMENT BY AUTHOR

This dissertation has been submitted in partial fulfillment of requirements for an advanced degree at Homi Bhabha National Institute (HBNI) and is deposited in the Library to be made available to borrowers under rules of the HBNI.

Brief quotations from this dissertation are allowable without special permission, provided that accurate acknowledgement of source is made. Requests for permission for extended quotation from or reproduction of this manuscript in whole or in part may be granted by the Competent Authority of HBNI when in his or her judgment the proposed use of the material is in the interests of scholarship. In all other instances, however, permission must be obtained from the author.

Bhawik Kumar Jain

DECLARATION

I, hereby declare that the investigation presented in the thesis has been carried out by me. The work is original and has not been submitted earlier as a whole or in part for a degree / diploma at this or any other Institution / University.

Bhawik Kumar Jain

List of Publications arising from thesis

Journals

1. **Identificaion and charcterization of GRIP domain Golgin PpImh1 of *Pichia Pastoris*.****Jain, BK**, Thapa, PS, Varma A, Bhattacharyya D., Yeast.2018 29 April. doi.org/10.1002/yea.3317.
2. Bhav M Papanikou Elyer P, Pandya K, **Jain BK**, Ganguly A, Sharma C, Pawar K, Austin J II, Day KJ, Rossanese OW, Glick BS, Bhattacharyya D. Golgi enlargement in Arf-depleted yeast cells is due to altered dynamics of cisternal maturation. J Cell Sci. 2014 Jan 1; 127(Pt 1):250-7. PMID: 24190882
3. Ganguly, A., Bhattacharjee, C., Bhav, M., Kailaje, V., **Jain, BK**., Sengupta, I., et al. and Bhattacharyya D. Perturbation of nucleo-cytoplasmic transport affects size of nucleus and nucleolus in human cells. FEBS Letters. 2016 Vol 590:631-643.
4. **Jain BK**, Bhattacharyya D. Golgin Imh1 mediates cisternal stacking in Golgi appratus of budding yeast *Pichia pastoris* (Manuscript under preparation)
5. Prasanna Iyer, Madhura Bhav, **Bhawik Kumar Jain**, Sudeshna Roy Chowdhury, Dibyendu Bhattacharyya. Vps74p controls Golgi size in Arf1-dependent manner. FEBS Letters. 2018 October. Article DOI: 10.1002/1873-3468.13266

Conferences

- 1) Poster presentation on the topic entitled “**Unstacking the stacking problem of the Golgi**” atASCB-EMBO 2017 meeting, December 2-6, 2017 Philadelphia, USA.

- 2) Poster presentation on the topic entitled “**Golgin protein Imh1 plays role in cisternal stacking of Golgi apparatus in the budding yeast *Pichia Pastoris***” at International conference of cell biology (ICCB 2018) held at CCMB Hyderabad, 2018, India.

- 3) Platform presentation on the topic entitled “**Unstacking the stacking problem of the Golgi**” at National Research scholars meet 2017, held at ACTREC, 2017, India

Bhawik Kumar Jain

**This thesis is dedicated to my beloved
family and teachers for their endless
support and constant encouragement**

Acknowledgements

I wish to take this opportunity to thank everyone who had been instrumental in making this long journey a rewarding and truly an indelible one. Foremost, extend my deepest gratitude to my thesis research advisor Dr.Dibyendu Bhattacharyya, for introducing me to the field of protein trafficking, guidance, encouragement, advice and constant support on countless occasions during my PhD tenure.Thank you for giving me an opportunity and freedom to expose myself to the world of research.

I would like to express my gratitude to Dr. Shubhada Chiplunkar, Director, ACTREC for providing excellent infrastructure, encouragement and endless supports throughout tenure. I am thankful to Dr. Sudeep Gupta, Dy. Director, CRC, ACTREC and Dr. HKV Narayan, Dy. Director, ACTREC for their support and help at different levels. I am also thankful to Dr. Rajiv Sarin (former Director) and Dr. Surekha Zingde (former Dy. Director).My sincere thanks to the funding agencies, Sam-mystery and HBNI for supporting the international travel to present my work at an international conference.

I am grateful to all my Doctoral Committee Chairpersons Dr. Rita Mulherkar, Late Dr.Rajiv Kalraiya (Ex.Chairperson),Dr.Sorab Dalal(Chairperson), and members Dr. Milind Vaidya,Dr. Prasanna Venkatraman, for their invaluable input, advice and support in shaping and refining my research work.

I would like to acknowledge all the members of Bhattacharyya Lab. I am thankful to Sanjay and Mansi for their excellent technical help. I thank all my colleagues, Madhura, Abira, Prasanna, Kaushal, Chumki, Ketakee, Pravin, Naini, Sudeshna, Shreosi and Roma for their constant support and healthy discussions during last six years. They really made difficult times easier for me with

tons of jokes, funny fights & laughter.Countless amazing food parties & tea sessions will always be cherished.

My Very special thanks to members of CIR, Imaging facility and EM facility staff, Uday Dandekar sir, Vaishali, Tanuja, Jayraj, Vinita Sawant, Siddhi. I am thankful to the Director's office (Mrs. Pritha Menon and Mrs. Lata Shelar), Programme office (Mrs. Maya Dolas), Administration, Accounts, Dispatch, Purchase, Stores and Photography department for their constant support throughout the tenure.

Special appreciation also goes out to my friends, Gopal, Pratik, Abha, Prajish, Saujanya, Bhushan, Jacinth and Sameer for their moral support as well as Friday parties, birthday celebrations and creating cheerful environments throughout last six years. I especially thank Gopal and Pratik for their ever-present unconditional support for scientific and personal work. I am also thankful to Pankaj Thapa for all the scientific discussion and experimental help.

I dedicate my warmest gratitude to all my family members for their love & constant faith in me, even when I couldn't explain to them what I was doing. They have always given me the latitude to develop my interest in whatever I'm passionate about and have always been happy and proud of my accomplishments.

Bhawik Kumar Jain

Table of content

Synopsis	1
List of Figures	17
List of Tables	18
Abbreviations.....	19
1. Introduction.....	20
1.1 Background of thesis	21
1.2 Hypothesis	22
1.3 Objectives	23
1.4 Work done	23
2. Review of literature.....	24
2.1 Organelle	25
2.2 Biological importance of organelle size and shape control mechanism.....	25
2.3 The secretory pathway.....	27
2.4 The Golgi apparatus	29
2.5 Transport through the Golgi apparatus.....	30
2.6 Cisternal stacking	32
2.7 Role of GRASPs in Golgi stacking	33
2.8 Protein Glycosylation	34
2.9 Yeast Golgi apparatus	35
2.10 Golgins	36
2.11 Vig4	37
2.12 Sec7	38
2.13 Imh1	39
2.14 ARL – (ADP-Ribosylation factor-Like).....	39

2.15 GRIP domain.....	40
2.16 COY 1 (CASP of Yeast)	40
2.17 SGM1 (Slow growth on Galactose and Mannose).....	40
2.18 Rud3 (Relieves Uso1-1 transport Defect)	41
3. Materials and Methods.....	42
3.1 Molecular biology methods	
3.1.1 Preparation of ultra-competent E. coli	43
3.1.2 Bacterial Transformation.....	44
3.1.3 Plasmid DNA isolation.....	44
3.1.4 Agarose gel electrophoresis.....	46
3.1.5 Polymerase chain reaction (PCR).....	47
3.1.6 Quick change mutagenesis	49
3.1.7 Gene cloning.....	50
3.2 Microscopy& Image Processing	
3.2.1 Preparing the Cells	55
3.2.2 Imaging Parameters	56
3.2.3 Deconvolution.....	57
3.2.4 ImageJ	57
3.2.5 Average Project.....	58
3.3 Basic Yeast Techniques	
3.3.1 Yeast strain: PPY12 (his4, arg4)	58
3.3.2 Retrieving strains from the yeast collection	58
3.3.3 Growing yeast log phase culture.....	59
3.3.4 Freezing Yeast.....	59
3.3.5 Yeast transformation.....	60
3.3.6 Replica plating for screening transformants	60

3.3.7	Genomic DNA isolation	61
3.3.8	Checking fluorescence signal in upright microscope for screening	62
3.3.9	Manipulating Yeast Genome	63
3.3.10	Yeast Live Cell Imaging	64
3.3.11	Electron microscopy of yeast	64
3.4	Statistical tests.....	66
3.5	Protein expression and purification protocol	
3.5.1	Cloning, expression and purification of <i>PpImh1</i>	66
3.5.2	Biophysical studies of purified protein	67
3.5.3	SDS PAGE and Western Blotting.....	68
3.6	Yeast Two-hybrid interaction assays.....	70
4.	Identification and characterization of GRIP domain Golgin from <i>Pichia pastoris</i>	
4.1	Introduction	72
4.2	Result	
4.2.1	Identification and characterization of GRIP domain.....	73
4.2.2	Protein expression, Purification and biochemical analysis of purified His6-tagged <i>PpImh1</i>	76
4.2.3	<i>PpImh1</i> forms parallel homodimer	77
4.2.4	Electron microscopy data suggests that <i>PpImh1</i> forms parallel homodimer with splayed N terminus	80
4.3	Discussion	82
5.	Golgin <i>PpImh1</i> mediate cisternal stacking of Golgi apparatus in budding yeast <i>Pichia pastoris</i>	
5.1	Introduction	85
5.2	Results.....	87
5.2.1	Assay system to monitor cisternal stacking in <i>Pichia Pastoris</i>	87

5.2.2	Deletion of Golgin PpIMH1 in Pichia pastoris dual color strain results in cisternal unstacking phenotype.....	87
5.2.3	WT Full-lengthPpIMH1 could rescue the Ppimh1 Δ deletion phenotype, but a version PpImh1 lacking the coiled coil domain fails to rescue such phenotype	90
5.2.4	Overexpression of PpImh1GRIP domain alone can cause unstacking phenotype while overexpression of only PpImh1 Coiled coil domain alone causes no such effect	92
5.2.5	Arl1 and Arl3 knockout display cisternal unstacking phenotype.....	94
5.2.6	Golgi Localization of PpImh1	97
5.2.7	PpImh1 is required for endosome to TGN trafficking	98
5.2.8	PpImh1 N terminal is indispensable for vesicle capture function.....	99
5.2.9	PpImh1 N terminal is dispensable for cisternal stacking function of PpImh1	100
5.3	Discussion	102
6.	Summary and conclusion	
6.1	Summary and conclusion.....	105
6.2	Future perspective	108
7.	Bibliography.....	110
	Appendix	126
	Publication	146



HomiBhabha National Institute

Ph.D. PROGRAMME

- 1. Name of the Student:** Mr. Bhawik Kumar Jain
- 2. Name of the Constituent Institution:** TMC-ACTREC
- 3. Enrolment No.:** LIFE09201204008
- 4. Title of the Thesis:** “Study to investigate the mechanism that controls cisternal stacking in Golgi apparatus”
- 5. Board of Studies:** Life Sciences

SYNOPSIS

1. Introduction:

One of the fundamental properties of eukaryotic cell is their ability to maintain organelle size, shape, and number that are appropriate for different growth and differentiation states[1]. Organelles are specialized organization to perform different regulatory or biochemical processes with distinct morphologies. For example, single spherical nucleus, reticulated networks of endoplasmic reticulum, mitochondria, Golgi apparatus etc. Cell possesses an active mechanism to build and maintain such structures. Altered organelle size and shape leads to improper cell function. It is likely that metabolism and/or signaling get affected by organelle size. One approach of reprogramming organelle size and shape can result into reprogramming cellular state or behavior. Here comes the concept of organelle directed medicine to cure diseased cells[2, 3]. We are interested in studying the process that controls and maintains the size and shape of intracellular organelles, such as the Golgi apparatus. This Golgi apparatus lies at the heart of the

secretory pathway and performs numerous functions including modification of secretory cargoes, their sorting and delivery to various destinations, which may be inside or outside the cell[4]. The Golgi apparatus has a characteristic structure comprising flattened membrane discs called cisternae that is conserved amongst nearly all eukaryotes[5]. In most cells, these cisternae are present in ordered stacks. Newly synthesized proteins arrive at the cis face of the stack, pass through medial cisternae, and then arrive at the trans face of the stack. During this time, glycoproteins are processed by an ordered sequence of resident Golgi enzymes. These enzymes show a polarized distribution in which early-acting enzymes are concentrated in cis cisternae while late-acting enzymes are concentrated in trans cisternae. Finally, the fully processed proteins are sorted into transport carriers at the trans-Golgi network (TGN).

Mostly the basic structure of Golgi apparatus is conserved, the structural organization of stacking differs between species. For example, in plant cells, the cisternae are arranged together to form stacks whereas in mammalian cells these stacks are linked by tubules forming the Golgi ribbon structures. The cisternae in *S.cerevisiae* cells are dispersed throughout the cell and not stacked, whereas those in another budding yeast *Pichia pastoris* cells are stacked[6]. The Golgi cisternae in most eukaryotes are organized into stacks, but the mechanisms that generate this organization have not been clear. Golgi stacks can be converted to individual cisternae by protease treatment, suggesting that protein cross-bridges hold the cisternae together[7]. The Golgi apparatus undergoes disassembly and reassembly process during the cell cycle, which is regulated by phosphorylation of the GRASP proteins, suggesting GRASPs as a stacking factor[8]. Mammalian cells contain two GRASP proteins GRASP65 and GRASP55 localized to early and medial Golgi cisternae respectively[9]. Single knockout of any of the GRASPs results in a minor effect on Golgi morphology. However double depletion of GRASP55+GRASP65 disperses Golgi

ribbon structure in individual cisternae and tubule-vesicular structures[10]. During cell cycle when cells exit mitosis, GRASP proteins are dephosphorylated after Cdk1 inactivation, enabling GRASPs to oligomerize and Golgi stacks to reform. GRASPs are peripheral membrane proteins on the cytoplasmic face of the Golgi cisternae that form trans-oligomers through their N-terminal GRASP domain, and thereby function as adhesive force to stick adjacent cisternae together into a stack and to link Golgi stacks into a ribbon, suggesting oligomerization as a mechanism of cisternal stacking. These studies suggest GRASPs as a major cisternal stacking factor.

Although GRASPs are associated with Golgi and pre-Golgi compartments in many organisms, cisternal stacking is unlikely to be the sole function of these proteins. Higher plants contain prominent Golgi stacks but no detectable GRASP homologs. Even in mammalian cells, GRASPs have been implicated in processes distinct from Golgi stacking. Morphological studies uncovered requirements for GRASP65, GM130, and GRASP55 in the lateral fusion of mammalian Golgi stacks into a Golgi ribbon. Moreover, GRASPs seem to have non-structural roles in secretion. GRASP65 and GRASP55 bind to the cytosolic tails of certain cargo proteins and facilitate their transport through the secretory pathway. GRASP homologs in *Dictyostelium* and *Drosophila* were shown to be important for unconventional secretory pathways that bypass the Golgi. These findings suggest that the activities of GRASPs have diversified during evolution, and they highlight the importance of defining the primary, conserved function of the GRASP family.

If GRASPs are considered as major cisternal stacking factor, their structural role should be conserved. In budding yeast *Pichia pastoris* deletion of GRASP homologue, GRH1 has no effect on Golgi stacking and this situation can be extended to plant cells where no GRASP homologue is identified[11, 12]. These studies suggest that in case of yeast and plants; where no

of the GRASP homolog has been either identified or found to be necessary for Golgi stacking, the new adhesive interaction of existing Golgi proteins could potentially mediate cisternal stacking. It has been reported that efficient stacking occurs in the absence of GRASP65/55 when either Golgin is overexpressed. This result suggests Golgins as an alternative cisternal adhesion force [13, 14]. The Golgins are long coiled-coil domain proteins which are shown to be important for Golgi structure maintenance and vesicle tethering. Knockdown of Golgin97, Golgin245, GCC185 shown to affect the Golgi structure, suggesting a role of Golgins in Golgi structure maintenance [15-17].

In our study, we are trying to identify the stacking factor using budding yeast *Pichia pastoris*. *Pichia pastoris* provides an excellent tool to study cisternal stacking where we can study the individual Golgi stack and adhesion between two individual Golgi cisternae. Therefore, the key question that remains to be answered is: What is the conserved stacking factor which holds these cisternae together in yeast, plant & other eukaryotic system. We have used combination of genome wide mutations analysis and directed mutations in yeast system as an approach.

2. Rationale:

Intracellular membrane trafficking is a coordinated process in the eukaryotic cell. Cargo carrying vesicles transport ER synthesized proteins and lipids to compartments where modifications occur, deliver them to their final destinations (Glick & Nakano, 2009). The Golgi apparatus plays a central role in the processing, sorting, and secretion of various cargo molecules destined for various intracellular and extracellular destinations. The Golgi apparatus basically consists of cisternae which are flat membrane sacs of discoid shape. The Golgi cisternae display variable shape in different species: from dispersed cisternae in *S.cerevisiae* to stacked cisternal structure in *Pichia pastoris* and to laterally connected ribbon

of cisternal stacks in metazoans, but the mechanisms that generate this organization have been not clear. Understanding the cisternal stacking mechanism may lend insight into the significance of cisternal stacking in cellular physiology.

3. Aim and Objectives:

3.1. Investigation of cisternal Stacking mechanism in Golgi apparatus

- 3.1.1. To develop an assay system to monitor cisternal stacking
- 3.1.2. To isolate and characterize temperature sensitive mutant of budding yeast showing cisternal unstacking phenotype and functional complementation
- 3.1.3. Identification of stacking gene by Restriction enzyme mediated integration (REMI)
- 3.1.4. Directed mutagenesis

3.2. Characterization of physiological significance of cisternal stacking

- 3.2.1. To check the effect of cisternal unstacking on cell growth
- 3.2.2. To check effect of cisternal unstacking on transport

4. Materials and methods:

4.1. Yeast strains and Plasmids

Experiments with *Pichia pastoris* were carried out using the prototrophic wild-type strain PPY12 and its derivatives. General methods for growth and transformation of *P. pastoris* have been described previously [18]. Yeast cells were grown at 30°C at 200 rpm. *Pichia pastoris* transformation was performed using electroporation method (Ref). Gene sequences were obtained from NCBI database.

We have used pUC19 backbone vectors (pUC19-His4, pUC19-Arg4, pUG6, pUC19-Hygro, pIB1, pIB2, pIB4) for genomic integrant and expression studies.

4.2. Preparation of ultra-competent cells

E.coli strain DH5 α MCR was made ultra-competent for the transformation of ligated DNA or plasmid vectors. A single colony was inoculated in 250 ml SOB broth and incubated at 18°C /250 rpm till O.D.600 reached ~0.4. The cells were harvested by pelleting down at 4°C and re-suspended in 80 ml of Transformation buffer (TB) followed by incubation on ice for 10 min and centrifugation. The cell pellet was re-suspended in 18.6 ml TB. 1.4 ml (7%) DMSO was added to the cells and mixed completely. 200 μ l aliquots of the cells were made in sterile microfuge tubes and snap frozen in liquid nitrogen followed by storage at -80°C.

4.3. Genomic DNA isolation from yeast cells

10ml yeast culture was grown overnight. The culture was spun for 5min, 3000 rpm. R.T. Supernatant was removed & pellet was resuspended in 0.5 ml MQ. Again cells were spun at room temperature and supernatant was removed carefully. The pellet was disrupted by vortexing briefly. Cells were re-suspended in 200 μ l breaking buffer (2% Triton X-100, 1% SDS, 100mM NaCl, 10mM Tris-Cl pH8, 1mM EDTA, pH 8). 0.3 g (200 μ l in vol.) glass beads and 200 μ l phenol (cold)/chloroform was added. The mixture is vortexed at highest speed for 3min. 200 μ l T.E buffer is added, vortexed briefly. Micro centrifuged for 5 min, highest speed/R.T. The aqueous layer is transferred to fresh tube. 1 ml 100% ethanol (ice cold) is added, mixed by inversion. The vials centrifuged for 3 min at high speed at room temperature. Supernatant is removed and re-suspended pellet in 0.4 ml 1 XT.E. Buffer. 3 μ l of 1mg/ml DNase-free RNase A is added, mixed and incubated 5 min at 37°C. 10 μ l of 4M Ammonium acetate and 1ml of 100% ethanol is added. The contents of vials were mixed by inversion, again incubated at -20°C & centrifuged 10-15 min,

room temperature. Supernatant is discarded and pellet is allowed to air dry. DNA is dissolved in 100 µl TE buffer and stored in -20°C.

4.4. *Pichia Pastoris* transformation protocol

Pick a single colony of your *Pichia* strain to grow in 10 ml YPD overnight at 30°C in a 100 ml sterile flask. Inoculate 50 mL YPD in a 250 mL flask with 0.1-0.5 ml of the overnight culture. Grow overnight again to an O.D. of 1-1.5. Add 1 ml of 1M DTT and 1M HEPES and keep it at 30 degree shaker for 15 mins. Centrifuge the cells at 3000rpm for 3 minutes at 4°C. Resuspend the pellet with 50 mL of ice cold, sterile water. Centrifuge the cells as in step 3, and then resuspend the pellets in 50 mL of ice-cold, sterile water. Centrifuge the cells again, then resuspend in 20 ml of ice-cold 1M sorbitol. Centrifuge the cells again, then resuspend the pellet in 200 µl of ice-cold 1M sorbitol. Keep the cells on ice, mix 40 µL of the cells and add linearized DNA prepared and then transfer to an ice-cold 0.2 cm electroporation cuvette. Be sure to tap the cells down to the bottom of the cuvette. Pulse the cells *Pichia* (25 µF, 200 ohm, 2000 V). Immediately add 1 ml of ice-cold 1M sorbitol to the cuvette. Transfer the cuvette contents to a sterile 1ml tube. Centrifuge at 5000rpm for 1 min. Remove 800µl of contents from tube and plate remaining on selection plates.

4.5. Live cell imaging yeast mutants in laser confocal microscope

Confocal imaging was performed with either a Leica SP5 or a Zeiss LSM 780 for 4D imaging, or a Zeiss LSM 510 META or LSM 710 for single time-point measurements, equipped with 100X or 63X 1.4 NA objectives. Cells grown to log phase at 25°C or 30°C in nonfluorescent or minimally fluorescent SD medium were immobilized on glass bottomed dishes (Cell E&G, Houston, TX, USA) using Concanavalin A (Sigma-Aldrich) as previously described [8], and were imaged at room temperature. Single- or dual-color

data sets were obtained using separate excitation and capture of red and green signals, with a pinhole of 1.0–1.2 AU and with line averaging of 4 to improve the signal-to-noise ratio. The pixel size was 70–90 nm. Optical sections were 0.25–0.40 μ m apart, and, 15–20 optical sections were collected to span an entire cell. Zstacks were collected at intervals of 2–4 seconds. To limit photo damage, laser illumination was minimized and confocal scans were carried out as quickly as possible.

5. Results:

5.1. To develop an Assay system to monitor cisternal stacking

To monitor the cisternal stacking in yeast we have used *Pichia pastoris* as model system which has stacked Golgi. To study the cisternal stacking in live cell condition under high end microscopes, the first necessity was to develop proper early Golgi and late Golgi marker tagged with different fluorescent proteins. For this purpose Vig4 as early Golgi marker and Sec7 as late Golgi marker were selected. Different Fluorescent proteins were tagged with either of them to make the final construct. We have tagged early Golgi protein Vig4 with msGFP (msGFP-Vig4) and late Golgi protein Sec7 with 6xDsRed (Sec7-6xDsRed), which shows green and red spots next to each other with overlapping yellow region.

5.2. Golgin *PpIMH1* Knockout affects cisternal stacking

Golgin *PpImh1* deletion results in an increase in intercisternal distance. This result suggested a slight alteration in the Golgi cisternal stacking, which was confirmed by electron microscopy of *PpImh1* knockout cells. In *PpImh1* knockout cells, there was an increase in intercisternal distance between medial and trans-Golgi. Furthermore, the total

area cover by the entire Golgi stack and intercisternal angle were perturbed. These experiments define that Imh1 depletion affects cisternal stacking between medial and Trans Golgi.

5.3. Coiled-coil domain of *PpIMH1* is essential for cisternal stacking function *PpIMH1*

To *PpImh1* is Golgin, Golgi resident proteins containing the N-terminal head domain, Golgi localizing C-terminal GRIP domain and long central coiled-coil domains. As a starting point of analysis, we tested whether full-length *PpImh1* can rescue the unstacking phenotype or not. The additional deletion constructs *PpImh1*(150-1100) Δ was generated for the individual domain. Full-length *PpImh1* was fully competent to rescue the unstacking phenotype. But *PpImh1* (150-1100) Δ was not able to rescue the unstacking phenotype. *PpImh1* (150-1100) residues show high predictability to form the coiled coil. To further refine precise determinants needed for cisternal Stacking, deletion of coiled-coil domain 150–1100 within the context of the full-length protein yielded a construct that was showing the cisternal unstacking phenotype. These results suggest that *PpImh1* (150-1100) domains, which has shown high probability to form coiled-coil domain are crucial for cisternal stacking.

5.4. Overexpression of GRIP domain results in cisternal unstacking phenotype

The GRIP domain of TGN Golgin acts as Golgi localizing signal. Expression of GRIP domain tagged with GFP in cells shown that it localizes to the TGN. Furthermore, it can act as a dominant negative mutant by competing with endogenous GRIP domain-containing proteins for binding to Arl1. To test whether overexpression of coiled-coil domain and GRIP domain in *Pichia pastoris* cells, we expressed GRIP domain and *PpCC*domain under the methanol inducible AOX1 promoter. Overexpression of coiled-

coil does not show any effect on cisternal stacking, but GRIP domain overexpression resulted in cisternal unstacking phenotype.

5.5. Arl1 and Arl3 knockout display cisternal unstacking phenotype

Deletion of both the *PpArl3* and *PpArl1* in *Pichia pastoris* cells results in cisternal unstacking phenotype. These results lead us to propose a model in which the nucleotide cycle of Arl3p regulates Golgi localization of Arl1p, which, when activated by nucleotide exchange, recruits Imh1p to the Golgi via its GRIP domain.

5.6. Golgi Localization of *PpImh1*

The hallmarks of GRIP domain Golgins is to their localization to TGN. To test what is the exact localization of *PpImh1*, we tagged the *PpImh1* with GFP & check its localization with respect to early and late Golgi. GFP-*PpImh1* was showing overlapped with both cis Golgi and trans-Golgi marker. Upon measuring the percent of the green spot on the red spot, we confirmed that it's co-localizing with both cis and trans-Golgi. These results suggest us that Imh1 could be localized to the medial compartment as it mediates the stacking between medial & trans-Golgi.

5.7. Sequence alignment and characterization of GRIP domain of *PpImh1*

With sequence alignment studies of *Pichia pastoris* using PSI-BLAST, we identified the single GRIP domain containing protein in *Pichia pastoris*, *PpImh1*. To examine the whether or not *PpImh1* GRIP domain is capable of localizing to the Golgi, we tagged the GRIP domain with mGFP and expressed it in *Pichia pastoris* cells. We found that *PpImh1* forms a punctate pattern which mostly corresponds to the Golgi.

5.8. Expression, Purification and Analysis of purified His6-tagged PpImh1

To understand the structural properties of PpImh1, we overexpressed His-tagged PpImh1 in Rosetta2DE3 cells and purified it using Nickel affinity chromatography and gel filtration. We confirmed the purified protein using mass spectrometry analysis and western blot against His-tagged PpImh1. CD spectroscopy suggests that imh1 contains 85% α -helical structure. To further understand the nature of the alpha-helical structure, coils analysis showed the probability of coiled-coil formation. This prediction asserts that PpImh1 has a domain that comprises a coiled-coil structure.

5.9. Yeast Two-Hybrid analysis and DLS analysis indicates PpImh1 forms parallel homodimer

To determine whether PpImh1 forms oligomer or not, we performed yeast two-hybrid assay. A strong interaction was observed between the full-length PpImh1 constructs, PpImh1-pGAD and PpImh1-pGBDU, confirming that PpImh1 forms oligomer. We further confirm it by Native-PAGE and DLS.

5.10. EM data suggests that PpImh1 forms parallel homodimer with splayed N terminus

To further elucidate the nature of the dimer, we visualized purified PpImh1 under transmission electron microscope. We observed that the PpImh1 particles exhibit two profiles, either a 'Y' shaped or a clustered form. Majority of individual PpImh1 particles seemed to form a 'Y' shaped structure which appeared at a significant frequency of 24 %. The clustered or network-like profiles may represent assemblies of the 'Y' shaped forms of PpImh1 or other differently folded forms of PpImh1.

5.11. Imh1 knockout affects the cell growth and endosome to TGN transport

We first want to check whether deletion of Imh1 has any effect on the growth of wild

type *Pichia pastoris* cells, we checked the growth of IMH1 knockout cell and Wild type cells. Growth curve analysis suggest us that imh1 knockout delay the growth of *Pichia pastoris* cell. Mammalian homologue of Imh1 regulates the endosome to TGN transport. Therefore we wanted to check whether *Pichia pastoris* Imh1 perform similar function or not. The status of cargo protein which shuttle between endosome to TGN was validated in *Ppimh1Δ* strain .To test this we tag one of the cargo proteins Tlg1 with GFP and check its localization status in imh1 deletion cells and in wild type *Pichia* cells. We observed that in case of wild type cargo protein was localized to Trans Golgi, protein Sec7 but upon Imh1 del Tlg1-GFP was not localized to the Golgi. It shows that imh1 regulates the transport between TGN and endosomes. A short well-conserved region at the N-terminus of TGN Golgin has been shown to be necessary and sufficient to nucleate the capture of endosome-to-Golgi carriers (Wong et al., 2017). To validate whether similar region of PpImh1 is functionally conserved or not, we deleted the N terminal 100Amino acids residues of endogenous PpImh1. We observed that in such strain fails Tlg1 fails to localize in Golgi, suggesting that endosome to Golgi vesicle capturing function is compromised. These results further confirm that the deletion of only 1-100 amino acids residues of endogenous PpImh1 is sufficient to abolish vesicle capture function of PpImh1.

6. Summary and significance of the study:

- a.** Imh1 deletion strains display cisternal unstacking between medial and trans Golgi
- b.** Coiled coil domain of Imh1 is essential for cisternal stacking
- c.** Arl1 and Arl3 deletion strains results in cisternal unstacking phenotype
- d.** PpImh1 co-localize with both early and late Golgi marker.
- e.** Imh1 knockout strain affects transport between endosome and TGN

- f. GRIP domain of PpImh1 is important for Golgi localization
- g. PpImh1 comprised of high degree of alpha helical coiled coil domain
- h. PpImh1 form parallel homodimer and has splayed N terminus.

In conclusion, our study mostly supports our hypothesis that the long coiled-coil domain could potentially mediate dimerization of Golgin molecules residing on two different Golgi Cisterna and multiple such dimerized Golgin pairs can bring two Golgi cisternae together to form a stack. *PpImh1* coiled-coil domain form parallel homodimer. Our data suggest that *PpImh1* mediates the cisternal stacking of TGN and medial Golgi. We also have shown that *PpImh1* has two distinct functions, cisternal stacking and vesicle capturing function. It appears that its cisternal stacking function is independent of the vesicle capturing function since deletion of vesicle capture domain (Imh1 (1-100)) has no effect on cisternal stacking. But the deletion of the coiled-coil domain which is essential for cisternal stacking affect vesicle capture functions. That further suggests that stacking is indispensable for vesicle capture.

7. References

1. Marshall, W., *Size control in dynamic organelles*. Trends Cell Biol, 2002. **12**(9): p. 414-9.
2. Marshall, W.F., *Engineering design principles for organelle size control systems*. Semin Cell Dev Biol, 2008. **19**(6): p. 520-4.
3. Handwerger, K.E. and J.G. Gall, *Subnuclear organelles: new insights into form and function*. Trends Cell Biol, 2006. **16**(1): p. 19-26.
4. Nakamura, N., J.H. Wei, and J. Seemann, *Modular organization of the mammalian Golgi apparatus*. Curr Opin Cell Biol, 2012. **24**(4): p. 467-74.
5. Klumperman, J., *Architecture of the mammalian Golgi*. Cold Spring Harb Perspect Biol, 2011. **3**(7).
6. Lowe, M., *Structural organization of the Golgi apparatus*. Curr Opin Cell Biol, 2011. **23**(1): p. 85-93.
7. Cluett, E.B. and W.J. Brown, *Adhesion of Golgi cisternae by proteinaceous interactions: intercisternal bridges as putative adhesive structures*. J Cell Sci, 1992. **103** (Pt 3): p. 773-84.
8. Wang, Y. and J. Seemann, *Golgi biogenesis*. Cold Spring Harb Perspect Biol, 2011. **3**(10): p. a005330.
9. Zhang, X. and Y. Wang, *GRASPs in Golgi Structure and Function*. Front Cell Dev Biol, 2015. **3**: p. 84.
10. Bekier, M.E., 2nd, et al., *Knockout of the Golgi stacking proteins GRASP55 and GRASP65 impairs Golgi structure and function*. Mol Biol Cell, 2017. **28**(21): p. 2833-2842.

11. Levi, S.K., et al., *The yeast GRASP Grh1 colocalizes with COPII and is dispensable for organizing the secretory pathway*. Traffic, 2010. **11**(9): p. 1168-79.
12. Ito, Y., T. Uemura, and A. Nakano, *Formation and maintenance of the Golgi apparatus in plant cells*. Int Rev Cell Mol Biol, 2014. **310**: p. 221-87.
13. Lee, I., et al., *Membrane adhesion dictates Golgi stacking and cisternal morphology*. Proc Natl Acad Sci U S A, 2014. **111**(5): p. 1849-54.
14. Ramirez, I.B. and M. Lowe, *Golgins and GRASPs: holding the Golgi together*. Semin Cell Dev Biol, 2009. **20**(7): p. 770-9.
15. Derby, M.C., et al., *The trans-Golgi network golgin, GCC185, is required for endosome-to-Golgi transport and maintenance of Golgi structure*. Traffic, 2007. **8**(6): p. 758-73.
16. Lu, L., G. Tai, and W. Hong, *Autoantigen Golgin-97, an effector of Arl1 GTPase, participates in traffic from the endosome to the trans-golgi network*. Mol Biol Cell, 2004. **15**(10): p. 4426-43.
17. Lu, L. and W. Hong, *Interaction of Arl1-GTP with GRIP domains recruits autoantigens Golgin-97 and Golgin-245/p230 onto the Golgi*. Mol Biol Cell, 2003. **14**(9): p. 3767-81.
18. Sears, I.B., et al., *A versatile set of vectors for constitutive and regulated gene expression in Pichia pastoris*. Yeast, 1998. **14**(8): p. 783-90.

8. Publications in Refereed Journals:

a. Published:

1. **Jain BK**, Thapa PS, Varma A, Bhattacharyya D. Identification and characterization of GRIP domain Golgin PpImh1 from Pichia pastoris. Yeast. 2018;1–8. <https://doi.org/10.1002/yea.3317>.

Manuscript under preparation

Jain BK, Bhattacharyya D. Golgin Imh1 mediates cisternal stacking in Golgi apparatus of budding yeast *Pichia pastoris*

b. Accepted: Nil

c. Communicated: Nil

d. Other Publications

1. Bhavé M Papanikou EIyer P, Pandya K, **Jain BK**, Ganguly A, Sharma C, Pawar K, Austin J II, Day KJ, Rossanese OW, Glick BS, Bhattacharyya D. Golgi enlargement in Arf-depleted yeast cells is due to altered dynamics of cisternal maturation. J Cell Sci. 2014 Jan 1; 127(Pt 1):250-7. PMID: 24190882
2. Ganguly, A., Bhattacharjee, C., Bhavé, M., Kailaje, V., **Jain, BK**, Sengupta, I., et al. and Bhattacharyya D. Perturbation of nucleo-cytoplasmic transport affects size of nucleus and

I. Book/Book Chapter: Nil

II. Poster Presentation

- 1) Poster presentation on the topic entitled “**Unstacking the stacking problem of the Golgi**” at ASCB-EMBO 2017 meeting, December 2-6, 2017 Philadelphia, USA.
- 2) Poster presentation on the topic entitled “**Golgin protein Imh1 plays role in cisternal stacking of Golgi apparatus in the budding yeast *Pichia Pastoris***” at International conference of cell biology (ICCB 2018) held at CCMB Hyderabad, 2018, India.
- 3) Platform presentation on the topic entitled “**Unstacking the stacking problem of the Golgi**” at National Research scholars meet 2017, held at ACTREC, 2017, India

Signature of Student: *Bhawik Kumar Jain*

Date: *27/04/2018*

Doctoral Committee:

S.No.	Name	Designation	Signature	Date
1.	Dr. Sorab N. Dalal	Chairperson	<i>S. N. Dalal</i>	<i>27/4/18</i>
2.	Dr. Dibyendu Bhattacharyya	Guide & Convener	<i>D. B. Bhattacharyya</i>	<i>27/4/18</i>
3.	Dr. Milind M. Vaidya	Member	<i>M. M. Vaidya</i>	<i>27/4/18</i>
4.	Dr. V. Prasanna	Member	<i>V. Prasanna</i>	<i>02/05/18</i>

Forwarded through:

S. V. Chiplunkar
Dr. S.V. Chiplunkar
Director, ACTREC
Chairperson, Academic &
Training Programme, ACTREC

Dr. S. V. Chiplunkar
Director
Advanced Centre for Treatment, Research &
Education in Cancer (ACTREC)
Tata Memorial Centre
Kharghar, Navi Mumbai 410210.

Dr. K. Sharma
Dr. K. Sharma,
Director, Academics,
T.M.C.
PROF. K. S. SHARMA
DIRECTOR (ACADEMICS)
TATA MEMORIAL CENTRE,
PAREL, MUMBAI

List of Figures

Figure 1.1 Golgi organization varies among different cells and species	21
Figure 2.1 Concept of Organelle Directed Medicine.....	26
Figure 2.2 The secretory pathway	28
Figure 2.3 Model of Golgi transport.....	31
Figure 2.4 Yeast Golgi apparatus	35
Fig3.1 <i>Pichia pastoris</i> gene deletion strategy	63
Figure 4.1 GRIP domain of <i>PpImh1</i> is important for Golgi targeting.....	74
Figure 4.2 The Conserved residue of GRIP domain is essential for Golgi targeting	75
Figure 4.3 Biophysical Characterization of <i>PpImh1</i>	76
Figure 4.4 <i>PpImh1</i> forms parallel dimer	78
Figure 4.5 Negative-stain EM of purified <i>PpImh1</i>	80
Figure 5.1 Two color <i>Pichia pastoris</i> strain (early Golgi msGFP-VIG4, Sec7-6xDsRed.M1)	87
Figure 5.2 Intercisternal distance is significantly increased in case of <i>Ppimh1</i> Δ cells.....	88
Figure 5.3 Schematic representation of <i>PpImh1</i> (Based on coiled coil analysis)	90
Figure 5.4 Full-length <i>PpIMH1</i> could rescue the <i>Ppimh1</i> Δ deletion phenotype.....	91
Figure 5.5 Overexpression of <i>PpImh1</i> GRIP domain alone can cause unstacking phenotype while overexpression of only <i>PpImh1</i> Coiled coil domain alone causes no such effect.....	93
Figure 5.6 Localization of iGFP-Imh1GRIP and iGFPImh1CC in <i>Pichia pastoris</i> cells.....	94
Figure 5.7 Localization of iGFP-Imh1 in <i>arl1</i> Δ and <i>arl3</i> Δ knockout cells	95
Figure 5.8 Intercisternal distance was increased in <i>arl3</i> Δ and <i>arl1</i> Δ cells	96
Figure 5.9 Localization of <i>PpImh1</i> to the Golgi	98
Figure 6.10 <i>Ppimh1</i> N terminal 100 amino acids are essential for endosome to Golgi transport.....	99
Figure 5.11 <i>Ppimh1</i> N (1-100) Δ has no effect on cisternal stacking.....	101
Figure 5.12 Model depicting the dual function of <i>PpImh1</i>	103

List of tables

Table 2.1 The canonical Human Golgins and orthologues.....	37
Table 3.1 Contents of PCR reaction	48
Table 3.2 Typical PCR cycle	48
Table 3.3 Contents of PCR reaction for site directed mutagenesis	49
Table 3.4 Cycling conditions for PCR for site directed mutagenesis	50
Table 3.5 Content of PCR reaction.....	51
Table 3.6 Typical Ligation Reaction Calculation.....	54
Table 3.7 Component of Ligation reaction	54
Table 3.8 Reaction mixture of resolving gel of SDS PAGE.....	68
Table 3.9 Reaction mixture of a stacking SDS-PAGE gel	69
Table 4.1 Mass Spec Analysis of PpImh1	77
Table 4.2 Quantification of PpImh1 profiles by electron microscopy.....	81
Table List of yeast strains used in the study	142
Table List of plasmids used in the study	144
Table List of primers used in the study.....	145

Abbreviations

WT	Wild Type
CC	Coiled coil domain
BSA	Bovine Serum Albumin
EDTA	Ethylene Diamine Tetra Acetic acid
DTT	1, 4-Dithioerythritol
SDS	Sodium dodecyl sulphate
SOB	Super Optimal Broth
SOC	Super Optimal Catabolite
COV (%)	Percentage Coverage
LB	Luria Bertani
EM	Electron Microscopy
SDS PAGE	Sodium dodecyl sulfate polyacrylamide gel electrophoresis
PCR	Polymerase Chain Reaction
GFP	Green fluorescent protein
YPD	Yeast Peptone Dextrose
SD	Synthetic Dextrose
TEMED	N, N, N', N',-Tetramethylethylenediamine
TGN	Trans Golgi network
ER	Endoplasmic reticulum
COPI	Coat protein complex I
COPII	Coat protein complex II
GTP	Guanosine triphosphate
kDa	Kilo Dalton
HEPES	4-(2-hydroxyethyl)-1-piperazineethanesulphonic acid
SEM	Standard error mean

1. Introduction

1.1 Background of thesis

The fundamental features of a cell such as a number, polarity, size, shape, and dynamics of intracellular organelles are precisely controlled by a complex mechanism [1]. However, the mechanism that controls the sizes & shapes of the organelles are poorly understood. These mechanisms are possibly different for different organelles.

Intracellular membrane trafficking is a coordinated process in the eukaryotic cell. Cargo carrying vesicles transport ER synthesized proteins and lipids to compartments where modifications occur, deliver them to their final destinations [2]. The Golgi apparatus plays a central role in the processing, sorting, and secretion of various cargo molecules destined for various intracellular and extracellular destinations [3]. Our focus is to study the mechanisms that control the shape, and morphology of the Golgi apparatus.

One of the fundamental unanswered question regarding the exotic nature of Golgi shape is: how the Golgi cisterna are held together? The Golgi apparatus basically consists of cisternae which are flat membrane sacs of discoid shape. This cisterna primarily forms a stack in most of the species from budding yeast *Pichia pastoris* to metazoans with few exceptions as in *S.cerevisiae* where the Golgi apparatus display dispersed cisternae. However, the mechanism the regulate the stacked cisternal structure in *Pichia pastoris* or fine-tune the laterally connected ribbon of cisternal stacks in metazoans is still poorly understood [4].

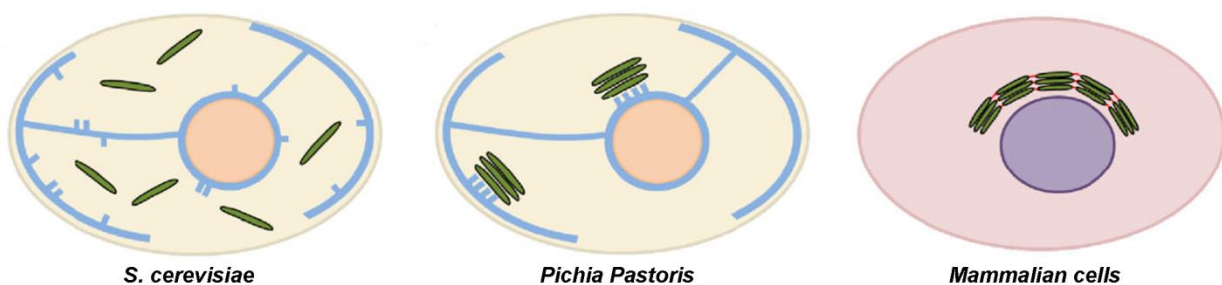


Figure 1.1 Golgi organization varies among different cells and species [5].

In *S. cerevisiae*, individual Golgi cisternae present throughout the cytoplasm. *Pichia. pastoris*, cisternae are aligned in parallel to generate the Golgi stack. In case of mammalian cells, more than few Golgi cisternal stacks are connected together to form a Golgi ribbon-shaped structure.

Moreover, alterations in the shape of the Golgi apparatus are observed during different physiological conditions as well as in many diseases. Golgi fragmentation has been observed in neurological disorders like Alzheimer's and specific tumor types [6-8]. Almost nothing is known about the significance of such alterations

Although few groups have shown the involvement of certain factors which maintain the specific shape and size of the Golgi apparatus, the complete regulation mechanism is still not clear. Despite years of research it remains poorly understood how Golgi shape, and organization is regulated. Our aim is to understand what are the factors which mediate cisternal stacking of the Golgi apparatus.

1.2 Hypothesis

The Golgi apparatus attribute typical structure that is conserved in almost all eukaryotes consists of flattened membrane discs called cisternae that are layered on top of each other to generate the Golgi stack. Smaller eukaryotic organisms contain one or more isolated Golgi stacks per cell, while invertebrates the stacks are connected to form the Golgi ribbon [4]. Despite such long research and understanding with the Golgi apparatus, there remain many questions regarding how this organelle is organized and how it carries out its diverse functions. It suggests the existence of an active mechanism that controls the cisternal stacking of Golgi apparatus. If indeed such a mechanism exists, what are the factors which maintain the specific organization of Golgi apparatus? And what is the physiological significance of cisternal stacking? Our hypothesis is that we will use budding yeast *Pichia pastoris* as a model system which contains 2-3 stacked Golgi

units per cell. With the use of different methods, we will try to identify the factor which plays role in Golgi cisternal stacking.

1.3 Objectives

- I. Investigation of cisternal stacking mechanism in Golgi apparatus
- II. Characterization of physiological significance of cisternal stacking

Detailed objectives

I. Investigation of cisternal stacking mechanism in Golgi apparatus

- A. To develop an assay system to monitor cisternal stacking
- B. Identification of cisternal stacking factor

II. Characterization of the physiological significance of cisternal stacking

- A. To check the effect of cisternal unstacking on transport
- B. To check the effect of cisternal unstacking on cell growth

1.4 Work done

The results and discussion of the work carried out under above-mentioned objectives are presented as two chapters with the following headings:

Chapter 5- Identification and characterization of GRIP domain Golgin *PpImh1* of *Pichia pastoris*

Chapter 6- Golgin *PpImh1* mediate cisternal stacking of Golgi apparatus in budding yeast *Pichia pastoris*

2. Review of literature

2.1: Organelles

An organelle is one of the several structures with specialized functions and shape bounded by a membrane and suspended in the cytoplasm of a eukaryotic cell. Eukaryotes have the most structurally complex cell type and consist of many smaller interior compartments, most of which is also enclosed by lipid membranes that resemble the outermost cell membrane. The examples of organelles are Nucleus, Mitochondria, Golgi apparatus, Lysosome, Endoplasmic reticulum, chloroplast etc. [1].

Organelles always optimize their structures to their functions. Different biochemical and regulatory functions are performed among different organelles, for example, the elongation steps of fatty acid biosynthesis occur inside the Endoplasmic reticulum (ER) but fatty acid beta-oxidation occurs within mitochondria. The size, shape, and number also vary for different organelle; the nucleus is mostly spherical, while ER is the reticulated network. Size, shape, and numbers of different organelles are well maintained and their alterations are often associated with different pathophysiological conditions. For example, the enlarged vacuole in *fab1* mutants of budding yeast leads to improper karyogamy and fitness defects. Mitotic spindle length defects can result in faulty chromosome separation. Cilia and flagella that are too long or short result in defective motility [1, 9].

2.2: Biological importance of organelle size and shape control mechanism

Organelles are reaction vessels of the cell where different biological reactions take place. For an effective manufacturing process, the size and shape of the reaction vessel are equally important as reactants and products. Likewise, organelle size inside the cell would influence the rates of biochemical reactions [9]. It can be speculated that metabolism is also influenced by size of

organelles, as in certain cells size of organelles are increased compared to other cell types like in case of secretory cells, the requisite for a high rate of flux of secreted proteins is met by overproliferation of ER and Golgi apparatus, enlarged lipid droplets in adipose cells, and also increase the number of mitochondria as a function of respiratory state [10] .

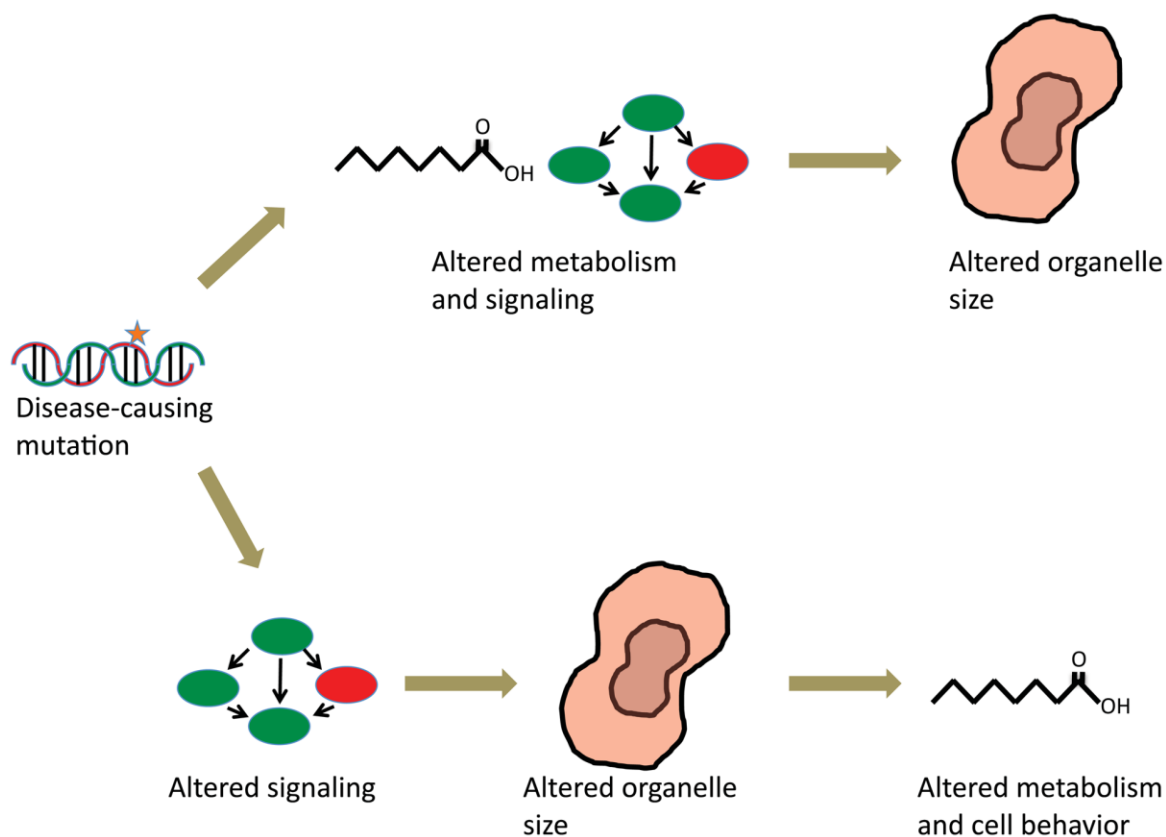


Figure 2.1 Concept of Organelle Directed Medicine [9]

If we hypothesize that organelle size and shape influence metabolism and cellular signaling, then change of organelle size and shape can scale back the altered organelle and can be used as a novel strategy for reprogramming metabolism and signaling pathway as a direct application in medicine [10]. The concept of organelle directed medicine can be extrapolated to shape of the organelle as well probably.

2.3: The secretory pathway

George Palade initiated the documentation of the ultra-structural perspective to understand how cargo proteins are secreted and membranes are assembled in the eukaryotic cells by using transmission electron microscopy that preserves membranes for ultrastructural analysis. George Palade used the technique of pulse-chase autoradiographic tracing of newly synthesized zymogen proteins. He observed the labeled proteins moving progressively from the endoplasmic reticulum (ER) through the Golgi complex and storage granules to the cell surface [11]. In every cell, the proteins, once synthesized on the ribosomes on rough ER, enter into the Golgi apparatus for post-translational modifications steps before they can be sorted to their final destination and become functionally active. To achieve this goal, cells use the secretory pathway, which involves the transport of newly synthesized proteins through a series of cellular compartments and subsequent sorting of them via different type of transport vesicles to their destination. Once synthesized, these proteins enter the lumen of ER. Proteins that enter the secretory pathway have an N-terminus ER signal sequence. This sequence guides the proteins being synthesized to the rough ER. Newly synthesized proteins in the ER are incorporated into small transport vesicles emerging from specialized sub-domains of ER called ER exit sites (ERES). The vesicles that carry newly synthesized proteins from the ER to the Golgi apparatus are COPII coated vesicles. Transport between ER & Golgi apparatus is bidirectional. Transport from ER to Golgi is called anterograde transport & the traffic from Golgi to ER is called retrograde transport. An important complex involved in the retrograde transport is the COPI coated vesicles. From the cis-Golgi, certain proteins, mainly ER-localized proteins, are retrieved to the ER via COPI vesicles. COPI vesicles are also important in intra-Golgi transport in a retrograde direction.

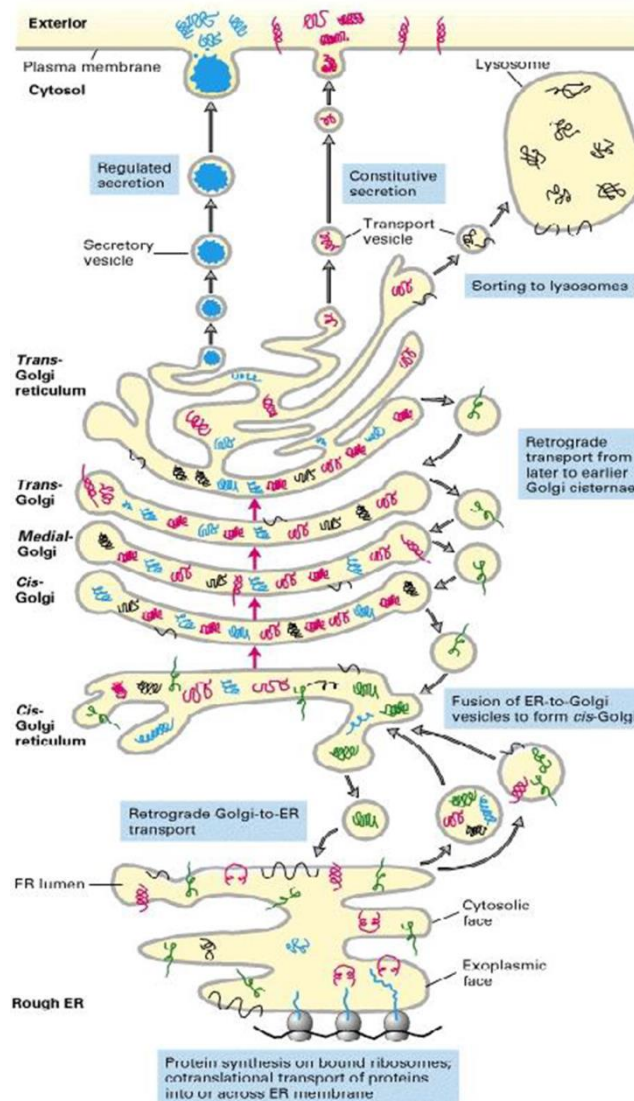


Figure 2.2 The secretory pathway

The schematic diagram explaining secretory pathway inside a cell. (Adopted from Molecular cell biology by Lodish H, Berk A, Zipursky SL, et al.)

Transport between ER & Golgi apparatus is bidirectional. Transport from ER to Golgi is called anterograde transport & the traffic from Golgi to ER is called retrograde transport. An important complex involved in the retrograde transport is the COPI coated vesicles. From the cis-Golgi, certain proteins, mainly ER-localized proteins, are retrieved to the ER via COPI vesicles. COPI vesicles are also important in intra-Golgi transport in a retrograde direction. A cargo protein once

arrives at cis cisterna travels towards the trans face of Golgi apparatus through various post-translational modification steps. At the trans-Golgi network, they are sorted & packaged into a different type of transport vesicles depending on destination. The cargo proteins are then delivered to their respective location within the cell or plasma membrane or are secreted outside the cell. In all cell types, at least some of the secretory proteins are secreted continuously. Examples of such constitutive (or continuous) secretion include collagen secretion by fibroblasts and secretion of serum proteins by hepatocytes [11, 12].

2.4: The Golgi apparatus

In 1898 Camillo Golgi was the first to visualize, describe, and ultimately name the Golgi complex. Using a histochemical impregnation method, involving the reduction and deposition of silver, he defined the Golgi in neuronal cells as a reticular apparatus stained by the “black reaction” (Golgi 1898)[13]. In the many years of ultrastructural research that have followed, the visualization of the Golgi has gone hand-in-hand with the developing EM techniques [14]. The function of this organelle as important organelle for glycosylation & protein secretion was uncovered by Neutra and Leblond and Palade, Jamieson, and coworkers in 1966, 1967. Compartmentalization of Golgi resident enzymes was reported by Novikoff and Goldfischer in 1961 from classic histochemistry data. Erik Fries & Rothman reconstituted the vesicle transport in cell-free extracts of tissue culture cells for the first time in 1980. Reconstitution in vitro of ER-to-Golgi transport was done by Becker and Balch in 1987. Dunphy& Rothman discovered that glycosylation pathway is compartmentalized within the Golgi stack in the cis to trans direction in 1983. Purification of cytosolic components required for the cell-free transport reaction yielded NSF, soluble NSF attachment proteins (SNAPs), Soluble NSF Attachment Protein receptor (SNAREs) by Rothman and colleagues. These experiments also resulted in discovering COPI vesicles 1986 by Orci and

Glick. Orci established that COPI vesicles carry the VSV-G protein between Golgi stacks. The process of retrograde transport from Golgi to ER was discovered by Munro and Pelham in 1987. Pierre Cosson and Francois Letourneur discovered that retrograde traffic is carried by COPI vesicles. This led to confusion about the exact function of COPI vesicles. ER-Golgi intermediate compartment (ERGIC) was isolated by Schweizer et al in 1988. COPII coat was discovered in 1994 by Barlow et al. Lippincott-Schwartz & colleagues for the first time in 1990, made use of BrefeldinA, a fungal metabolite to study ER to Golgi transport & revealed that Golgi resident glycosyltransferases are not statically localized to Golgi. In 2006 direct pieces of evidence to support cisternal maturation came from two groups simultaneously [15, 16]. Even after these reports, many modifications of vesicular transport & cisternal maturation models are being proposed till now. Despite these many observations, a generalized acceptance of any particular model for Golgi biogenesis is still lacking; however, a majority of the researchers presently accept the cisternal maturation model [15, 16].

2.5: Transport through the Golgi apparatus

The Golgi cisternae contain enzymes that process sequentially protein and lipid glycosylation. There are a different model by which cargo transport to the Golgi stack, the well-accepted model is cisternal maturation. In cisternal maturation model, cargo is retained inside the Golgi cisternae that gradually mature to newer cisternae in a cis to trans direction [15, 16].

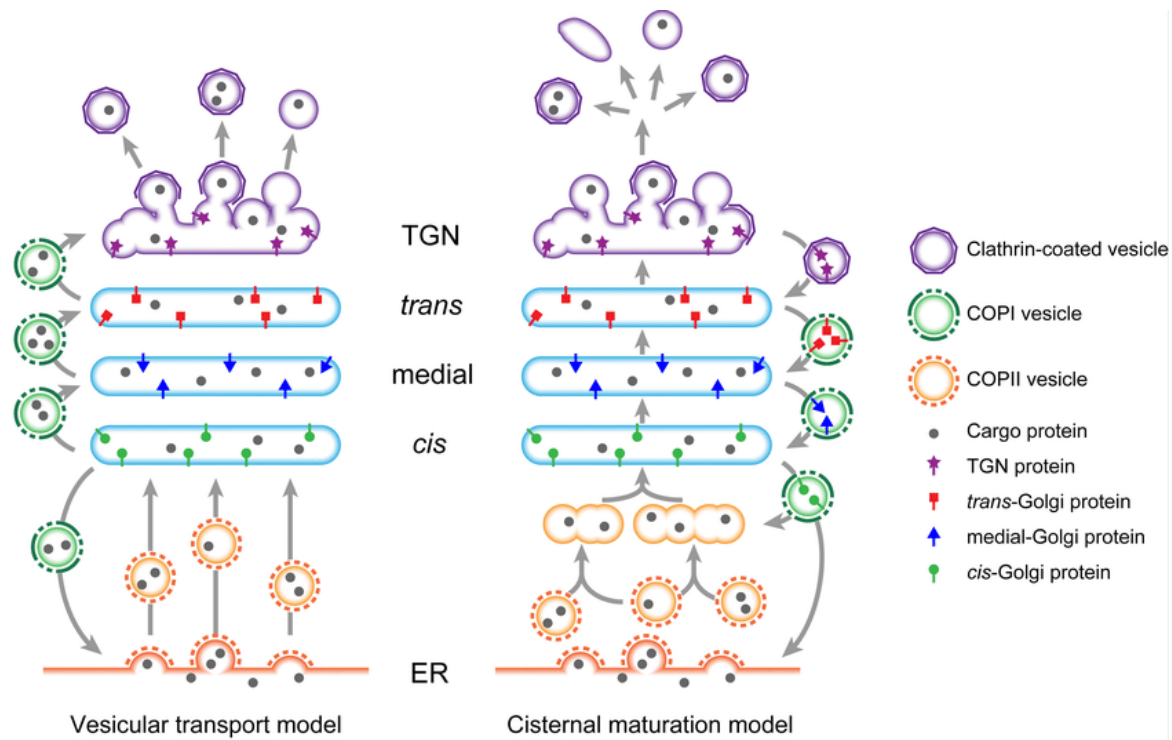


Figure 2.3 Model of Golgi transports [17]

Cisternae mature by the continual recycling of Golgi enzymes in retrograde vesicles that bud from the rims of ‘later’ cisternae and fuse with adjacent ‘earlier’ cisternae. Another model for transport is by tubular connectivity between different cisternae in the Golgi stack. Even though the support for these transport mechanisms are not yet clear, it is possible that certain cargo transported by this mechanism. Regardless of how cargo passage through the Golgi stack, it is clear that active mechanisms exist to maintain the cisternal identity [18].

2.6: Cisternal stacking

The Golgi apparatus plays a central role in the processing, sorting, and secretion of various cargo molecules destined for various intracellular and extracellular destinations. The Golgi display variable shape in different species: from dispersed cisternae in *S. cerevisiae* to stacked cisternal structure in *Pichia pastoris* and to laterally connected ribbon of cisternal stacks in metazoans. But the mechanisms that regulate such exotic organizations have not been clear [4].

Earlier reports showed the presence of proteinaceous bridge holding Golgi cisternae together [19]. Candidates bridging proteins are the GRASPs (Golgi Reassembly and Stacking Proteins) GRASP65 and 55, that localize to cis and medial Golgi cisternae respectively [20]. In lower eukaryotic cells like budding yeast possess single GRASP protein [21]. It was established that both GRASP65 and 55 mediate cisternal stacking by in vitro assay for post-mitotic assembly of rat liver Golgi stacks, suggesting a role as Golgi stacking factors [20, 22, 23]. Single knockout of GRASP65 has partial loss of stacking. Double knockout of GRASP65 and 55 seems to have a minor effect on Golgi stacking, but it affects Golgi ribbon formation suggesting that GRASPs laterally link adjacent cisternae in the Golgi ribbon [24, 25]. A recent study using high-resolution quantitative electron microscopy has tried to resolve this discrepancy. Knockdown of any of GRASP alone results in a slight but consistent reduction in the number of cisternae within a stack, while double knockdown of both GRASPs completely disrupts stack formation, resulting in vesiculation of Golgi cisternae. These experimental results robustly hold up that GRASPs have essential roles in Golgi cisternal stacking.

2.7: Role of GRASPs in Golgi cisternal stacking

GRASP55 & GRASP65 were identified by in vitro cisternal stacking during the cell cycle. GRASPs are 400 amino acid long protein containing N terminal and C terminal domain [20, 22]. The N terminal domain is comprised of PDZs domain which has the ability of oligomerization. This PDZ domain is conserved in most of the species [26, 27]. GRASPs are localized to Golgi membrane via myristoylation of a glycine at position 2[28, 29]. The Golgin 45 is thought to be the receptor for GRASP55 [30], whereas the GM130 recruits GRASP65 [31, 32]. The GM130 C-terminus contains a characteristic PDZ-ligand that interacts with the binding pocket of PDZ2 in GRASP65[28]. Knockout of either GRASP55 or 65 has a minor effect on Golgi stacking but double knockout of GRASPs disperse the Golgi ribbon structure in single Golgi cisternae, suggesting GRASPs as major stacking factor[24]. GRASPs protein mediate cisternal stacking by mode of trans oligomerization of PDZ domain [33, 34]. GRASPs has been also involved in other function than cisternal stacking, in Dictyostelium and yeast they are involved in the unconventional secretory pathway for transport of AcbA upon starvation condition [35-37]. It has been shown that using yeast genetics, the pathway has been dissected and involves the formation of starvation-dependent specialized autophagosomes called CUPS (compartment for unconventional protein secretion) near ER exit sites (ERES). CUPS are enriched in autophagosomal markers and they require both autophagy and ESCRT machinery for their formation [38]. Grh1 is also required for CUPS formation where it is enriched and where it could act to tether these structures to the plasma membrane [36]. Indeed, unlike classical autophagosomes, which fuse with endosomes/lysosomes, CUPS are thought to fuse with the plasma membrane [39]. Mammalian GRASPs appear to have a role to play in N-linked glycosylation, not only at the Golgi but also at the initial steps of the process in the ER. Through a

thorough analysis of the N-glycans by mass spectrometry, depletion of GRASP55 (but not GRASP65) was shown to result in an extensive decrease in N-linked glycans borne by glycoproteins [40]. GRASPs also involved in sorting of integrins from the ER in follicle cells covering the oocyte in *Drosophila* ovaries [41].

2.8: Effect of Golgi fragmentation on Protein trafficking, Protein and lipid glycosylation, and cargo sorting

The Golgi in *S. cerevisiae* does not form a cisternal stack; that suggest cisternal stacking is not essential for cell survival. But in higher eukaryotes, Golgi cisternae are arranged in a stack and also form a Golgi ribbon. In spite of very early observation of such exotic morphology of Golgi, the biological reason for such cisternal stacking remains poorly understood.

Double knockout of GRASPs (55+65) results into the disorganization of the Golgi cisternal stack but does not have any effect on cell death, confirming that it's not essential for cell survival [24, 40]. Disruption of cisternal stacking results in an increase trafficking of the integrins, VSVG, and cathepsin D. Golgi fragmentation increases the speed and effectiveness of COPI vesicle formation in vitro [70]. Golgi cisternal unstacking results in missorting of the cathepsin D precursor to the extracellular space, suggesting that cisternal stacking make sure that cargo sorting occurs when cargo reaches TGN [40].

Double depletion of GRASPs decreases glycoprotein glycosylation and glycan complexity but there was no effect on expression and localization of Golgi enzymes. It also results in decreases N-linked oligosaccharides on the cell surface, with a reduction in both high-mannose and complex-type glycans. GRASP depletion also affects global N-linked glycoprotein glycosylation. These reports suggest that possibly the formation of Golgi stack is important to ensure a proper flux for protein trafficking and accurate glycosylation [24, 40].

2.9: Yeast Golgi apparatus

The yeast Golgi apparatus came into limelight by the very first discovery of identification of 23 complementation groups important for a secretory pathway in *S.cerevisiae* [71]. Like all other eukaryotes, yeast Golgi can be divided into functionally different cis, medial & trans cisternae which carry out different steps of posttranslational modification.

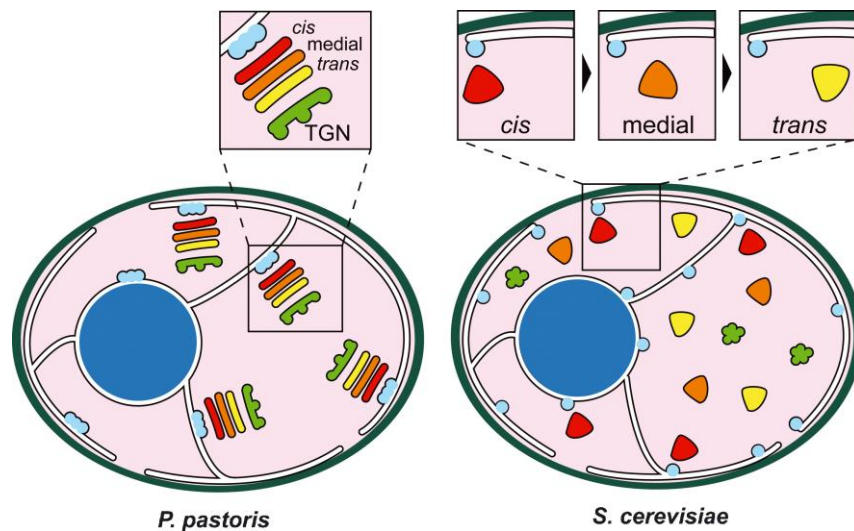


Figure 2.4 Yeast Golgi apparatus

Early acting enzymes like α -1,6-mannosyltransferases (Och1, Mnn9) localize to cis cisternae. Also, Golgi-ER retrieval enzymes like Erd2, Rer1 localize to early cisternae. Later acting enzymes such as -1,2-mannosyltransferases (Mnn2) and α -1,3-mannosyltransferases (Mnn1) define medial & trans cisternae. Many yeast species like *Pichia pastoris* [72, 73], *Schizosaccharomyces pombe* show stacked Golgi cisternae like higher eukaryotes. But *S. cerevisiae* shows a unique Golgi structure in which the Golgi cisternae are unstacked & they are seen floating throughout the cytoplasm [74].

2.10: Golgins

Golgins are Golgi localized long coiled-coil domain protein. Golgins proteins form coiled-coil structure and their C terminal domain mediates Golgi localization. These proteins are well conserved throughout the evolution [75]. The term “Golgins” as defined by being a protein that is found on the Golgi and predicted to form a homodimeric parallel coiled-coil over most of its length. Golgins were initially identified as Golgi localized antigens recognized by antibody from patients suffering from the autoimmune disease [76]. Golgin coiled-coil proteins are found on the cis-face of the Golgi, around the rims of the stack and on the trans-face of the Golgi. GM130, p115, and GMAP-210 localize to the cis-Golgi, the GRIP domain Golgins (golgin-97, golgin-245) localize to trans-Golgi, and TMF, CASP, golgin-84, and giantin are present on Golgi rims [77]. C-terminal domains of most Golgins interact with activated small Rab GTPases, allowing recruitment to specific regions of the Golgi [78, 79]. They are predicted to form parallel homodimeric coiled-coils over most of their length, and this elongated ‘rod-like’ structure would allow them to extend up to 300 nm away from the surface of the Golgi, thus making them ideal candidates to mediate the contact with incoming vesicles [80, 81].

Protein	Alternative names	Human gene symbol	<i>D. melanogaster</i>	<i>C. elegans</i>	<i>S. cerevisiae</i>	<i>A. thaliana</i>
GM130	golgin-95	GOLGA2	CG11061	F33G12.5	<i>BUG1</i>	
GMAP-210	Trip230 CEV14	TRIP11	CG7821	Y111B2A.4	<i>RUD3</i>	At3g6157 At2g46180
golgin-160	Mea-2 IIGP165 GCP170	GOLGA3				
golgin-84	RFG5	GOLGA5	CG17785	T24B1.1		At1g18190 At2g19950
CASP		CUX1 (alt)		Y54F10AM.4c (ceh-44)	<i>COY1</i>	At3g18480
giantin	macrogolgin GCP372	GOLGB1	CG6450 (lva)			
golgin-97		GOLGA1	CG4840 (cbs)		<i>IMH1</i>	At5g66030
golgin-245	p230 tGolgin-1	GOLGA4	CG3493	F59A2.2/6		
GCC88		GCC1	CG10703	C15C7.2.1 (klp-8)		
GCC185		GCC2	CG3532	T05G5.9		
TMF	ARA160	TMF1	CG4557	F39H12.1	<i>SGM1</i>	At1g79830

Table 2.1 The canonical Human Golgins and orthologues [75]

Single knockdown of Golgin affects Golgi structure suggesting their role in Golgi structure maintenance [82-84]. Recently electron microscopy study suggests that in double depleted GRASPs cells expression of Golgin rescue the Golgi ribbon formation, suggesting a role of Golgins as a stacking factor in the organism which does not have GRAPs homolog [85].

2.11: Vig4-GDP-mannose transporter

Vig4 is a Golgi membrane protein containing multiple transmembrane domains. Vig4 of *Pichia pastoris* is a homolog of Vrg4 of *S. cerevisiae*. The function of this protein is to transport GDP-mannose inside the Golgi lumen. The mutations in Vrg4 cause defects in N-linked, O-linked glycosylation of proteins & mannosylation of sphingolipids [86]. Vrg4 also perform other functions like to retrieve ER-localized BiP from Golgi & maintaining normal membrane morphology [87]. Vig4 localizes to the early Golgi membrane with help of several transmembrane domains. Vrg4 is

present as an oligomer. C terminal domain of Vrg4 is required for its assembly into oligomers. The Vrg4 lacking N-terminal domain is stable and multimerize but is mislocalized to ER. This suggested that the N-terminal domain is important for correct localization of the protein to Golgi membranes. Golgi mannosyltransferases are type II membrane proteins having a short cytosolic N-terminal domain followed by a transmembrane domain to anchor the enzymes to the Golgi membrane [88]. The transmembrane domain is followed by a non-conserved stem and a more conserved C-terminal globular catalytic domain. To label Vig4 with fluorescent protein like GFP, GFP is often attached to N terminus of Vig4 so as to achieve proper folding of GFP which is much better in cytosol than in Golgi lumen [15, 89, 90].

2.12: Sec7- SECretory protein

Sec7 is Guanine nucleotide exchange factor (GEF) for ADP ribosylation factors (Arfs). It is a very large size protein of 226 kDa. Sec7 was identified through a mutation that causes a defect in secretion or protein transport [71]. Sec7 is essential for proliferation of Golgi and vegetative growth of cells. The catalytic activity of Sec7 resides in 200 amino acid residues domain called the Sec7 domain [91]. The sec7 domain contains “glutamic finger “which is important for its activity [92]. This domain is conserved throughout the evolution. Sec7 is sensitive to Brefeldin A treatment. Sec7 localizes to Golgi membranes via its HDS1 domain by interaction with activated Arf1, forming a positive feedback loop & stabilizing its localization. Also, the autoinhibition caused by Sec7 C-terminus is relieved after its stable recruitment to the membrane [93]. Arf1, Arl1, Ypt1 affect the membrane localization of Sec7 & ypt31/32 can stimulate the GEF activity of Sec7 [94]. Sec7 localizes to late Golgi cisternae [95]. Sec7 is peripheral membrane protein abundantly present on the late Golgi membrane. Sec7 was used as a marker to label late Golgi in many studies. Late Golgi cisternae can be labeled with Sec7-GFP or Sec7-mcherry [15, 73, 96].

2.13: Imh1- Integrin's and Myosin's significant Homology

(Shares with Integrin's and Myosin's significant Homology) [97]. Imh1 is Yeast homolog of GRIP domain Golgins. Golgins are Golgi localized proteins which function in Golgi structure maintenance and vesicle tethering. Imh1 was first identified as a suppressor of YPT6 null mutant. It was able to rescue the temperature-sensitive growth phenotype and missorting of carboxypeptidase [97]. Imh1 contains High alpha helical repeats. Imh1 contains C terminal Golgi localizing GRIP domain [98]. GRIP domains contain conserved tyrosine residue. Mutation of conserved tyrosine to alanine abolishes localization of GRIP domain Golgin from Golgi [99]. GRIP domain Golgins are recruited to the Golgi via ARF-like GTPases Arl1 and Arl3. Cells lacking either of two, Arl1p and Arl3p GRIP domain does not localize to the Golgi. In vitro binding experiments demonstrated that activated Arl1p-GTP binds specifically and directly to the Imh1p GRIP domain. Arl1p Colocalizes with Imh1p-GRIP at the Golgi and Golgi localization of Arl1p was regulated by the GTPase cycle of Arl3p. These results suggest a cascade in which the GTPase cycle of Arl3p regulates Golgi localization of Arl1p, which in turn binds to the GRIP domain of Imh1p and recruits it to the Golgi [100]. The imh1 central region contains High alpha helical repeats which form a coiled-coil domain.

2.14: ARL – (ADP-Ribosylation factor-Like)

Arl1 and Arl3 are Ras family small GTPases [101]. Arl1 is localized to the TGN. In budding yeast, arl1 and arl3 null mutants are viable and have minor defects in protein sorting in the TGN [33, 34, 35, 36]. The plasma membrane of yeast arl1 null mutant cells is hyperpolarized, leading to defects in ion homeostasis, suggesting that Arl1 regulates the localization or activities of ion transporters [37, 38, 39].

GRIP domain binds to Arl1–GTP and GRIP domains proteins shown to be both necessary and sufficient for their localization to the Golgi[100]. GRIP domain Golgins regulates endosome-to-Golgi transport via tethering of endosome-derived vesicles to the TGN [84]. Arl3 and Arl1 sequentially work in cascade and Arl3 activate Arl1 which recruits Imh1 to the Golgi [100, 102].

2.15: GRIP domain

GRIP domain is a conserved protein domain. The GRIP (golgin-97, RanBP2alpha, Imh1p, and p230/golgin-245) domain is found in different Golgi localized Golgin proteins. GRIP domain is C terminal region present on the majority of Golgin molecule which mediates targeting of the proteins to the Golgi [99].

2.16: Coy1 (CASP of Yeast):

COY1 encodes a protein that is the homolog of mammalian CASP in *S. cerevisiae*. It also belongs to the conserved family of coiled-coil proteins. *COY1* deletion in *S.cerevisiae* does not affect the viability of cells, but strikingly restores normal growth of those cells that lack the Golgi soluble NSF attachment protein receptor Gos1p. Besides the extensive coiled-coil region in the cytosolic N terminus, Coy1 has got a C Terminal Transmembrane Domain (TMD). There are conserved Histidine and Tyrosine residues in the middle of TMD. The conserved histidine is necessary for Coy1p's activity in cells lacking Gos1p while the conserved Tyrosine is necessary for the Golgi targeting of the particular protein [103]. Coy1 plays an indirect role in the retrograde transport between the early Golgi compartments. It regulates the COG-complex dependent fusion of COPI vesicles in the retrograde pathway [104].

2.17: Sgm1 (Slow growth on Galactose and Mannose):

Sgm1 was first identified in yeast as a protein with extensive coiled-coil motifs that interacts to the GTP bound form of Rab-6 like GTPase Ypt6 [105]. Sgm1 has got a similar overall structure across

different species. This structure consists of a large coiled-coil region, flanked by short non-coil domains, with a separate short coiled-coil region at the C terminus. The human protein with the strongest similarity to this structure is TMF, TATA element modulatory factor [106]. Sgm1 is known to be recruited to the Golgi membranes by Ypt6. The C terminal coiled-coil domain of Sgm1 has got the site for interaction with Ypt6 and is necessary for the localization of the protein to the Golgi membrane [106].

2.18: Rud3 (Relieves Uso1-1 transport Defect)

The coiled-coil protein Rud3p has been found to be on the cis-Golgi. Rud3p was identified as a suppressor of temperature-sensitive mutations in Uso1p (the yeast homolog of the p115) and Sec34p (a subunit of the COG complex)[107]. Deletion of Rud3p results in defects in the Golgi processing of N-linked glycans. Rud3 localizes to early Golgi. Rud3 is a mammalian homolog of GMAP-210. C terminal domain of Rud3 GRAB domain is important for Golgi targeting. This recruitment is mediated by the combined action of the GTP-binding protein Arf1p and the membrane protein Erv14p [108].

3. Materials and Methods

3.1: Molecular biology methods

Host strain: E. coli DH5 α

Luria-Bertani (LB) (HI Media) medium: Luria Broth powder (20g) was dissolved in 800 ml deionized milliQ (D/W) and the volume was adjusted to 1 liter with milliQ and sterilized by autoclaving. For making LB-agar plates, 20g bacteriological grade agar powder was dissolved and sterilized by autoclaving and poured in 90 mm sterile plates.

Antibiotics:

Final Concentrations for Ampicillin and Kanamycin are 50 μ g/ml and 30 μ g/ml respectively.

3.1.1: Preparation of ultra-competent E. coli:

Higher competency is very important to ensure high transformation efficiency that often helps in cloning. DH5 α was made ultra-competent for the transformation of recombinant/routine plasmid vectors.

Super-optimal broth (SOB): Dissolve all the following ingredients in milliQ, 2% Bactopeptone (HI media), 0.5% yeast extract (HI media), 10mM NaCl (Merck), 2.5mM KCL (Merck), 10mM MgCl₂, 10mM MgSO₄ and autoclave to sterilize.

Super-optimal catabolite (SOC) media: To 98ml of sterile SOB, add filter sterilized 2M glucose and autoclaved 2M MgCl₂.

Transformation buffer (TB): 100 ml of D/W; 10 mM PIPES(Sigma), 15 mM CaCl₂, 250 mM KCl, adjusted pH to 6.7 with 5N KOH, 55 mM MnCl₂, filter sterilized through 0.2 μ membrane filter.

Protocol: E. coli DH5 α cells were streaked on LB agar plate and incubated overnight at 37°C. A single colony is inoculated in 250 ml SOB medium and incubated on refrigerated shaker incubator with 200 RPM at 18°C until OD600 reaches to 0.6. Incubate the flask on ice for 10 minutes and spin the culture at 2500g (3500 RPM) for 10 minutes at 4°C. Resuspend the cells very gently in 80 ml of ice cold transformation buffer and again keep on ice for another 10 minutes. Spin the mixture at 2500 x g (3500 RPM) for 10 minutes at 4°C. Resuspend the cells gently in 20 ml of ice cold transformation buffer. Incubate on ice for 10 minutes. Add DMSO to a final concentration of 7% (1.4 ml) and mix by pipetting up and down. Aliquot 100 μ L of cells in a tube and freeze the vial in liquid nitrogen and stored at -80°C.

3.1.2: Bacterial Transformation[109]

Ultra-competent cells (100 μ L aliquots) were taken out from -80°C and thawed on ice. 10 μ L (50-100 ng) of DNA added to 100 μ L thawed competent cells (avoid disturbing cells by pipetting rather tap the tube gently). Cells were incubated on ice for 10 minutes. Heat shock was given to the vial by keeping in 42°C water-bath for 45 seconds. The cells were placed on ice immediately for 5 minutes. After 5 mins 200 μ L of ice cold SOC medium was added to the vial aseptically and incubated at 37°C with shaking at 180 RPM for 20 minutes. The cells were plated on appropriate antibiotic-containing LB agar plate and incubated at 37°C for 12-16 hours for colonies to appear.

3.1.3: Plasmid DNA isolation

Plasmid DNA was isolated by various methods.

3.1.3.1: QIAprep Spin Miniprep method

Reagent- Qiagen miniprep kit, as per the manufacturer's protocol.

QIAprep Spin Columns contain a unique silica membrane that binds up to 20 µg DNA in the presence of a high concentration of chaotropic salt and allows elution in a small volume of low-salt buffer.

A single colony was inoculated in 10ml of LB-amp/ LB-kan media and incubate at 37°C for 12-16 hours at 180 RPM bacterial shaker incubator. The bacterial culture was transferred in a 15ml tube and spin at room temperature for 5 minutes at 5000 RPM. The pellet was vortexed briefly and then resuspend in 250µl of Buffer P1 and transfer to a microcentrifuge tube (Ensure RNase A has been added to Buffer P1). Add 250µl of buffer P2 and invert the tube 4–6 times. Immediately add 350µl of buffer N3 and again invert the tube 4–6 times. Spin the lysate at 13,000RPM for 10 minutes. Add the clear supernatant very carefully to the QIAprep spin column. Spin the column for 30–60 seconds and discard the flow through. Add 600µl of buffer PE to wash the QIAprep spin column and again spin for 30–60 seconds. Discard the flow through. Wipe the column from outside so as to remove any residual buffer PE. Then place the column in a dry tube and spin at 13000 RPM for 2 minutes to remove any residual wash buffer. Now, place the QIAprep column in a clean 1.5 ml microcentrifuge tube. Add 50µl Buffer EB (pre-warmed at 65°C) to the center of the QIAprep spin column, let it stand for 2 minutes. Centrifuge for 2 minutes at 14000 RPM to elute Plasmid DNA.

3.1.3.2: Plasmid DNA isolation using TELT buffer

This is a quick and cost-effective protocol for preparing plasmid DNA which was mainly used during regular screening for positive clones in all the cloning experiments.

TELT buffer [50mM Tris-Cl (Sigma) pH7.5, 62.5mM EDTA (Fischer Scientific) pH8, 0.4% Triton X100(Sigma), 2.5M LiCl (Sigma)], Lysozyme (Sigma) (50mg/ml), 70% ethanol, Absolute alcohol (Merck), TE buffer.

The bacterial culture was inoculated in 1.5ml LB-antibiotic (Amp/Kan) media and incubated at 37°C, for 12-16 hours at 200 RPM. Cells were pellet down at 14000 RPM for 1 minute at 4°C . The supernatant was discarded and the pellet was resuspended in 150µl TELT buffer and vortex briefly. Add 5.7µl lysozyme (Stock 50mg/ml) to the same and mix well. Incubate the vial on ice for 1 minute. Incubate the vial in boiling water bath for 1 minute. Immediately place the vial on ice for 10 minutes. Spin at 4°C at 15000 RPM for 10 minutes and collect supernatant in a new vial. Add 330µl chilled absolute alcohol and incubate at 80°C for 30 minutes. Spin at 4°C at 15000 RPM for 10 minutes. Add 200µl chilled 70% ethanol for washing the DNA pellet and again centrifuge at 15000 RPM at 4°C for 5min. Dry the pellet so as to remove all remaining alcohol and re-suspend in 20µl TE buffer.

3.1.4: Agarose gel electrophoresis

Agarose gel electrophoresis is a routinely used method for the analysis and preparation of DNA molecules. Various size DNA fragments can be separated on agarose gels using different concentrations of agarose.

Ethidium bromide 0.5 µg/ml

6X Gel loading dye: 1.2ml glycerol, 1.2ml 0.3mM EDTA, 300µl of 20% SDS, 160 µl of 0.5% Bromophenol blue stock, nuclease free water to make up volume to 10ml.

Sodium Borate (SB) buffer: 10mM NaOH pH 8.5 adjusted with boric acid for 1X SB buffer.

Agarose powder was weighted as per requirement of percentage of gels (depends on the size of DNA fragments), for example, to make a 0.8% agarose gel, add 0.48g of agarose powder in a glass flask, to which add 60ml of 1X sodium borate (SB) buffer. The mixture was microwaved for 2

minutes so that agarose powder melts and the gel dissolves. Boiling mixture was allowed to cool down so as to add ethidium bromide (to visualize DNA) at a final concentration of 1µg/ml (stock 10mg/ml) and mixed well without creating bubbles and pour the mixture into the gel tray, place comb to create wells. Once the gel is solidified, remove the comb. Pour 1X SB buffer (running buffer) to the tank containing agarose gel. Dilute DNA sample (Plasmid DNA, PCR fragments, restriction digestion fragments, ligated DNA) with 6X gel loading dye (to make a final concentration of 1X). Standard 1Kb or 100bp ladders were run in parallel to understand the size of DNA fragments being analyzed. DNA bands were visualized using gel documentation system.

3.1.5: Polymerase chain reaction (PCR)

The PCR technique provides specific DNA amplification of the sequence of interest from a template (yeast genomic DNA / plasmid DNA /cDNA) with the help of two oligonucleotide primers that bind to opposite strands in a sequence-specific manner. A thermostable DNA polymerase is used for extension of the primers at 3' end. Phusion high fidelity DNA polymerase was used for PCR amplification.

1. A typical mixture of a PCR reaction includes the following additive

	Components	Final concentration
1	H ₂ O	To make up the volume
2	5X buffer HF/GC	1X
3	10mM dNTP mixture	200µM
4	Forward primer	0.5µM
5	Reverse primer	0.5µM

6	Template DNA	50ng (Plasmid DNA)100ng (Genomic DNA or cDNA)
7	DNA polymerases	0.02 U/ μ l

Table 3.1 Contents of PCR reaction

2. Thaw all the samples on ice and add all the reagents as per the order stated in the table above, followed by a short spin of the PCR tube after addition of all the components. Transfer quickly to the thermocycler preheated to the denaturation temperature (98°C) so as to start the reaction.

Typical PCR cycle:

Cycle step	Temperature	Time	Cycles
<i>Initial denaturation</i>	<i>98°C</i>	<i>3 minutes</i>	<i>1</i>
<i>Denaturation</i>	<i>98°C</i>	<i>30 seconds</i>	
<i>Annealing</i>	<i>Lower T_m+3</i>	<i>30seconds</i>	<i>30-34</i>
<i>Extension</i>	<i>72°C</i>	<i>60 seconds /Kb</i>	
<i>Final extension</i>	<i>72°C</i>	<i>8 minutes</i>	<i>1</i>
<i>Final hold</i>	<i>4°C</i>	<i>Forever</i>	

Table 3.2 Typical PCR cycle

Check the PCR product on an agarose gel.

3.1.6: Quick change mutagenesis[110]

Quick change mutagenesis was used to introduce either point mutation or insertion or deletion of a few bases in a gene of interest with the help of high fidelity PfuTurbo polymerase. Prepare an oligo mix by mixing 5 μ l of each forward and reverse primer (from 100 μ M stock) and 40 μ l of ddH₂O(1:10dilution). Template concentration should be between 40-60ng/ μ l.

The reaction was set up as follows:

Components	Volume(μ l)
H ₂ O	15.3
10X buffer for PfuTurbo	2
10mM dNTPs	0.4
Primer mix(1:10dilution)	0.4
Template DNA(40ng/ μ l)	1
PfuTurbo polymerases	0.4 (20U)

Table 3.3 Contents of PCR reaction for site-directed mutagenesis

Cycling conditions for quick change mutagenesis:

Cycle step	Temperature	Time	Cycles
<i>Initial denaturation</i>	<i>95°C</i>	<i>30s</i>	<i>1</i>
<i>Denaturation</i>	<i>95°C</i>	<i>30s</i>	
<i>Annealing</i>	<i>55°C</i>	<i>60s</i>	<i>18</i>
<i>Extension</i>	<i>68°C</i>	<i>2min/Kb</i>	
<i>Final extension</i>	<i>68°C</i>	<i>8min</i>	<i>1</i>

Table 3.4 Cycling conditions for PCR for site-directed mutagenesis

3.1.7: Gene Cloning[111]

In gene cloning, plasmid DNA is cleaved with one or more RE in order to get blunt/cohesive ends and then foreign DNA fragment of variable sizes with compatible ends are ligated. The ligated heterogeneous mix is then transformed into a suitable bacterial host to propagate the clones. The resulting transformed recombinant clones are then screened by RE digestion to confirm the recombinant clone. Different strategies are used to clone a fragment of DNA in a plasmid vector, for example, PCR based cloning, sticky end based directional cloning etc.

3.1.7.1: Restriction Digestion

Restriction enzymes or restriction endonucleases cut at a specific site in the template DNA. The components of preparative and analytical restriction digestion reaction were as follows:

Components	Preparative	Analytical
Plasmid DNA	1 µg	100ng
H ₂ O	To make up the volume to	To make up the volume to
10X buffer	5µl	1µl
BSA	If required	If required
Enzyme	5U (1µl)	1U (0.2µl)

Table 3.5 Content of PCR reaction

1. Add all the components in a microcentrifuge tube.
2. Add the enzyme in the end.
3. Briefly vortex the tube followed by short spinning the tube.
4. Incubate the tube at 37°C for 2-4 hours in a water bath (or, at any other temperature if mentioned specifically for a particular enzyme).
5. For any vector preparation in a cloning method, add 1µl alkaline phosphatase (FastAP) (NEB) in the reaction tube and incubate for another 1 hour (Alkaline Phosphatase removes the 5'-phosphate groups of DNA from both the termini of the digested vector so as to avoid the self-ligation of the vector).
6. Analyze the digested DNA fragment on an agarose gel.

3.1.7.2: Purification of restriction digested DNA or PCR product

For cloning of digested DNA fragments (either vector or insert), it is very important to purify them to remove nucleotides, primers, enzymes, mineral oil, salts, agarose, ethidium bromide, and other impurities from DNA samples before setting up ligation reaction.

Nucleotide removal kit (Qiagen), Gel extraction kit (Sigma)

QIA quick Nucleotide Removal Kit was used to remove DNA impurities during all cloning procedures. Columns contain a silica membrane assembly for binding of DNA in high-salt buffer and elution with prewarmed water. The protocol is as follows-

Add 5 volumes of Buffer PN to 1 volume of the reaction sample and mix them homogeneously. Transfer the mixture in a QIA quick spin column, placed in the 2ml collection tube. Centrifuge the tube for 1 min at 6000 RPM, discard the flow-through. Add 600µl of buffer PE to the column and centrifuge for 1 min at 6000 RPM. Discard the flow through. Wipe the column from outside so as to remove any residual buffer PE. Then place the column in a dry tube and spin at 13000 RPM for 2 minutes to remove any residual wash buffer. Now, place the column in a clean 1.5 ml microcentrifuge tube. Add 50µl pre-warmed (at 50°C) autoclaved water to the center of the column, let it stand for 2 minutes, and centrifuge for 2 minutes at 14000 RPM to elute pure DNA. To increase the concentration of the pure DNA, freeze the DNA by keeping the Eppendorf tube at -80°C for 20 minutes, once frozen, then concentrate the DNA in a Speed-Vac at 4°C until the volume reduces]

3.1.7.3: Purification of DNA fragments from agarose gel

For cloning of digested DNA fragments (either vector or insert) or to get any pure PCR product, sometimes DNA bands of specific size had to be cut from agarose gel followed by removal of agarose from DNA samples before setting up ligation reaction. GenElute Gel Extraction Kit (Sigma) was used to purify DNA fragment from agarose gels. Place the agarose gel containing DNA band of interest in a gel doc machine under UV light to visualize DNA. Cut the DNA band from the gel using sharp scalpel pre-sterilized with 70% alcohol (Remove as much as excess

agarose to increase the yield). Make small pieces of the DNA band and place them in an Eppendorf. Add 3 volume of the Gel Solubilization Solution to the gel slice. (For every 100mg of agarose gel, added 300 ml of Gel Solubilization Solution). Incubate the gel mixture at 60°C for 10-15 minutes with intermittent vortexing. In the meantime, add 500 ml of the column preparation solution to the binding column and centrifuged for 1 minute. Discard the flow through. Add 1 gel volume of 100% isopropanol and mix homogeneously. The solubilized gel solution mixture was then added to the binding column and centrifuged for 1 minute at 6000rpm. The flow-through liquid was discarded. Add 600µl of buffer PE to the column and centrifuge for 1 min at 6000 RPM. Discard the flow through, Wipe the column from outside so as to remove any residual buffer PE. Place the column in a dry tube and spin at 13000 RPM for 2 minutes to remove any residual wash buffer. Now, place the QIAprep column in a clean 1.5 ml microcentrifuge tube. Add 50µl pre-warmed (at 50°C) autoclaved water to the center of the column, let it stand for 2 minutes, and centrifuge for 2 minutes at 14000 RPM to elute pure DNA. [To increase the concentration of the pure DNA, freeze the DNA by keeping the Eppendorf tube at -80°C for 20 minutes, once frozen, then concentrate the DNA in a SpeedVac at 4°C until the volume reduces]

3.1.7.4: Ligation reaction

DNA ligase enzyme creates a phosphodiester bond between a 5'- phosphate termini and a 3'- hydroxyl group of two different DNA fragments and ligates the vector and insert DNA.

Method-

Components	Molar ratio	Concentration($\mu\text{g}/\mu\text{L}$)	Length (in base pair)	Max Volume
Vector	1	$x\mu\text{g}/\mu\text{L}$	Size in bp	Available vol.
Insert	3	$y\mu\text{g}/\mu\text{L}$	Size in bp	Available vol.

Table 3.6 Typical Ligation Reaction Calculation

Measure the concentration of purified vector and insert DNA fragments. The typical ratio of vector: insert used was 1:3 which can vary depends on the size of either vector or insert. Calculate the amount of vector and insert fragment required to achieve 1:3 molar ratio as per the following table in any insilico ligation calculator. Add the components of the ligation reaction as mentioned in the following table-

Components of the ligation	Total volume (10 μL)
Nuclease-free water	To make up the volume
10X T4DNAligase buffer	1 μL
Vector	As calculated from the above table
Insert	As calculated from the above table
T4 DNA Ligase	200U

Table 3.7 Component of Ligation reaction

Always set up a positive control (any plasmid DNA of same concentration without vector and insert, to check if transformation worked) and a negative control (another ligation mixture without insert fragment). Incubate the reactions at 22°C for 2-4 hours or at 16°C for overnight. Transform all the three-reaction mixture in E. coli cells and check for positive clones.

3.1.7.5: Screening of recombinant bacterial clones

Clones have to be screened for the presence of the specific insert. If the test plate contains more colonies compare to the negative control plate, then only proceed for clone screening. Ideally, in the negative control plate, there should not be any colonies.

Method-

Replica plate transformants on LB-Amp or LB-Kan plates and inoculate in 1.5ml antibiotic containing LB broth. Incubate Eppendorf tubes at 37⁰C for 12-16 hours at 200 RPM. (Each clone was given a specific miniprep number for documentation). Following day, isolate plasmid DNA using TELT buffer protocol. Set up restriction digestion for the clones along with vector control DNA in which one restriction enzyme present in the vector DNA and another enzyme is present in the insert DNA to confirm the presence of an insert in the final clone. Analyze the digested fragment in agarose gel electrophoresis.

3.2 Microscopy& Image Processing[115]

3.2.1: Preparing the Cells

A yeast culture was inoculated from a healthy preculture and grown overnight in 5 mL non-fluorescent minimal medium (NSD) in a 50-mL baffled flask. Aim to image the cells at an OD₆₀₀ of ~0.5. Use a MatTek dish with a high precision 0.170 mm cover glass bottom. Prepare the dish with ConA: pipette 250 µL ConA onto the dish, wait for 15 mins, wash thoroughly with dH₂O, and let it dry. Just before imaging, adhere cells to the dish: pipette 250 µL from your culture onto the dish, wait for 10 mins and rinse gently several times with NSD by pipetting. Leave 2-3 mL of fresh NSD in the dish.

3.2.2: Imaging Parameters

Following parameters were used for the live cell imaging using Leica SP8 imaging platform.

- 100x objective (NA=1.4 or higher)
- Frame size: 256 x 128 (width x height)
- Zoom: 7
- Pixel size: 60-70 nm
- XY scan direction: bidirectional, phase = 3.15,
- Pinhole: 1.2 AU
- Line averaging: 8
- Slice thickness: approximately 0.3 μm
- Bit depth: 8-bit is almost always adequate
- Laser settings for green and red fluorescence channels:
 - 488: 3-10%, HyD, collection window = 495-550 nm, gain = 400-500
 - 561: 3-10%, HyD, collection window = 575-750 nm, gain = 400-500
- PMT for bright field, gain = 300-350; store in blue channel of RGB images

3.2.3: Deconvolution

Images were deconvoluted using Huygens professionals. First raw Lif file was opened by Huygens professionals, then we have to go to > Parameter wizard. In the case of raw Lif file, it will provide the NA (1.35), excitation/emission, pixel size, step size, and wavelengths. After that click the “Next” arrows to proceed through the wizard. The images were cropped using cropper then click “Next” for the background, try “Auto” first, and click “Accept”. Leave the values for maximum iterations, etc., but change the signal-to-noise ratio to 10. Once all the parameters are set we have to click “Deconvolve. If the deconvolved image is satisfactory click “Accept, to next channel. We will repeat for the other fluorescence channel. When we reach the bright field channel, click “All done.” We have to select appropriately deconvolved or original image, and click “Next”. We have to choose the red as Ch-0, green as Ch-1, and bright field as Ch-2 and then click “Done”. The deconvolved image will be saved as Tiff 8 bit to decon folder.

3.2.4: ImageJ

In ImageJ, we have to process the deconvoluted images. We will open the images using File > Import > Image Sequence, select your “decon” folder. We have to select Image >Hyperstacks> Stack to Hyperstack, choose order “XYZ” and input the appropriate number of channels, slices per stack, and frames. We have to select mode as grey scale and click “OK”. Then split the merge channels and select C2 for C1 and C1 for C2, keep C3 for C3 and save as tiff file. Then we have to convert each channel from 8 bit to 16 bit. After that, we will select choose Process > Math > multiply and multiplication factor will be 256. To adjust the brightness we will select Image > Adjust > Brightness/Contrast. For each of the three channels, in turn, press the Auto button in the B&C window.

3.2.5: Average Project

To project the Z project, select Image > Stacks > Z Project and choose “Average Intensity” and press OK. Wait for the projection to finish. If desired, adjust the brightness and contrast of the individual channels as described above. We will save the individual channel in the PNG format and merged image in TIFF file format.

3.3 Basic Yeast Techniques[116]

3.3.1: Yeast strain: PPY12 (*his4*, *arg4*)

Media preparation: Media were prepared as indicated on the bottles by dissolving the powder in distilled water & autoclaved for sterilization. Drop out media were prepared for selection of clones after transformation. These were prepared by adding yeast nitrogen base, glucose, CSM without a particular amino acid for selection in a proportion as indicated on media bottles. They were sterilized by autoclaving. (YPD ready mix powder, synthetic complete media powder SD, Yeast nitrogen base, glucose, complete supplementary mixture, CSM without URA/ TRP/ LEU).

3.3.2: Retrieving strains from the yeast collection

To retrieve the yeast strain from the freeze down, first UV sterilizes the laminar hood and keep a YPD plate / auxotrophic dropout plate in the hood. Then identify the appropriate vial (Labelled location number) from -80°C. Remove the vial from -80°C and keep it on ice. We will use a sterile toothpick to take small amount of the frozen cell and streak on YPD plate or auxotrophic dropout plate (only for strains containing episomal plasmids). Incubate at 30°C for 2days.

3.3.3: Growing yeast log phase culture

To grow yeast cells, A single colony was inoculated from the plate in 5ml YPD broth or dropout broth in a preculture tube. Preculture tube will be incubated at 30° C, 200rpm for 48hrs. The saturated pre-culture (Cells should be settled at the bottom of the tube, and the whole bottom of the tube should be filled with cells). We will inoculate the 0.1% from saturated pre-culture for a log phase culture in the baffled flask (No other than this flask so as to maintain proper aeration and further good results).

3.3.4: Freezing Yeast

We have used 15% glycerol prepared in distilled water sterilized by autoclaving

Method-

Yeast cells were inoculated in pre-culture tube overnight until the culture is saturated. Once the culture is saturated, we will plate 400µl cell suspension from saturated pre-culture on 2 YPD plates or plates of selection medium. YPD Plates will be incubated at the appropriate temperature until lawn growth appeared. For each strain, two cryovials were prepared by placing 1.5ml sterile 15% Glycerol in each vial. A location number for freeze down of the strain was obtained by making a new entry in the Filemaker yeast database of the lab. Each vial was labeled with this location number on the top. The details of the strain were written on the side of cryovials. We will use a small sterilized tip, about a third of the lawn (YPD plates) or an entire lawn (selective plates) was scraped off and re-suspend in one of the vials. The similar procedure will be repeated for the second vial. The vials will be kept in the respective yeast freeze down box in the -80°C freezer. One vial was placed in standard collection, and an identical vial was kept in the backup collection.

The Complete information about the strain has to be entered in the Filemaker yeast database of the lab.

3.3.5: Yeast transformation[117]

Pichia pastoris cells were transformed by the high-efficiency electroporation method. A single colony of *Pichia* strain was grown in 6 ml YPD overnight at 30°C, 200rpm. Once the saturated growth is attained the growth, inoculate the 0.1 percent of the culture in 50mL YPD in a 250 mL flask with 0.1-0.5 ml of the overnight culture. The culture was allowed to grow overnight again to an O.D. of 1-1.5. Once it reaches 1.0 OD, add 1ml of 1M DTT and 1M HEPES and keep it at 30-degree shaker for 15 mins. After 15 mins centrifuge the cells at 3000 rpm for 3 minutes at 4°C. The pellet will be resuspended with 50 mL of ice-cold, sterile water and centrifuge the cells. The similar step will be repeated and resuspend the pellet in 50 mL of ice-cold, sterile water. After that centrifuge the cells again, and resuspended in 20 ml of ice-cold 1M sorbitol. Cells will be washed with 1M sorbitol and then resuspend the pellet in 200 μ L of ice-cold 1M sorbitol. We will keep the cells on ice and take 40 μ L of the cells and add linearized DNA prepared and then transfer to an ice-cold 0.2 cm electroporation cuvette, tap the cells down to the bottom of the cuvette. Now cells are ready for the electroporation, we will pulse the *Pichia* cells (25 μ F, 200-ohm, 2000 V). Immediately, after the pulse adds 1 ml of ice-cold 1M sorbitol to the cuvette. We have to transfer the cuvette contents to a sterile 1ml tube and centrifuge at 5000rpm for 1 min. Remove 800 μ L of contents from tube and plate the remaining amount on selection plates.

3.3.7: Replica plating for screening transformants

The replica plating was performed to select the transformants on the selective plate. For that grids and lines were made on a fresh plate and put numbers on the plate. We can replica plate as much as

a colony from transformation plate (after colony appears) in a new plate to screen for positive transformants. Replica plate will be incubated at the 30°C incubator for 24 hours.

3.3.8: Genomic DNA isolation [118, 119]

Breaking buffer: 2 % (v/v) Triton X-100, 1% (v/v) SDS, 100 mM NaCl, 10 mM Tris- Cl, pH 8.0 1 mM EDTA, pH 8.0, Distilled H₂O(sterile)

Method-

A single colony was inoculated from a replica plate in preculture tube (5-6 ml)/ Eppendorf tube (1ml). It will be allowed to grow overnight at 30°C 200 RPM. Overnight culture will be Spin for 5 minutes at 3000 RPM at room temperature. The supernatant will be discarded and wash pellet (resuspend, spin and discard the supernatant) with 0.5mL MQ. Cell pellet will be vortex briefly and add 200µl of freshly prepared breaking buffer and resuspend cells. We will add 0.3 g (200 µl in vol.) small glass beads and 200 µl phenol (cold)/chloroform. The mixture is vortexed at highest speed for 3min to achieve cell lysis. Once the cell is lysed we will add 200 µl 1X TE buffer and give a brief vortex. Cells will be centrifuge at highest speed for 5 min, at room temperature and the aqueous layer will be transferred to a fresh tube. We have to add 1ml 100% ethanol (ice cold), mix by inverting tubes and incubate tubes at -20°C for 1 hour for DNA precipitation. Again, we will centrifuge tubes for 5-10 minutes at the highest speed at room temperature and resuspend pellet in 0.4 ml in 1X TE Buffer. To degrade RNA, 3µl RNaseA (Stock 10 mg/ml) will be added, mix and incubate for 5 min at 37°C to remove RNA contamination. After that add 10 µl of 4M Ammonium acetate and 1ml of 100% ethanol mix by inversion and incubate at -20 ° C for 1 hour. Finally, centrifuge tube at room temperature for 10-15 min at 14000 RPM and air-dry pellet. Resuspend DNA pellet in 20µl TE buffer. Store at -20°C.

3.3.9: Checking in an upright microscope for screening

To check whether our desired strain is showing fluorescence signal, small amount of colony will, be taken from replica plate and resuspend in 20µl of SD media. The slides & coverslips will be cleaned with Colin and air-dried. The cell suspension will be put on on t h e slide and the coverslip placed from the top on this suspension. We will seal the coverslips with transparent nail polish and put a drop of immersion oil on the coverslip and slide was placed on the microscope stage for observation. Cells were focused in the bright field & then fluorescence was checked by selecting an appropriate fluorescent filter.

3.3.10: Manipulating Yeast Genome

Gene targeting by homologous recombination is one of the most powerful and important techniques available for studies in yeast. A gene at its normal chromosomal location can be removed or replaced with an allele created in vitro, such that the only genetic difference between the initial strain and the final strain is that particular allele. Therefore, phenotypes conferred by null mutations or any other types of mutations can be analyzed. Genes can also be modified to be fused to the coding sequence for fluorescent proteins, such as green fluorescent protein (GFP). Because the epitope tag or fusion is made in the genomic context, the tagged gene is subject to native regulation. The properties of a strain containing the epitope tag or fusion can be compared to an isogenic wild-type strain that lacks the tag to study gene function, localization and regulation.

3.3.10.1: Gene deletion strategy[24]

Principle

Deletion of an entire open-reading frame (ORF) of a gene deletion creates a null mutation, allowing for the analysis of loss-of-function phenotypes. To generate a deletion, the gene sequence from start to stop codon is removed and is generally replaced with a selectable marker (Kanmax)

The vectors used for gene deletion was pUG6 (KanMXmarker). The open reading frame of *P. pastoris* IMH1 was deleted as follows. 1-kb sequences flanking the IMH1 coding sequence were amplified from genomic DNA using the primers IMH1NdeIFw and IMH1SalIRv (upstream) or IMH1XhoIFw and IMH1HpaIRv (downstream). The amplified fragments were digested with NdeI and SalI (for the upstream fragment) and XhoI and HpaI (for the downstream fragment). Upstream fragment was ligated with a pUC19Kanmax vector that had

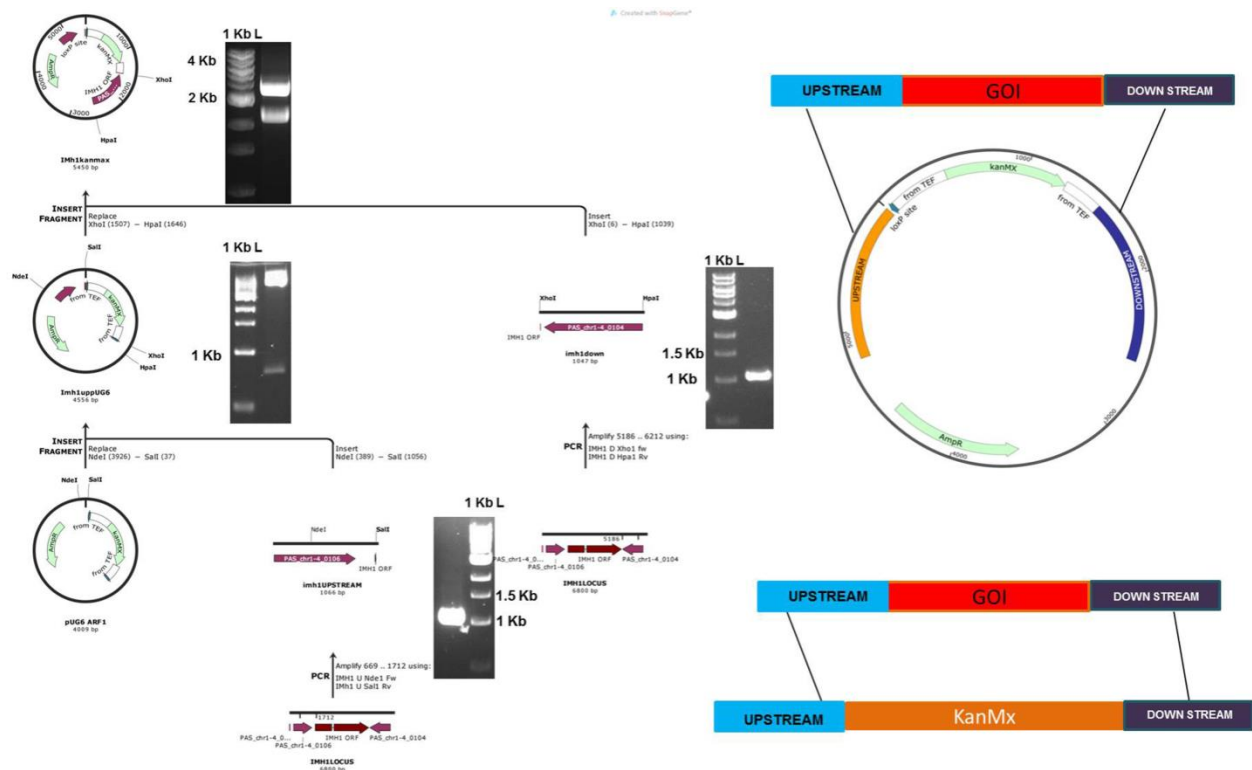


Fig3.1 *Pichia pastoris* gene deletion strategy

been digested with NdeI and SalI. The resulting plasmid was cut with XhoI and HpaI to ligate downstream fragment that results in pUC19-*PpIMH1*:: Kanmax. Finally, a 3.2-kb NdeI-HpaI fragment was excised from this plasmid and transformed into PPY12 cells. G418 positive transformants were screened by PCR to confirm that IMH1 had been deleted.

3.3.11: Yeast Live Cell Imaging

For Yeast cell imaging: ConcanavalinA was dissolved in distilled water to the concentration of 2mg/ml&100µl aliquots were made & stored at -20°C

Method-

In case of live cell imaging first, clean the glass bottom plate with Colin. After that treat the glass bottom plate with a 200µl aliquot of concanavalin-A for 15 minutes. Concanavalin-A will be removed the using a pipette and rinse the plate with milli-Q water. The plate will be air dried then add 200µl log phase yeast culture (OD₆₀₀ 0.5-0.6) to Con-A coated glass surface and incubate for 12 minutes at room temperature. After 12 mins remove the culture and wash gently with SD media so as to remove all unattached cells and add 1.5 ml of SD media for imaging.

3.3.12: Electron microscopy of yeast [99]

The cells were grown in a 50-ml yeast culture to an OD₆₀₀ of about 0.5. Once the cell reaches the 0.5OD filter the cells slowly on a 0.22 µM bottle-top filter down to a volume of about 5 ml. After that add 40 ml of ice-cold 50 mM KPi (pH 6.8), 1 mM MgCl₂, 2% glutaraldehyde and the fix it for 1 hr. on ice. The fixed cells will be Spin for 3 min at

3000 rpm at 4°. The pellet will be resuspended by vortexing in 25 ml ice-cold 50 mM KPi (pH 6.8). The same step will be repeated twice more, for a total of three washes. After completion of last wash resuspend the pellet in 1 ml 50 mM KPi (pH 6.8) and transfer the cell mixture to an Eppendorf tube. The remaining steps until resin polymerization are all done at room temperature. The cells will be resuspended in 0.75 ml freshly prepared 4% KMnO₄ and mix end-over-end for 30 min. [Note: KMnO₄ takes a while to dissolve with vigorous vortexing. This solution is a potent oxidizing agent, so use caution: wear gloves and safety glasses, and dispose of the waste in the container of the caustic liquid.] Again spin the cells for 1 min at 5000 rpm and resuspend the cells in 0.75 ml H₂O. The same step will be repeated twice more and resuspend the cells in 0.75 ml 2% uranyl acetate. (Sterile filter the uranyl acetate solution and store it at room temperature in the dark. If a precipitate form, discard the solution and prepare it fresh.) Cells will be mix end-over-end for 1 hr and Wash four times with H₂O. Meanwhile, we will prepare normal spurrs resin according to the formula given in the kit instructions. It is convenient to mix the resin components in a disposable plastic beaker placed on a balance in the hood. Mixing can be done with a glass rod. The cells will be dehydrated in the following graded series of EtOH solutions. After each spin (1 min at 5000 rpm) and resuspension, mix the cells end-over-end for 5 min. Start with a fresh, unopened bottle of water-free EtOH. 50%, 70%, 80%, 85%, 90%, 95%,100%, 100%,100%, 100%. Place the rack with the capsules in a vacuum desiccator, and degas for 15 min. After washing place the rack on a block of Styrofoam in an accurate temperature-controlled oven set at 68°C and allow the resin to polymerize for 36-48 hrs. The samples are now ready for sectioning and staining with lead citrate. Ultrathin sections were cut on ultra-microtome (Leica UC7, Germany) and collected on copper grids. Finally, sections contrasted with uranyl acetate and

lead citrate and micrographs were taken on Jeol 1400 plus Transmission Electron Microscopy (Japan) at 120 KeV to capture images in bright field mode.

3.4: Statistical tests

For every experiment, datasets are incorporated in Graph Pad Prism 6 software. Datasets are first checked for normal distribution by column statistics. If the distribution of the datasets were found to be not normal, then we performed the non-parametric test, which is a Mann-Whitney test. (In all mammalian results, mostly we performed Mann-Whitney Tests since the datasets were found to have a not normal distribution). Thus, significance tests were performed. If the distribution of the datasets were found to be normal, then we performed the unpaired student t-test. Graphs were plotted in column type mean with standard error mean or with range.

3.5: Protein expression and purification protocol [120, 121]

3.5.1: Cloning, expression, and purification of PpImh1

Full length PpImh1 was amplified using primers, PpImh1NdeIFw and PpImh1NotIRv. The amplified fragment was cloned in pET28a between NdeI and NotI sites. The resultant plasmid was then transformed into Rosetta2DE3 strain for expression. Transformed cells were grown in LB media containing Kanamycin (50ug/mL) and Chloramphenicol (34ug/mL). When the culture OD600 reached 0.6, it was induced with 0.4mM IPTG and grown overnight at 22°C, 180 rpm. Pellet from two-litre culture was re-suspended in 30mL of Buffer A (10mM HEPES, 300mM NaCl, 5% Glycerol, 0.1% Triton X-100, pH 8.5) and sonicated 6 times (60% amplitude, 1minute, 50% pulse) till clear suspension was obtained. This suspension was centrifuged at 14,000 rpm for 40 mins and the supernatant was allowed to bind the Ni-NTA beads (4mL, pre-equilibrated with buffer A) for 1 hour followed by washing with ten-bed volumes of wash buffer (10mM Imidazole

+ Buffer A). The bound protein was eluted (3mL) using elution buffer (200mM Imidazole + Buffer A). Elution fractions from affinity purification were loaded on 8% SDS Gel. The affinity eluted fraction was then concentrated to 1mL using 30kDa cutoff centricon (Amicon Ultra-15 Centrifugal Filter Units) and injected into the Gel filtration column for obtaining pure protein fractions.

3.5.2: Biophysical studies of purified protein

3.5.2.1: Circular Dichroism Spectroscopy

The secondary structure of the purified PpImh1 protein was characterized using Jasco J-810 (Japan), Circular Dichroism (CD) polarimeter. Far-UV CD scan of protein (30uM PpImh1 in 2.5mM HEPES pH 8.5, 50mM NaCl buffer) was collected in the 200–240 nm wavelength range at 20°C.

3.5.2.2: Dynamic Light Scattering

Dynamic Light Scattering (DLS) was performed using 70µl of FPLC purified fraction. The hydrodynamic radius of PpImh1 protein was calculated using DynaProNanoStar, Wyatt Technology. Before the DLS experiment, all the samples were filtered with 0.45 µm filter.

3.5.2.3: Negative staining to visualize purified PpImh1 [122]

Purified native PpImh1 was diluted to 10µM using distilled water, adsorbed to a 400-mesh formvar-coated copper grid (Nisshin EM Co, Ltd., Tokyo, Japan) and placed in 1% uranyl acetate solution for 10s. After drying, the samples were observed using a transmission electron microscope (JEM- 1400Plus; JEOL Ltd., Tokyo, Japan) at an acceleration voltage of 120 kV

3.5.3: SDS PAGE and Western Blotting:

3.5.3.1: Protein Estimation

Protein estimation was done using Bradford's reagent as per manufacturer's protocol using BSA (1mg/ml stock)

We have to add 1ml (1:4 diluted) Bradford reagent to each reaction and incubate samples for 10 minutes at room temperature. The optical density of the samples was measured at 595nm along with blank and standard curve is plotted. We have used 5µl of lysate for determination of protein concentration with reference to standards.

3.5.3.2: SDS-PAGE[123]

SDS-PAGE enables to separate proteins on the basis of their size and charge.

30% Acrylamide solution: 29g Acrylamide and 1g Bis-acrylamide(USB) were dissolved in distilled water on a magnetic stirrer overnight (O/N) at room temperature; The volume was made up to 100 ml and filtered through 0.45 µm filter and stored in a dark bottle at 4°C.

6X sample loading buffer: 50mM Tris.Cl (pH 6.8), 10% glycerol, 2% SDS, 1% β- mercapto-ethanol (BME) 0.1 % bromophenol blue.

Electrophoresis buffer: 25mM Tris base, 250 mM Glycine (pH 8.3) and 0.1% SDS Method: The resolving gel of 10% and 18% was made according to the following table

Component	Volume	Volume for
H ₂ O	3.2 ml	1 ml
30% Acrylamide mix	2.67 ml	4.8 ml
1.5M Tris pH 8.8	2 ml	2 ml
10%SDS	80 µl	80 µl

10%APS	80 μ l	80 μ l
TEMED	8 μ l	8 μ l

Table 3.8 Reaction mixture of resolving gel of SDS PAGE

Component	Volume for 5ml (4%)
H ₂ O	3ml
30% Acrylamide mix	0.67 ml
1M Tris pH 6.8	1.25 ml
10% SDS	50 μ l
10% Ammonium persulphate	50 μ l
TEMED	5 μ l

Table 3.9 Reaction mixture of a stacking SDS-PAGE gel

3.5.3.3: Wet transfer of proteins on PVDF membrane

The wet transfer method is used to transfer proteins separated on SDS-PAGE onto PVDF membrane for further analysis by immunoblotting.

High Glycine transfer buffer: 0.1M Tris, 0.19M Glycine, 20% methanol, 0.04% SDS.

3.5.3.4: Western Blotting[124]

Western blotting is an analytical technique which detects the presence of native or denatured proteins which are first electro-transferred onto a membrane and are then detected using protein-specific antibody.

Tris-buffered saline (TBS): 150/500 mM NaCl, 20 mM Tris (pH 7.4); Tris-buffered saline with Tween20 (TBS-T): 1X TBS + 0.1 % Tween 20; Blocking agent: 5% or

3% BSA in 1X TBS;

The membrane was blocked with either 0.3% BSA in TBST (for β Tubulin) or in 0.5% BSA in TBST (for His-Tag antibody) at room temperature for 2-3 hour. incubated with primary antibody (diluted in 1% BSA, TBST) for 1 hour [for β Tubulin (1:1000 dilution)] at room temperature or for overnight [for His-tag(1:5000 dilutions)] in the slow rocker. The membrane was washed 3 times in TBST for 10 minutes each in the high-speed rocker. The membrane was incubated with secondary antibody anti-mouse HRP (horseradish peroxidase) of 1:5000 dilution in 0.5% BSA for 1 hr at room temperature and give 3 washes in TBST for 10 minutes each in the high-speed rocker. The signal was detected by enhanced chemiluminescence (ECL+), by incubating the blot with a detection reagent for 5 min, followed by exposure to X-ray film and development.

3.6: Yeast Two-hybrid interaction assays[125]

Protein-protein interactions were tested using the yeast two-hybrid system. Interactions were tested between the proteins fused to the Gal4 DNA-binding domain and the Gal4 activation domain. *PpImh1* (full length), *PpImh1* (1-300), *PpImh1* (400-765) and *PpImh1* (725-1124) were PCR amplified from *P. pastoris* genomic DNA, with XmaI & SalI as the restriction sites. The digested amplified fragments were inserted into pGBDU (“bait”) and pGAD(“prey”) vectors digested with the same restriction enzymes. Plasmids were transformed into *S. cerevisiae* strain PJ694A using lithium acetate method (Gietz & Woods, 2002). Transformants were selected on SD Leu-Ura plates. Interactions were tested by plating the transformants on SD-Leu-Ura-His plates.

4. Identification and characterization of GRIP domain Golgin *PpImh1* from *Pichia pastoris*

4.1: Introduction

The Golgi apparatus, chiefly known to play an important role in the secretory pathway is universally present in all eukaryotic system [4]. Endoplasmic Reticulum(ER), serves as the primary site for protein synthesis, followed by subsequent folding and packaging into transport vesicles which are then delivered to Golgi [123]. There are many types of vesicles that participate in the secretory pathways. The cargo proteins that are to be transported via the anterograde pathway are usually carried by COPII vesicles or clathrin-coated vesicles. On the other hand, few ER resident proteins which are to be brought back to the ER in the retrograde pathway are carried by COPI vesicles [124]. A class of proteins called ‘Golgins’, are reported to mediate the upstream ‘tethering’ of any incoming vesicle to Golgi, before their fusion with the Golgi membrane, to form initial contacts [125]. Typically, Golgins are large alpha-helical coiled coil domain containing proteins that present at different Golgi locations. Golgins like GM130, p115, and GMAP-210 localize to the cis-Golgi, the GRIP domain Golgins (Golgin-97, Golgin-245, GCC88, and GCC185) localize to the trans-Golgi, and the third class of Golgins like TMF, CASP, Golgin-84, and Giantin are on Golgi rims [126]. Such specific localization of specific Golgins helps to capture the specific class of vesicles. For example, different ER born vesicles are usually captured by GM130, p115, and GMAP-210, Intra Golgi vesicles are captured by TMF, CASP, and Golgin-84, and vesicles from endosomes are captured by Golgin-97, Golgin-245, GCC88, and GCC185 [77].

The last class, previously mentioned, that captures the vesicles coming from endosomes, is a family of ‘Golgins’ that are targeted to the trans-Golgi by their C-terminal GRIP domains [99, 100]. Four such GRIP domain Golgins have been reported, in mammalian cells namely: Golgin97, Golgin245, GCC185, and GCC88. GRIP domain sequences have been identified in mammals, flies, plants, yeast (Imh1) and parasites [75]. The GRIP domain functions majorly as a TGN

targeting signal. TGN Golgins contain a high percentage (75–85%) of α -helical coiled coils. Golgins, such as GCC185 and Golgin97 form parallel homodimer. Recent studies using Atomic Force Microscopy suggested that GCC185 N terminus end forms a splayed end or Y shaped structure, which has an affinity for vesicle coming from the endosomes [127].

Pichia pastoris, a type of budding yeast happens to share structural and molecular similarities in secretory pathways to that of mammalian systems. Unlike *Saccharomyces cerevisiae*, *Pichia* is well-known for its highly efficient extracellular protein secretion, while displaying a stacked Golgi apparatus [73]. Moreover, most of the powerful yeast genetic manipulation tools are well established in *Pichia*. For all the above advantageous reasons, we decided to study the functional role of ‘Golgins’ in *Pichia pastoris*.

In the present study, we have identified and characterized the GRIP domain Golgin of *Pichia pastoris*, *PpImh1*. We have demonstrated that *PpImh1* contains the conserved GRIP domain. Biophysical studies & electron microscopy results suggest that *PpImh1* forms a parallel homodimer and a ‘Y’ shaped structure.

4. 2: Results

4.2.1: Identification and characterization of GRIP domain of *PpImh1*

The GRIP domain, whether expressed in mammalian cells or in budding yeast *S. cerevisiae*, always localizes to the Golgi. Also, overexpression of GRIP domain saturates the binding sites of endogenous GRIP domain proteins on the Golgi. These data suggest that the GRIP domain helps the Golgin to localize to Golgi. *S. cerevisiae* encodes a single GRIP domain containing protein, Imh1 which localizes to the Golgi [99, 100]. With sequence alignment studies of *Pichia pastoris* using PSI-BLAST, we identified the single GRIP domain containing protein in *Pichia pastoris*,

PpImh1. We compared the sequence of C terminal domain of different GRIP domain containing proteins (Human GCC185, HumanGCC88, Human Golgin97, Human Golgin245, *S. cerevisiae* Imh1 and *Pichia pastoris* Imh1) using PSI-BLAST (Fig 4.1A).

To examine whether *PpImh1* GRIP domain is capable of localizing to the Golgi, we tagged the GRIP domain with mGFP and expressed it in *Pichia pastoris* cells. We found that *PpImh1* forms a punctate pattern which mostly corresponds to the Golgi (Fig4.1B). When co-expressed along-with Sec7-DsRed, a trans-Golgi marker protein, mGFP tagged PpImh1 GRIP domain co-localized with Sec7-DsRed (Fig 4.1C).

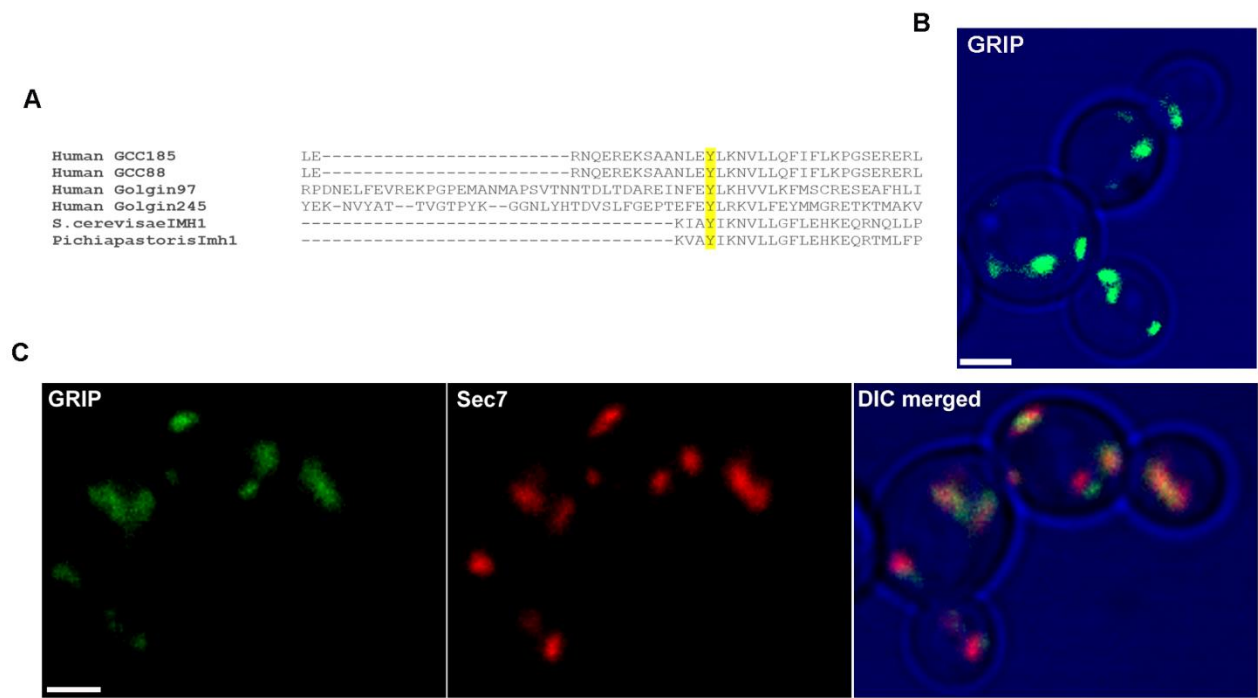


Figure 4.1 GRIP domain of *PpImh1* is important for Golgi targeting

(A) Alignment of the carboxy-terminal portions of the indicated proteins. C terminal domain of Golgins was aligned using PSI-BLAST Tool. (Human GCC185, Human GCC88, Human Golgin97, Human Golgin 245, *S. cerevisiae* Imh1, *Pichia pastoris* Imh1). The tyrosine conserved Residues that are identical (yellow) sequences are shaded. (B) Fluorescence confocal image of live Wild-type *Pichia pastoris* cells expressing GFP fused to the GRIP domain of the *PpImh1* protein. The fusions contained the carboxy-terminal (1030-

1125) residues of *PpImh1*. Scale bar 1 μ m. (C) Green fluorescent protein (GFP)-*PpImh1p*-GRIP fusion (encoding amino acids 1030-1125) was expressed in wild-type strains PPY12 expressing Sec7-6XDsRed which localize to Golgi compartments. Colocalization can be observed as yellow in the panels. Scale bar 1 μ m.

These results display agreement with previous studies that showed that GRIP domain containing protein localizes to the trans-Golgi/TGN. The conserved tyrosine residue of GRIP domain is essential for Golgi targeting (140). Our studies confirm, mutation of this conserved tyrosine aborts the Golgi targeting of *PpImh1* (Fig 4.2).

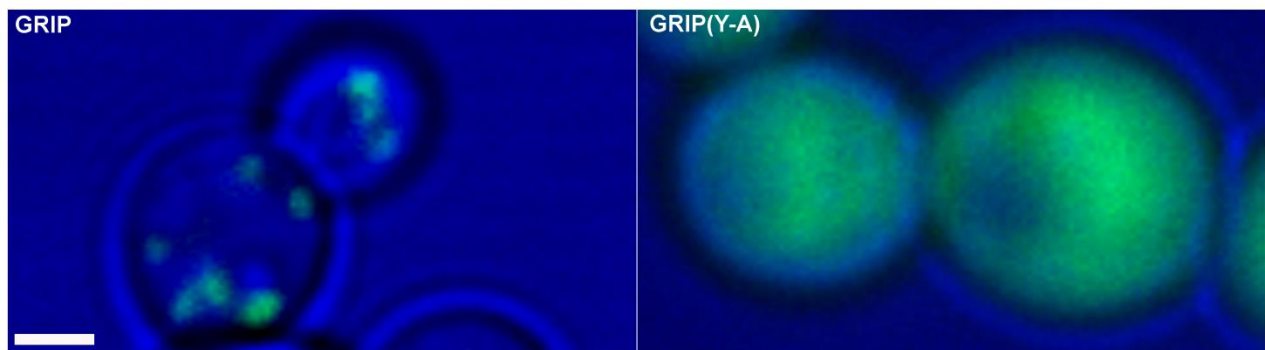


Figure 4.2 The Conserved residue of GRIP domain is essential for Golgi targeting

The Conserved residue of GRIP domain is essential for Golgi targeting. GRIP domain conserved residue tyrosine was replaced by alanine. Live cell imaging showed that GRIP domain protein doesn't localize to Golgi. Scale Bar 1 μ m.

It has been reported that Arl1 binds to the GRIP domain Golgins and recruits them to the TGN [128]. In order to check its role in the recruitment of *PpImh1* to the Golgi, we deleted *ARL1* from a *Pichia pastoris* strain expressing GFP-*PpImh1*. In an *arl1* Δ strain, GFP-*PpImh1* fails to localize to the Golgi and thus appears cytosolic (Fig 5.7).

4.2.2: Protein Expression, Purification and biochemical analysis of purified His6-tagged *PpImh1*

To understand the structural properties of *PpImh1*, we overexpressed His-tagged *PpImh1* in Rosetta2DE3 cells and purified it using nickel affinity chromatography (Fig 4.3A) and gel filtration (Fig4.3B). We confirmed the purified protein using mass spectrometry analysis (Table4.1) and western blot against His-tagged *PpImh1* (Fig4.3C). We also performed CD spectroscopy of purified recombinant His-tagged *PpImh1* to determine the nature of the secondary structure. The data plotted as ellipticity versus wavelength is shown in Figure 4.3D. The CD spectrum of Golgin *PpImh1* shows double minima at approximately 208 and 220 nm, which is a characteristic of the α -helical structure. This result was confirmed by non-linear least-squares analysis using the program K2D2, which yielded a best-fit to 85% α -helical structure.

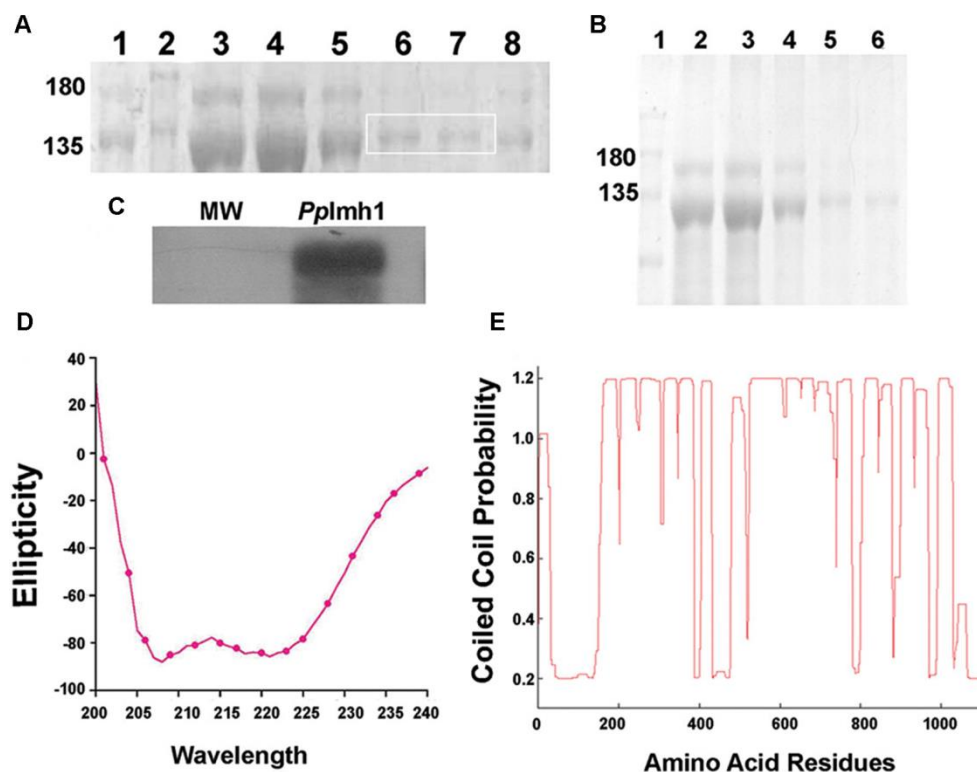


Figure 4.3 Biophysical Characterization of *PpImh1*

(A) Purified His6-tagged Imh1 analyzed by SDS/PAGE (8%) and stained with Coomassie Blue. Fractions obtained after affinity purification were loaded; Gel A 1 1-Beads after washing, 2-Protein Marker, 3 to 8-Affinity Elution fraction. Marked protein band at 130 kDa was excised from the gel and processed for In-Gel digestion and given for Mass spectrometry (Q-TOF 5600 Triple TOF AbSciex). The raw data was processed using Protein Pilot 4.5 and was aligned to FASTA of *P.pastoris* (Taxon ID- 4922, as on 21st June 2017) from UniProt. (B) The elution fraction was concentrated to 1ml and resolved for further purity using Sephadex 200 FPLC column; Gel 1-Concentrated affinity fraction, 2- Protein Marker, 3 to 6- FPLC elution. (C) Immunoblot using Anti-His antibody against His tagged *PpImh1*. (D) CD spectrum of purified His6-tagged *PpImh1* (30μM). Ellipticity is plotted as a function of wavelength (nm) for *PpImh1* (30μM)). The data are superimposed with the non-linear best-fit using the K2D2 program, yielding 85% α -helix, 1.24% β -strand. (E) Predicted probability of each amino acid in the sequences of the *PpImh1* to form coiled-coil using structure secondary structure prediction tool Coils.

Protein Group 1 Vesicular transport protein OS= Komagataella phaffii

(Strain ATCC 76273/CBS 7435 /CECT11047/NRRL Y-11430/Wegner 21-1) GN=IMH1 PE=4 SV=1

N	Unused	Total	%COV	Accession#	Name	Species	Peptides (95%)
1	290.64	290.64	91.8	trIF2QN571 F2QN57_KOMPC	Vesicular transport protein OS= Komagataella phaffii (strain ATCC 76273/CBS 7435 /CECT11047/NRRL Y-11430/Wegner 21-1) GN=IMH1 PE=4 SV=1	KOMPC	526

Protein sequence coverage - Vesicular transport protein OS=

Komagataella phaffii (strain ATCC 76273/CBS 7435 /CECT11047/NRRL Y-11430/Wegner 21-1) GN=IMH1 PE=4 SV=1

Table 4.1 Mass spectrometry analysis

To further understand the nature of the alpha-helical structure, coils analysis [129] showed the probability of coiled-coil formation (Fig 4.3E). This prediction asserts that *PpImh1* has a domain that comprises a coiled-coil structure.

4.2.3: *PpImh1* forms parallel homodimer

To determine whether *PpImh1* forms oligomer or not, we performed yeast two-hybrid assay in which full-length *PpImh1* was cloned into bait and prey vector. The two-hybrid assay strain PJ694A was transformed with bait and prey constructs and subsequently grown on the selective medium as described in the methods section. Interactions between *PpImh1* proteins were monitored by the ability of transformed yeast cells to grow in a medium lacking histidine. A strong

interaction was observed between the full-length *PpImh1* constructs, *PpImh1*-pGAD and *PpImh1*-pGBDU, confirming that *PpImh1* forms oligomer (fig 4.4A).

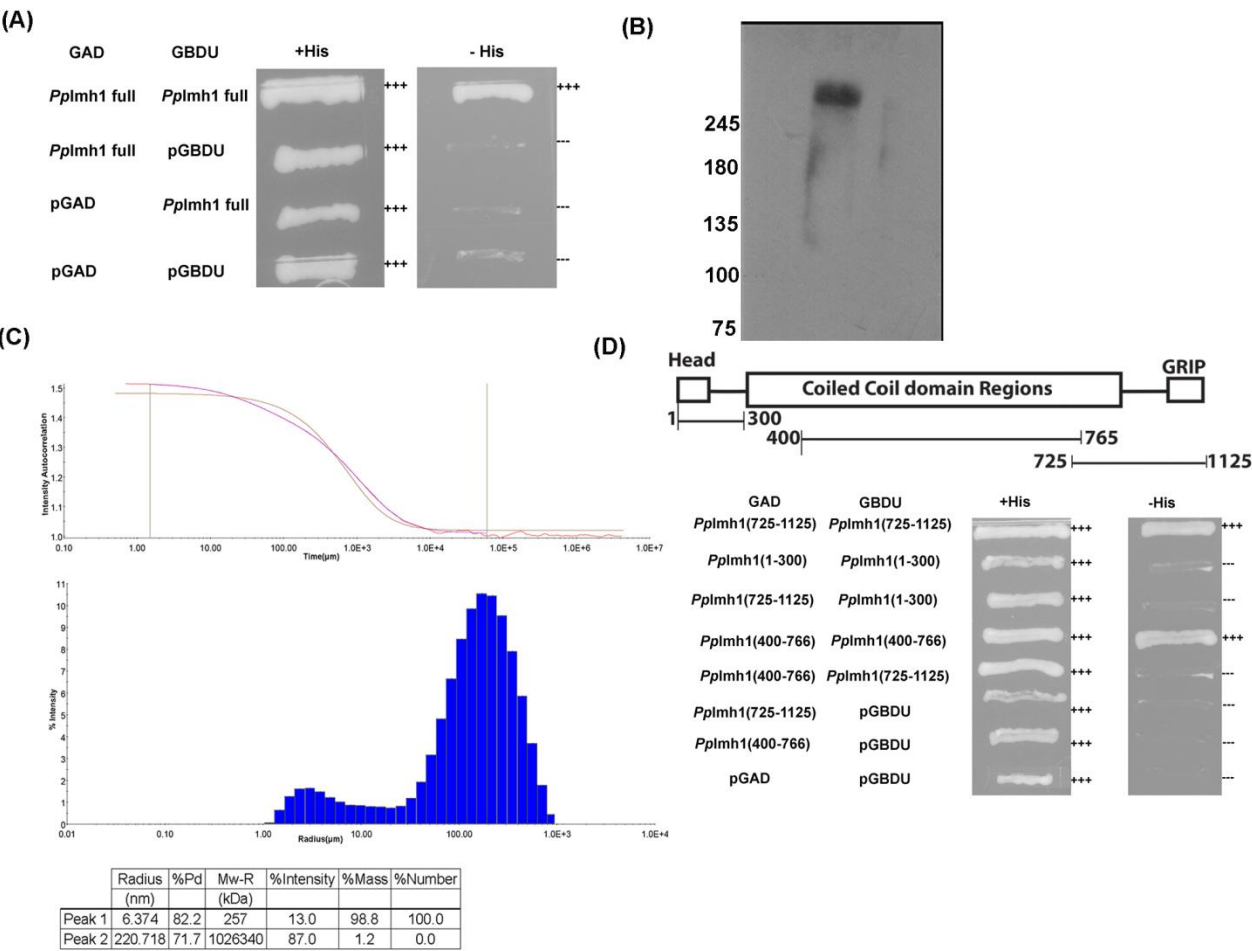


Figure 4.4 *PpImh1* forms parallel dimer

(A) To test whether *PpImh1* form dimer or monomer we used Yeast two-hybrid analysis. The “prey” vector encoded the full length of *PpImh1*, and the “bait” vector encoded the full-length *PpImh1* protein. Both vectors were transformed into *S. cerevisiae* tester strain. Growth on plates lacking histidine reflects an interaction. (B) Oligomeric status of *PpImh1*. Purified His tagged *PpImh1* was analyzed on Native PAGE, then transfer to nitrocellulose membrane for immunoblot using Anti His antibody. (C) DLS Data 1. Correlation function plot between intensity and time(us) 2. Intensity distribution plot between Percent Intensity and Radius(um). Plot showing multimodal polydisperse population with around 99% mass contributed by molecules estimated to have molecular weight ~260kDa. (D) To test whether *PpImh1* form parallel dimer or antiparallel dimer, we cloned *PpImh1* (1-300), *PpImh1* (400-765), *PpImh1* (725-1125)

fragments in bait and prey vector. Both the constructs were transformed into *S. cerevisiae* tester strain. Growth on plates lacking histidine reflects an interaction.

To investigate the oligomeric nature further, we analyzed the behavior of *PpImh1* using DLS. The correlation graph and fast decay time suggest that the mean radius of the particles is within the expected range for proteins which is usually between 1 to 100 μ s. It showed the estimated molecular weight of the *PpImh1* dimer to be around 260kDa, which is precisely double of the molecular weight of its monomeric form i.e., 130kDa (Fig 4.4C). We observed that polydispersity is high, which can be attributed to the multiple oligomeric states present in the protein sample. Such native dimeric state was also confirmed through native gel followed by western blot using an antibody against the His-tagged *PpImh1*, where it showed band around 260kDa (Fig 4.4B).

According to the results obtained through the above experiments, it can be concluded that *PpImh1* probably forms a homodimer. However, a dimer may be orientated in a parallel (head-to-head) or anti-parallel (head-to-tail) fashion. To distinguish between these possibilities, we utilized the yeast two-hybrid assay to analyze interactions between various N- and C-terminal truncated constructs. Strong self-interaction was observed between the coiled-coil regions and C-terminal [GAD-*PpImh1* (725-1124) with GBDU-*PpImh1* (725-1124) and GAD-*PpImh1* (400-765) & GBDU-*PpImh1* (400-765) (Fig 4.4D). However, no self-interaction was detected between N-terminal (1-300) regions. Neither any interaction was detected between C-terminal (725-1124) and N-terminal region (1-300). This result indicates, *PpImh1* probably dimerizes through the self-interactive central coiled-coil regions and C-terminal regions. However, the N-terminal domain does not mediate such dimerization either through self-interaction or interaction with the C-terminal region. All of these results together suggest that *PpImh1* forms parallel homodimers.

4.2.4: Electron microscopy data suggest that *PpImh1* forms parallel homodimer with splayed N terminus

To further elucidate the nature of the dimer, we visualized purified *PpImh1* under transmission electron microscope. We observed that the *PpImh1* particles exhibit two profiles: either a ‘Y’ shaped or a clustered form (Fig4.5A). Majority of individual *PpImh1* particles seemed to form a ‘Y’ shaped structure which appeared at a significant frequency of 24 % (Table 4.2). The clustered or network-like profiles may represent assemblies of the ‘Y’ shaped forms of *PpImh1* or other differently folded forms of *PpImh1*. Some particles had no head or short head which may be because of proteolysis or restricted conformation. The most biologically accepted form as per the function of Golgins would be a ‘Y’ shaped conformation as it favours the capturing of the vesicle by the N terminal splayed end. Yeast two-hybrid results indicate that the N-terminal region of *PpImh1* is monomeric and that the C-terminal region is dimeric (Fig. 4.5C).

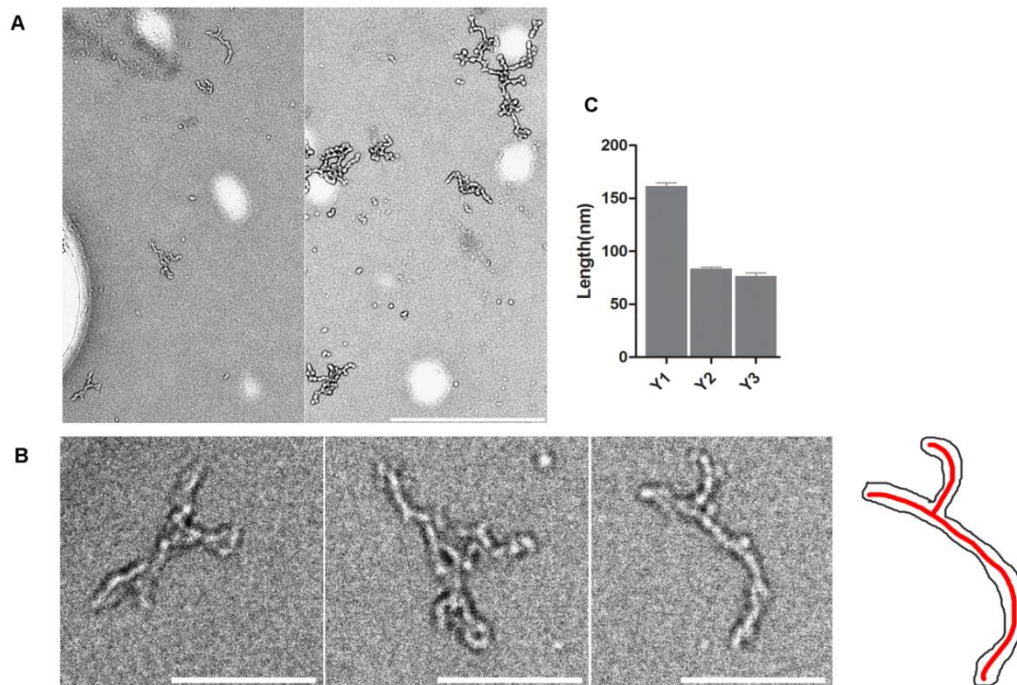


Figure 4.5 Negative-stain EM of purified *PpImh1*

(A) Purified *PpImh1* & control buffer sample was absorbed on the grid and stained with 1% uranyl acetate and observed using TEM (JEOL 1400 plus 120kV, USA) transmission electron microscopy at magnification 5000X. Representative images are shown. Y- Y-shaped profile is marked. Scale bar - 500nm.(B) Magnified representative image of Y-shaped profiles of *PpImh1* and Outline of predicted *PpImh1* structure. Scale Bar- 100nm (C) Measurement of length of each branch of Y shaped conformation of *PpImh1* using iTEM analysis software. The branch lengths were classified as Y1 (rod) & branches Y2 & Y3. The values are statically significant ($P < 0.0001$, Paired t-test).

Profile	Number	Ratio (%)
Y shaped	48	24
Cluster	154	76
Total	200	100

Table 4.2- Quantification of *PpImh1* profiles by electron microscopy

It is most probable that the ‘Y’ Shaped profile represents a parallel dimer with two branched monomeric N-terminal regions and a single dimeric C-terminal region. In the ‘Y’ shaped structure, the stalk represents the self-interacting coiled-coil domain. The splayed end represents N terminal domain which does not appear to self-interact or form dimer. The length of each branch of the ‘Y’ shaped profile was measured. The branch lengths were categorized as lower rods (Y1) and upper arms (Y2 and Y3) (Fig4.5B). The average lengths were 76, 86 and 161nm for Y3, Y2, and Y1 respectively. The difference in length between Y1 & Y2 or Y1&Y3 was significant; however, there was no significant length difference between the branches Y2&Y3, suggesting that one branch is significantly longer than the other two branches (Fig4.5C). It is to be noted that the combined size of self-interacting central and C-terminal domains of *PpImh1* is almost double to that for its non-interacting N-terminal domains. This quantification strengthens the fact that the ‘Y’ shaped structure represents a dimer of *PpImh1*. Lack of splayed structure on both sides of the

dimer further emphasizes the fact that *PpImh1* indeed forms parallel dimers, but not the anti-parallel dimers.

4.3: Discussion

We have identified the sole GRIP domain Golgin of *Pichia pastoris*. Arl1 binds to the GRIP domain and recruits Golgins to TGN. A conserved tyrosine residue of GRIP domain is essential for Arl1 interaction and subsequent Golgi targeting [99, 128]. In the case of mammalian cells, mutation of this tyrosine residue to alanine affects the localization of Golgin 97 & Golgin 245 [98]. *PpImh1* fails to localize to the Golgi when this corresponding tyrosine of its GRIP domain is mutated to alanine. This result indicates that sequence-specific interaction of GRIP domain is essential for Golgi targeting of GRIP domain protein.

Apart from the GRIP domain, TGN Golgins have a long coiled-coil domain and an N terminal head domain. TGN Golgins capture the vesicles of recycling endosomes through the N terminal head domain [130]. Their long coiled-coil domain possibly functions as a spacer to extend the vesicle capture domain [81, 127]. We have demonstrated that *PpImh1* also contains higher grade alpha-helical coiled coil domain which possibly performs the similar function.

Mammalian TGN Golgins such as GCC185, Golgin97 have been shown to form a parallel homodimer. Moreover, GCC185 also has been shown to form the 'Y' shaped dimeric structure with its N terminus forming a splayed end, which has an affinity to bind vesicles [127]. No such study has been reported yet on the capabilities of yeast Golgins to form such structures. Our yeast two-hybrid analysis suggests that *PpImh1* possibly forms a parallel homodimer. In addition, EM data confirms that *PpImh1* displays such 'Y' shaped structures. Golgin97, the mammalian

homolog of PpImh1 captures the vesicles which shuttle between endosomes and TGN. However, whether PpImh1 exhibits the same function requires further investigation.

**5. Golgin *PpImh1* mediate cisternal
stacking of Golgi apparatus in budding
yeast *Pichia pastoris***

5.1: Introduction

Intracellular protein trafficking is a coordinated process in the eukaryotic cell. Vesicles carry cargo proteins from the ER to compartments where modifications occur and deliver them to their final destinations [2]. The Golgi apparatus plays a central role in the processing, sorting, and secretion of various cargo molecules destined for various intracellular and extracellular destinations [3]. The Golgi apparatus basically consists of cisternae which are flat membrane sacs of discoid shape [134]. The Golgi cisternae display variable shape in different species: from dispersed cisternae in *S.cerevisiae* to stacked cisternal structure in *Pichia pastoris* and to laterally connected ribbon of cisternal stacks in metazoans, but the mechanisms that generate this organization have been not clear [4, 77]. The Golgi stacks can be converted to individual cisternae by protease treatment, suggesting that protein bridges hold cisternae together [22]. The Golgi apparatus undergoes disassembly and reassembly process during the cell cycle, which is regulated by phosphorylation of the GRASP proteins, suggesting GRASPs as a stacking factor [135]. Mammalian cells contain two GRASP protein GRASP65 and GRASP55 localized to early and medial Golgi cisternae respectively [136]. Single knockout of any of the GRASPs results in a minor effect on Golgi morphology. However, double depletion of GRASP55+GRASP65 disperses the Golgi ribbon structure in individual cisternae and tubulovesicular structures [27]. During the cell cycle, Golgi structure undergoes fragmentation when cells exit mitosis, GRASP proteins undergo dephosphorylation after Cdk1 inactivation, enabling GRASPs to oligomerize and Golgi stacks to reform. GRASPs are peripheral membrane proteins on the cytoplasmic face of the Golgi cisternae that form trans-oligomers through their N-terminal GRASP domain, and thereby function as the “biological adhesive” to stick adjacent cisternae together into a stack and to link Golgi stacks into

a ribbon, suggesting oligomerization as a mechanism of cisternal stacking [136]. These studies suggest GRASPs as a major cisternal stacking factor.

So, if GRASPs are considered as major cisternal stacking factors, their structural role should be conserved. In budding yeast *Pichia pastoris* deletion of GRASP homolog, GRH1 has no effect on Golgi stacking and this situation can be extended to plant cells where no GRASP homolog is identified [20, 24]. These studies suggest that in case of yeast and plants, where no of the GRASP homolog has been either identified or found to be necessary for Golgi stacking, an yet unidentified adhesive interaction of existing Golgi proteins could potentially mediate cisternal stacking.

A simple cisternal adhesion model has been proposed which suggests that adhesive energy that binds cisternae to each other at physiological equilibrium can be generated by many different combinations of Golgins+GRASPs or even in the absence of GRASPs. According to the report, efficient stacking occurs in the absence of GRASP65/55 when either Golgin is overexpressed [88]. This result suggests Golgins could be the alternative cisternal adhesion force. The Golgins are long coiled-coil domain proteins which are shown to be important for Golgi structure maintenance and vesicle tethering [137]. Knockdown of Golgin97, Golgin245, GCC185 shown to affect the Golgi structure, suggesting a role of Golgins in Golgi structure maintenance [85, 87, 138].

In our study, we have tested the role of GRIP domain Golgin PpImh1p in the Golgi structure using budding yeast *Pichia pastoris*. *Pichia pastoris* provides an excellent tool to study cisternal stacking where we can study the individual Golgi stack and adhesion between two individual Golgi cisternae.

5.2: Results

5.2.1: Assay system to monitor cisternal stacking in *Pichia Pastoris*

To study cisternal stacking, we have created an assay system in which early Golgi protein Vig4 is tagged with msGFP, and trans-Golgi protein Sec7 is tagged with 6XDsred. Live cells were imaged by fluorescence confocal microscopy. Golgi cisternae were visualized both with 2D projections and with 3D rendering for quantitative measurements. In wild-type cells, we observe that VIG-GFP and SEC7-6xDsRed.M1 forms elongated green and red signal representing early and late cisterna stacked in close proximity resulting in a ‘traffic light’ type of juxtaposed signal (Fig 5.1). The green and red signals are very close and almost located on the top of each other.

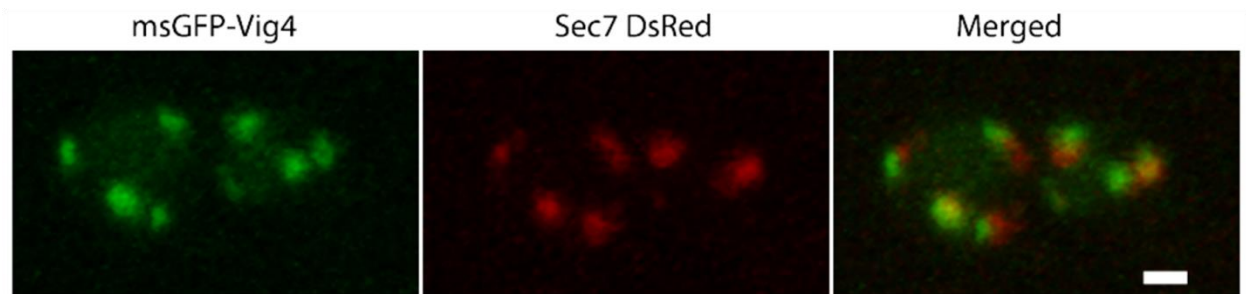


Figure 5.1 Two color *Pichia pastoris* strain (early Golgi msGFP-VIG4, Sec7-6xDsRed.M1)

Pichia pastoris Cells expressing msGFP-VIG4 and SEC7 DsRed.M1x6. Cells were grown in YPD media to log phase and imaged in Zeiss780 imaging system. Optical sections were collected every 200nm. Images were processed using ImageJ. The representative cell is shown. Scale bar: 1 μ m.

5.2.2: Deletion of Golgin *PpIMH1* in *Pichia pastoris* dual color strain results in a cisternal unstacking phenotype

We wanted to investigate the potential roles of GRIP domain containing Golgins in mediating cisternal stacking in budding yeast. In budding yeast *Pichia pastoris*, the only GRIP domain

containing Golgin is *PpImh1*[139]. So, we wanted to test whether the deletion of *PpImh1* has any effect on cisternal stacking or not.

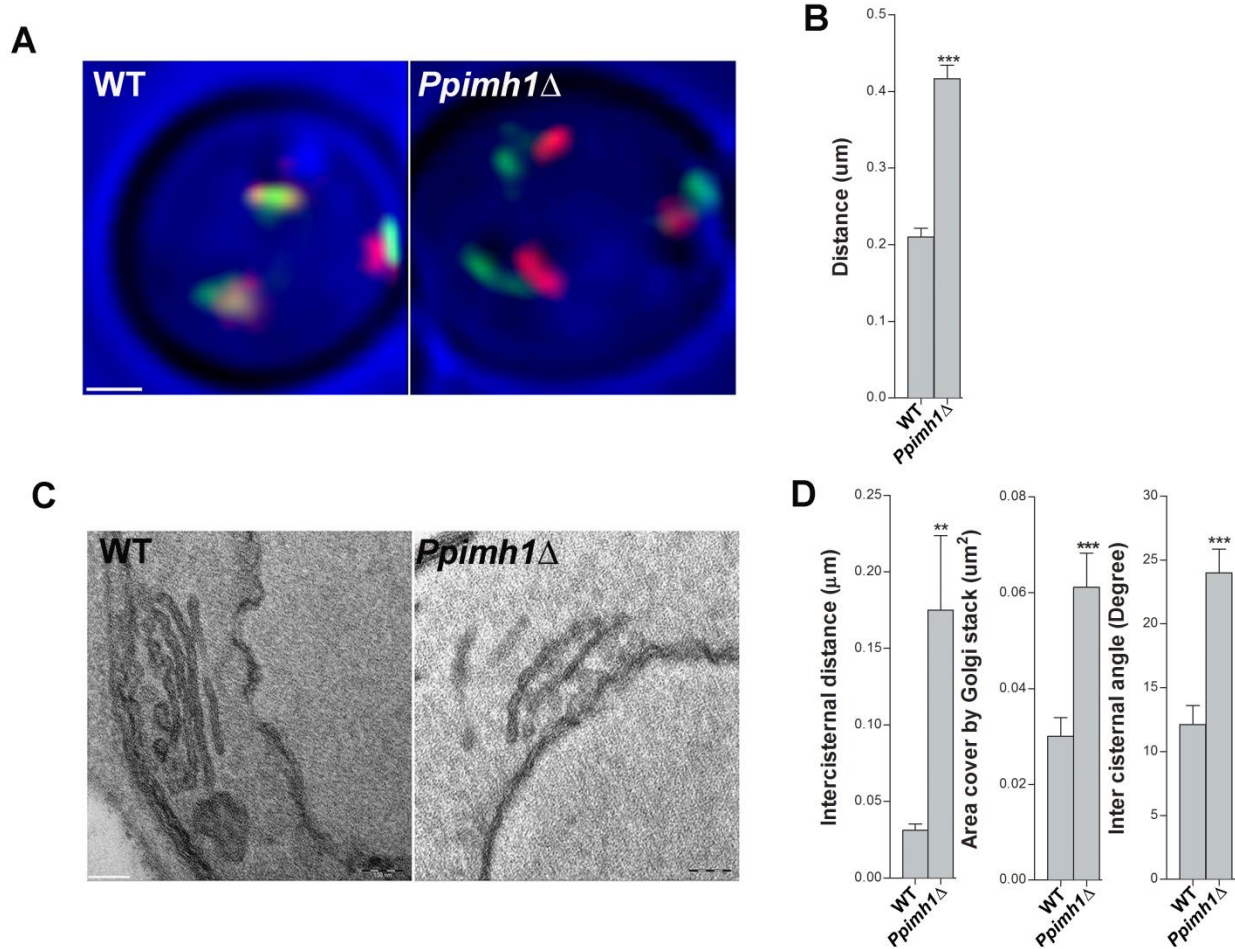


Figure 5.2 Inter-cisternal distance is significantly increased in the case of *Ppimh1*Δ cells.

(A) *PpIMH1* was deleted in *Pichia pastoris* Cells expressing msGFP-VIG4 and SEC7-DsRed.M1x6. Cells were grown in YPD media to log phase and imaged under a Zeiss LSM780 confocal microscope. Optical sections of 200nm thickness were collected for the entire volume of cells. Image hyper stack were deconvoluted using Huygens Pro and further filtered and Z-projected using ImageJ. Representative cells are shown. Scale bar: 1 μm. (B) The distance between the green and red spot was measured using Imarisx64 8.0.1 Biplane. To quantitate the inter-cisternal distance, images were opened in Imaris, the surface was filled using 3D rendering for a specific channel, then the individual surface was considered as a solid object, and center point was selected. By using pointer distance between one green and one red spot was measured. Values represent mean±SEM (60cells) student t-test ***P<0.0006. (C) To capture thin section electron micrograph of *Pichia pastoris* PPY12 wild-type and *Ppimh1*Δ strain, wild-type & *Ppimh1*Δ Cells were grown for log phase till 0.5 OD, concentrated using vacuum filter, fixed and resuspended in 0.75 ml 4%

KMnO₄ and mixed for one hr at room temperature. The cells were then washed and resuspended in 0.75 ml 2% uranyl acetate and mixed for one hr at room temperature. Finally, the cells were embedded in Spurr's resin; 50 ml of yeast culture yielded enough cells for three BEEM capsules. The resin was polymerized for two days at 68°C; sections were stained with uranyl acetate and viewed under an electron microscope (100 CXII; JEOL U.S.A. Inc.). The representative cells are shown; scale bar represents 100nm. (D) Quantitative data from thin section electrograph. Quantitative data from thin section electrograph were measured using iTEM software (i) Maximum inter-cisternal distance between two cisternae was measured by drawing the line between medial Golgi and TGN, (ii) Total area covered by entire Golgi stack, measured by drawing the entire Golgi stack area (iv) Angle between two cisternae, measured using drawing line on medial Golgi & TGN and angle between two lines were measured. Values represent mean±SEM (45 cells) student t-test ***P<0.0006.

In wild-type cells, we observe that Vig-GFP and Sec7-DsRed forms elongated green and red signal representing early and late cisterna stacked in close proximity. The green and red signals are very close and almost located on the top of each other. However, Golgin *PpImh1* depletion results in clear separation of these green and red signals allowing each cisterna to be visualized distinctly with no apparent overlap (Fig5.2A). This result suggests that *PpImh1* depletion causes a slight separation between Golgi cisternal stacks, which was confirmed by quantitative measurements from distance between the center of green and red spots through 3D rendering (Fig 5.2B).

To gain further insight of structural details, we resorted to electron microscopy of *PpImh1* deleted cells along with wild-type cells as a control. Electron microscopy data suggest that clearly there is an increase in inter-cisternal distance between medial and trans-Golgi in *PpImh1* depleted cells. Furthermore, it appears that TGN is positioned at an angle to the rest of the stack while one end in many cases is attached to the rest of the stack (Figure 5.2C). To quantitatively characterize this mutant phenotype, we have measured several parameters from the EM micrographs. We found that the inter-cisternal angle between TGN and medial Golgi was increased in *PpImh1* deletion strain as compared to the wild-type. Moreover, the total area covered by the entire Golgi stack was also

increased. These experiments indicate that *PpImh1* depletion affects cisternal stacking between medial and trans-Golgi. (Fig 5.2D)

5.2.3: WT Full-length*PpIMH1* could rescue the *Ppimh1*Δ deletion phenotype, but a version *PpImh1* lacking the coiled-coil domain fails to rescue such phenotype.

PpImh1 contains an N-terminal head domain, Golgi localizing C-terminal GRIP domain and long central coiled-coil domains. The long coiled-coil domains could potentially mediate dimerization of Golgin molecules residing on two different Golgi Cisterna and multiple such dimerized Golgin pairs can bring Golgi Cisternae together to form a stack. To test this hypothesis, we need to test whether the coiled-coil is essential for cisternal stacking or not. According to coiled-coil domain analysis (fig 5.3), the central region of *PpImh1* (150-1100) residues shows high predictability to form the coiled coil. Full-length *PpImh1* was fully competent to rescue the unstacking phenotype, but *PpImh1* (150-1070) Δ was not able to rescue the unstacking phenotype (Fig5.4A).

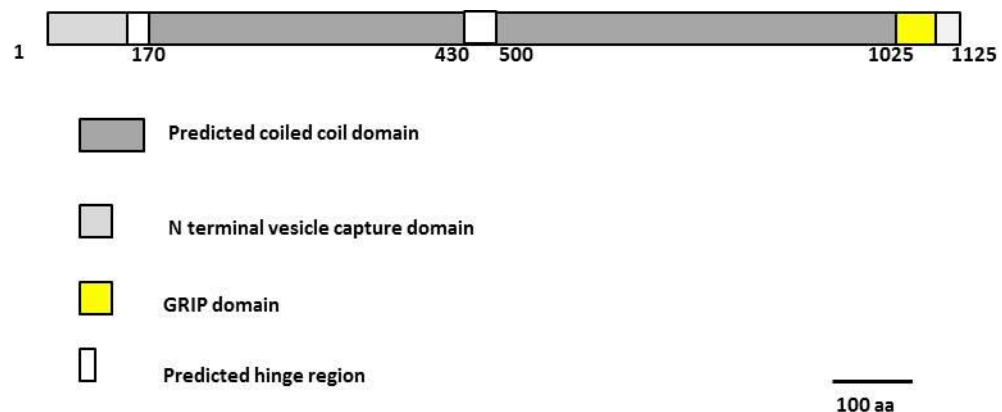


Figure 5.3 Schematic representation of *PpImh1* (Based on coiled-coil analysis)

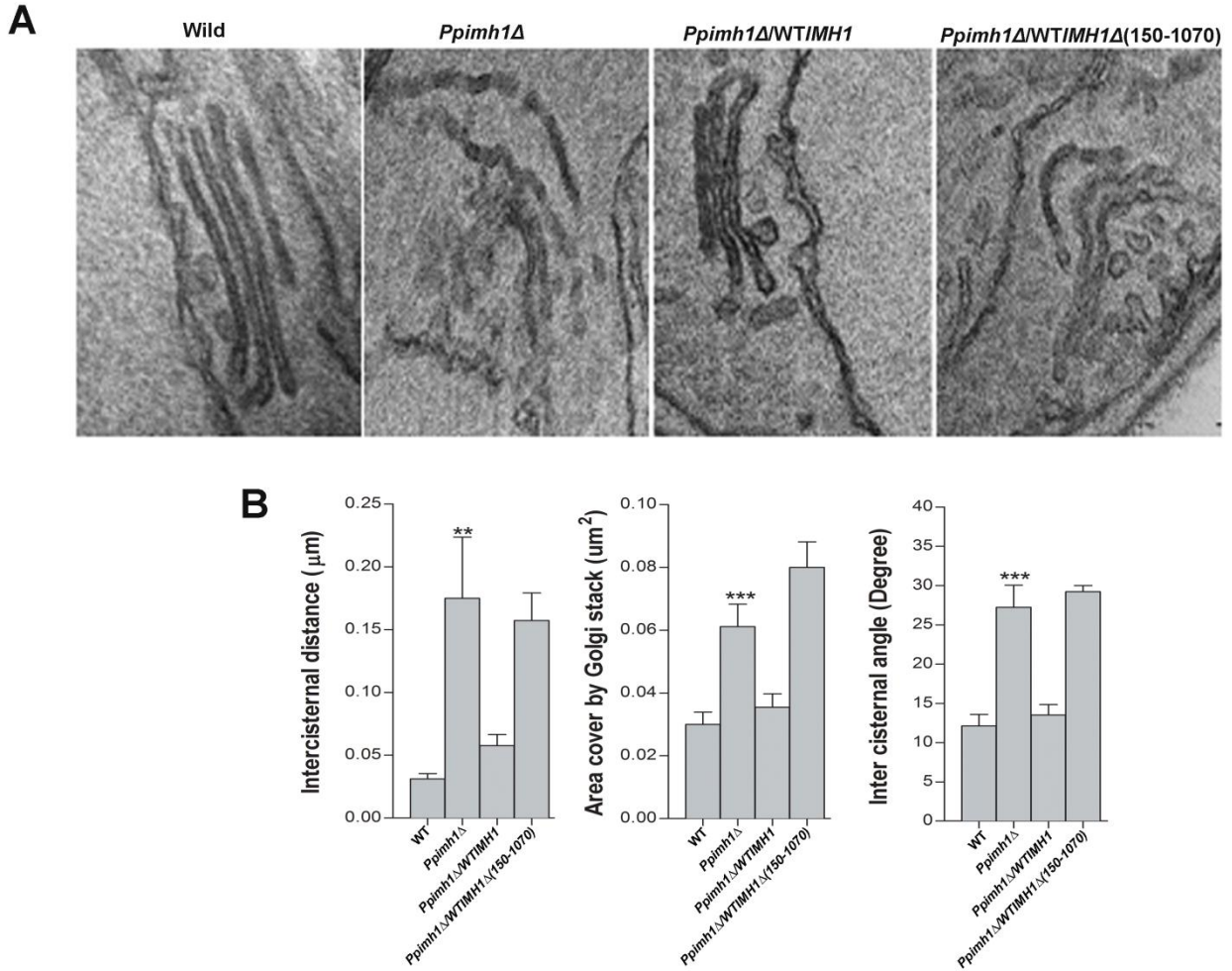


Figure 5.4 Full-length *PpIMH1* could rescue the *Ppimh1Δ* deletion phenotype

(A). Thin section electron micrograph of the *Ppimh1Δ* cells transformed with (i) Full-length *PpIMH1* (ii) *PpImh1Δ* (150-1070). The *Ppimh1Δ* strain was transformed with full-length *PpIMH1* and *PpImh1Δ* (150-1070) as a second copy. All the strains were grown until log phase then cells were concentrated, fixed and stained. Cells were embedded in Spurr's resin then sections were taken and observed under an electron microscope (100 CXII; JEOL U.S.A. Inc.) The representative cells are shown. Scale bar - 100nm. (B). Quantitative data from thin section electrograph were measured using iTEM analysis software (i) Maximum inter-cisternal distance between two cisternae, (ii) Area covered by the entire Golgi stack (iii) Angle between two cisternae. Values represent mean \pm SEM (45 cells) student t-test *** $P < 0.003$

We also found that the Inter-cisternal distance, area cover by the entire Golgi stack and inter-cisternal angle increase in the PPY12-*PpImh1* (150-1070) Δ rescue strain (Fig5.4B). These results

suggest that *PpImh1* (150-1070) domain, which has shown high probability to form coiled-coil domain is essential for cisternal stacking function of *PpImh1*.

5.2.4: Overexpression of *PpImh1*GRIP domain alone can cause unstacking phenotype while overexpression of only *PpImh1* Coiled-coil domain alone causes no such effect.

The GRIP domain of TGN Golgin acts as Golgi localizing signal. Expression of GRIP domain tagged with GFP in cells shown that it localizes to the TGN. Furthermore, it can act as a dominant negative mutant by competing with endogenous GRIP domain-containing proteins for binding to Arl1. If *PpImh1* is mediating the cisternal stacking through dimerization of coiled-coil regions, then it is conceivable that the overexpression of GRIP domains will saturate all the binding sites of *PpImh1*. Accordingly, such over-expression in *Pichia pastoris* cells may cause cisternal unstacking as dominant negative like phenotype as most of the endogenous *PpImh1* will not be localized to the Golgi. When we overexpressed GRIP domain under the methanol inducible AOX1 promoter, it resulted in cisternal unstacking phenotype (Fig 5.5A). We observed that GRIP domain overexpression results in an increase in inter-cisternal distance, the area cover by the entire Golgi stack and inter-cisternal angle (Fig 5.5B). However, similar overexpression of coiled-coil domain does not show any effect on cisternal stacking (Fig 5.5A, 5.5B).

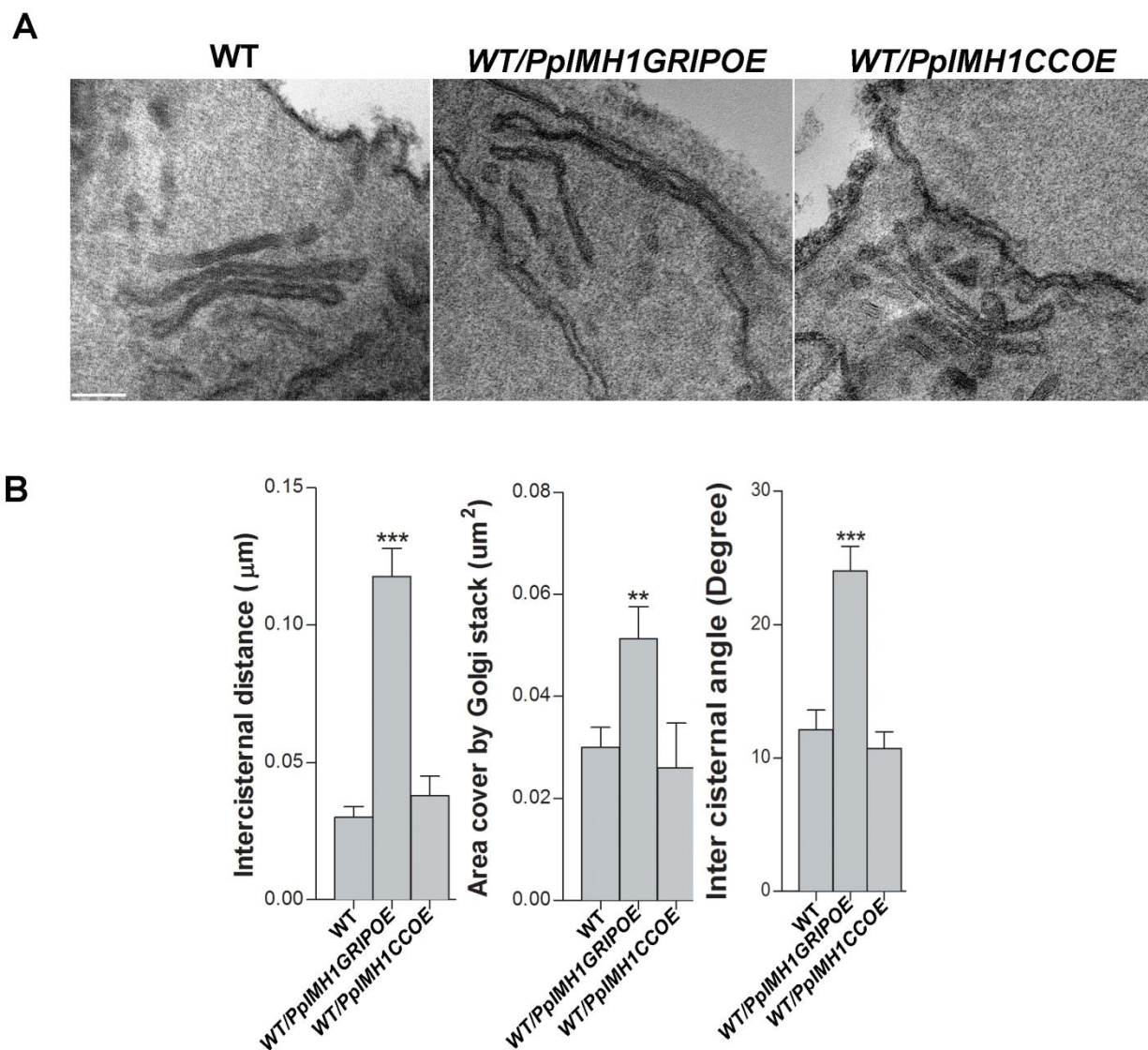


Figure 5.5 Overexpression of *PpImh1GRIP* domain alone can cause unstacking phenotype while overexpression of only *PpImh1* Coiled-coil domain alone causes no such effect.

(A). Thin section electron micrograph of *Pichia pastoris* wild-type cell overexpressed with *PpIMH1GRIP* domain and *PpIMH1CC*. *PpIMH1GRIP* and *PpIMH1CC* were cloned in a pIB4 vector under the control of methanol inducible promoter AOX1. Cells were grown till log phase in SYG (Glycerol) and induced by 1% methanol. Cells were concentrated, fixed and processed for thin section electron micrograph. Sections were observed under an electron microscope (100 CXII; JEOL U.S.A. Inc.) The representative cells are shown. Scale bar – 100nm) (B). Quantitative data from thin section electrograph were measured using iTEM analysis software (i) Maximum inter-cisternal distance between two cisternae, (ii) Area covered by the entire Golgi stack (iii) Angle between two cisternae. Values represent mean±SEM (45cells) student t-test ***P<0.005).

To further understand these results, we tagged *PpIMH1GRIP* domain and *PpIMH1CC* domain with GFP expressed under the AOX1 promoter. We observed that *PpIMH1GRIP* domain overexpression shows a typical punctate Golgi pattern, while *PpIMH1CC* overexpression which lacks GRIP domain, fails to localize to the Golgi (Fig 5.6). That, in turn, results in cytosolic accumulation of the coiled-coil domain and no effect on cisternal stacking.

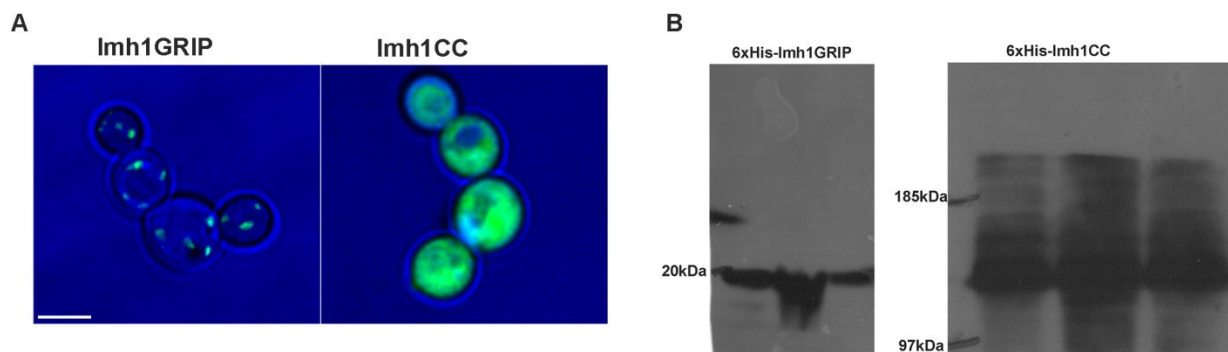


Figure 5.6 Localization of GFP-Imh1GRIP and iGFPImh1CC in *Pichia pastoris* cells.

(A). GFP-Imh1GRIP and GFPImh1CC were cloned into a pIB4 vector under the control of a methanol inducible AOX1 promoter. Constructs were integrated into the *Pichia pastoris* at His4 locus. Cells were grown to log phase in YPD and imaged in Leica SP8 imaging system. Optical sections were collected every 200nm. Images were processed and projected using Image J. Representative cell are shown. Scale bar: 1 μ m. B. Overexpression of Imh1GRIP and Imh1CC was analyzed on SDS PAGE, then transfer to nitrocellulose membrane for immunoblot using Anti His antibody.

5.2.5: Arl1 and Arl3 knockout display cisternal unstacking phenotype

Arl1p and Arl3p are divergent members of the ARF family of GTPases, referred to as ARF-like or ARL GTPases, and they are highly conserved with the human ARL1 and ARF-related protein (ARP) GTPases, respectively. Arl1-GTP interacts with the GRIP domain, and this interaction regulates the Golgi recruitment of Golgin-97[131].Arl1-Arl3 works in cascade, in which the GTPase cycle of Arl3p regulates Golgi localization of Arl1p, which in turn binds to the GRIP domain of Imh1p and recruits it to the Golgi. Arl3 and Arl1 are the reported to be receptors for the

GRIP domain proteins. To validate this in *Pichia pastoris*, we tagged the chromosomal copy of *PpIMH1* with GFP and transformed into *arl3* Δ , *arl1* Δ strains. GFP-Imh1 was found to be localized throughout the cytoplasm in case of *arl3* Δ , *arl1* Δ compare to the wild-type where it was localized to the Golgi (Fig 5.7). This suggests that both Arl3 and Arl1 are functionally conserved.

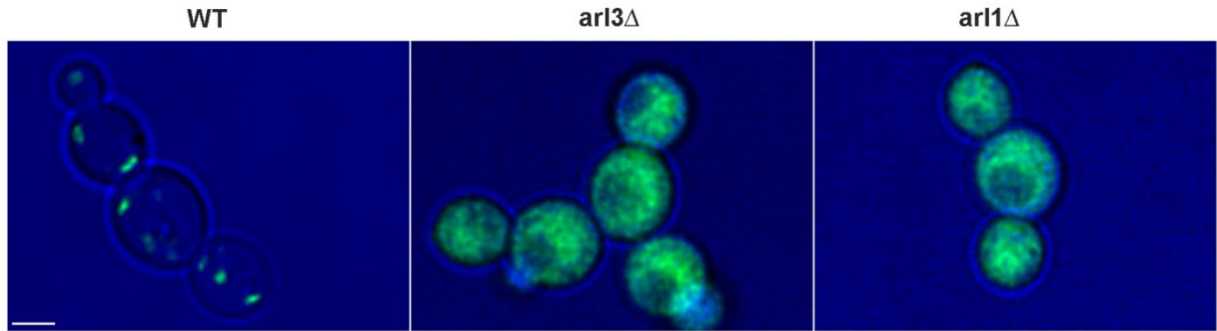


Figure 5.7 Localization of GFP-Imh1 in *arl1* Δ and *arl3* Δ knockout cells.

GFP-Imh1 was transformed into PPY12, *arl1* Δ , and *arl3* Δ strains. Cells were grown to log phase in YPD and imaged in Leica SP8 imaging system. Optical sections were collected every 200nm. Images were processed using Image J. Representative Cells are shown. Scale bar: 1 μ m.

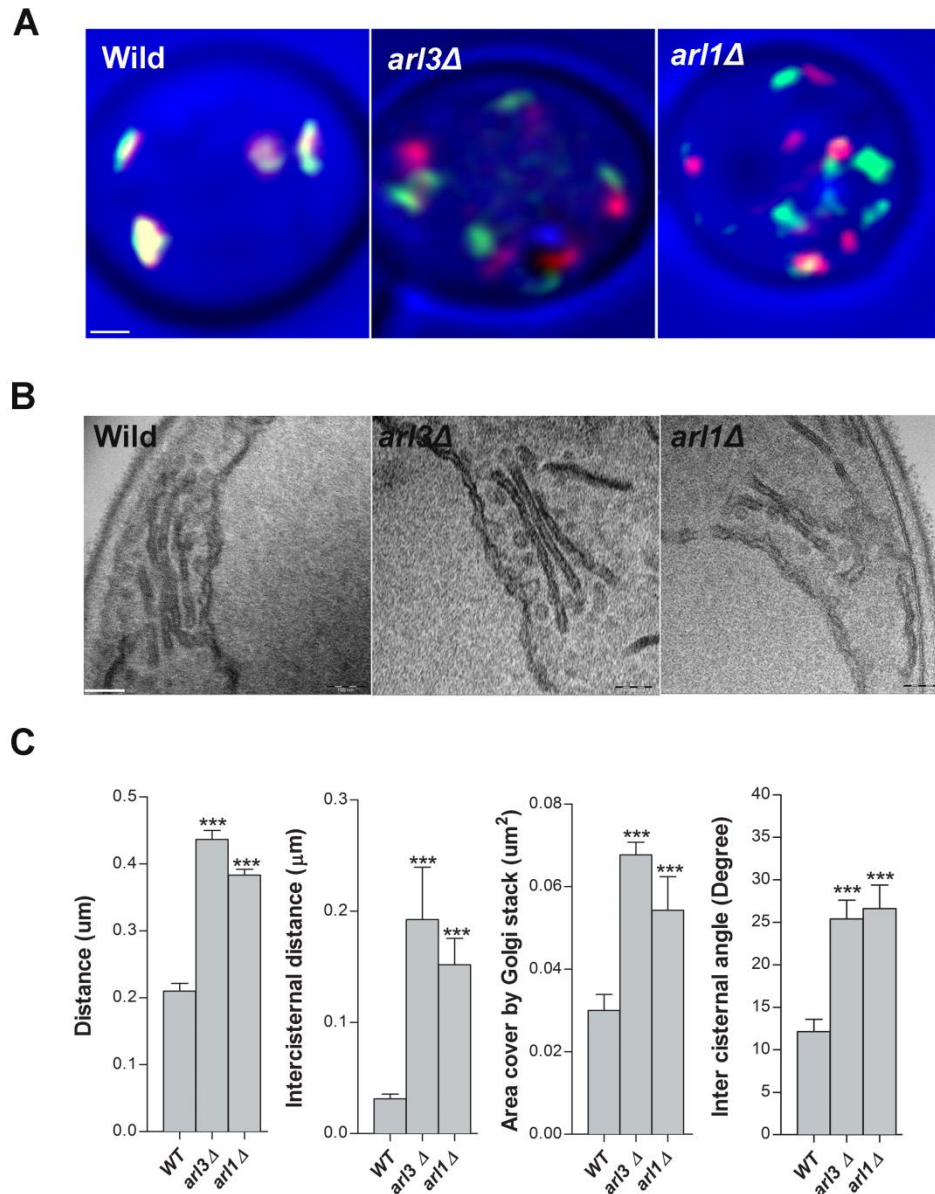


Figure 5.8 Inter-cisternal distance was increased in *arl3Δ* and *arl1Δ* cells

(A). *Pichia pastoris* strain expressing msGFP-VIG4 and SEC7-DsRed.M1x6 was deleted for *arl3Δ* & *arl1Δ*. Cells were grown to log phase and imaged under a Leica SP8 confocal imaging system. Optical sections of 200nm thickness were collected for the entire volume of cells. Image hyper stacks were deconvoluted using Huygens Pro and further filtered and Z-projected using ImageJ. Representative cells are shown. Scale bar: 1 μm. (B). Thin section electron micrograph of *Pichia pastoris* PPY12 wild-type, *arl3Δ*, and *arl1Δ* cells. *Pichia pastoris* WT, *arl3Δ*, and *arl1Δ* cells were grown until log phase. Cells were concentrated, fixed & stained. Sections were observed under an electron microscope (100 CXII; JEOL U.S.A. Inc.) The representative cell is shown. Scale bar – 100nm) (C). The distance between the green and red spot was measured using Imarisx64 8.0.1 Biplane. To quantitate the inter-cisternal distance, images were opened in

Imaris, the surface was filled using 3D rendering for a specific channel, then the individual surface was considered as the solid object, and center point was selected. By using pointer distance between one green and one red spot was measured. Values represent mean \pm SEM (60cells) student t-test ***P<0.0002. Quantitative data from thin section electrograph were measured using iTEM analysis software (i) Maximum inter-cisternal distance between two cisternae,(ii) Area covered by the entire Golgi stack (iii) Angle between two cisternae. Values represent mean \pm SEM (45cells) student t-test ***P<0.0002).

Since *PpImh1*'s recruitment to Golgi is dependent on Arl3-Arl1 function, we may hypothesize that depletion of both the Arl3 and Arl1 in *Pichia pastoris* cells should result in a cisternal unstacking phenotype. To test that, we created Arl3 and Arl1 knock out strain in wild-type two color Golgi strain. Indeed, we observed a cisternal unstacking phenotype in both the strains both through light microscopy and electron microscopy (Fig 5.8A, B). There was an increase in inter-cisternal distance, area cover by the entire Golgi stack and inter-cisternal angle (Fig 5.8C). These results once again strengthen our hypothesis that *PpImh1* indeed mediating the cisternal stacking of Golgi.

5.2.6: Golgi Localization of *PpImh1*

The hallmarks of GRIP domain Golgins is to their localization to TGN. The Golgin-97-GRIP domain is sufficient for the recruitment of Golgin-97 to TGN [131, 140]. To test what is the exact localization of *PpImh1*, we tagged the *PpImh1* with GFP & check its localization with respect to early and late Golgi. GFP-*PpImh1* was showing overlapped with both cis Golgi and trans-Golgi marker (Fig 5.9A). Upon measuring the percent of the green spot on the red spot, we confirmed that it's co-localizing with both cis and trans-Golgi (Fig 5.9B). These results suggest to us that *PpImh1* could be localized to the medial compartment. This result also fits well with our hypothesis that *PpImh1* mediates the stacking between medial & trans-Golgi.

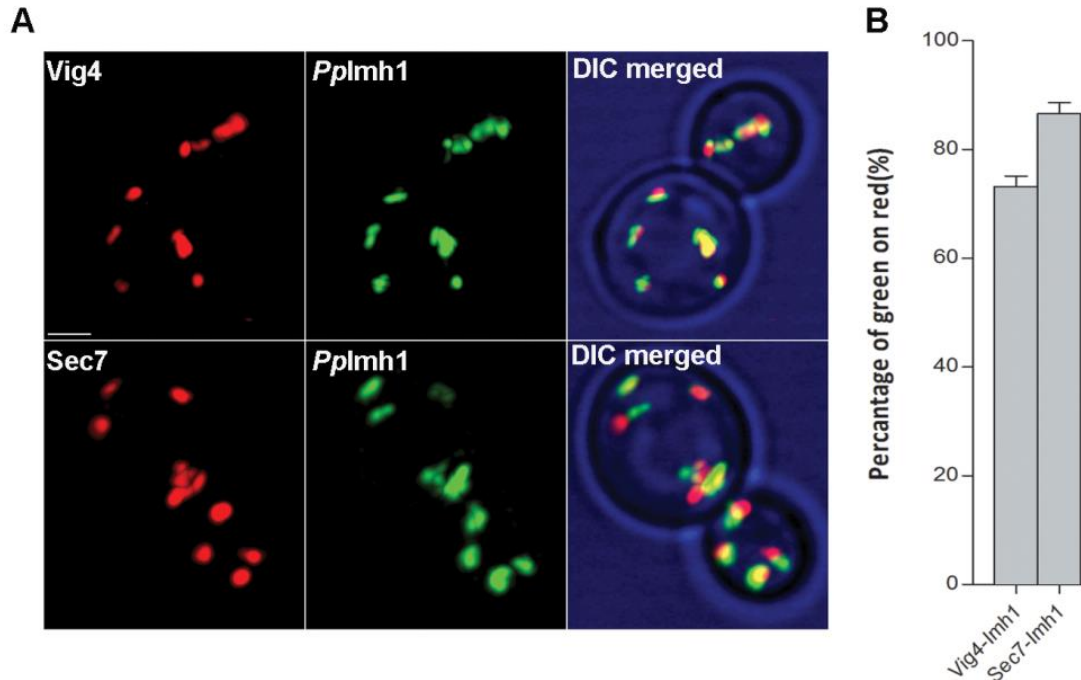


Figure 5.9 Localization of *PpImh1* to the Golgi

(A). Cells expressing GFP-*PpIMH1* were transformed with cis Golgi marker mcherry-VIG4 and trans-Golgi marker SEC7-DsRed.M1x6. Resulting strain (GFP-*PpIMH1* mcherry-VIG4) & (GFP-*PpIMH1*, SEC7DsRed.M1x6) were grown till log phase; images were taken under Leica SP8 confocal imaging system. Optical sections of 200nm thickness were collected for the entire volume of cells. Image hyper stack were deconvoluted using Huygens Pro and further filtered and Z-projected using ImageJ. Representative cells are shown. Scale bar: 1 μ m. (B). The overlap between two differently labeled punctate compartments was quantified. Colocalization for each pair was measured as the percentage of the GFP signal that overlapped with a mask created from the mCherry-Vig4, and Sec7-6xDsRed.M1 signal. Colocalization of the two markers was determined using ImageJ (60 cells). Values represent mean \pm SEM (60 cells).

5.2.7: *PpImh1* is required for endosome to TGN trafficking

Knockdown of individual mammalian GRIP domain proteins can result in, defects in the retrograde traffic of some cargo proteins from endosomes to the TGN [82, 85, 86, 141, 142]. It has also been suggested that some GRIP domain proteins are associated with outgoing or incoming cargo vesicle trafficking in TGN [142]. Golgin 97, the mammalian homolog of *PpImh1* has been implicated in recycling endosome trafficking. To test whether depletion of *PpImh1* has any effect

on endosome to TGN trafficking, we GFP-tagged one of the cargo protein Tlg1 which shuttles between endosome to TGN. We checked the localization of GFP-Tlg1 in wild-type *Pichia pastoris* cells, which shows that Tlg1 localized to TGN (Fig 5.10). Furthermore, we checked the localization of Tlg1 in *Ppimh1Δ*, *Ppimh1 Δ (150-1070)* cells. In the case of *PpImh1Δ* as well as *PpImh1 (150-1070) Δ* cells, Tlg1 was not localized to the TGN. It was showing ‘spotty’ peripheral localization which is supposed to be endosome. It suggests that *PpImh1* depletion affects the endosome to TGN trafficking.

5.2.8: *PpImh1* N terminal is indispensable for vesicle capture function

A short well-conserved region at the N-terminus of TGN Golgin has been shown to be necessary and sufficient to nucleate the capture of endosome-to-Golgi carriers [133].

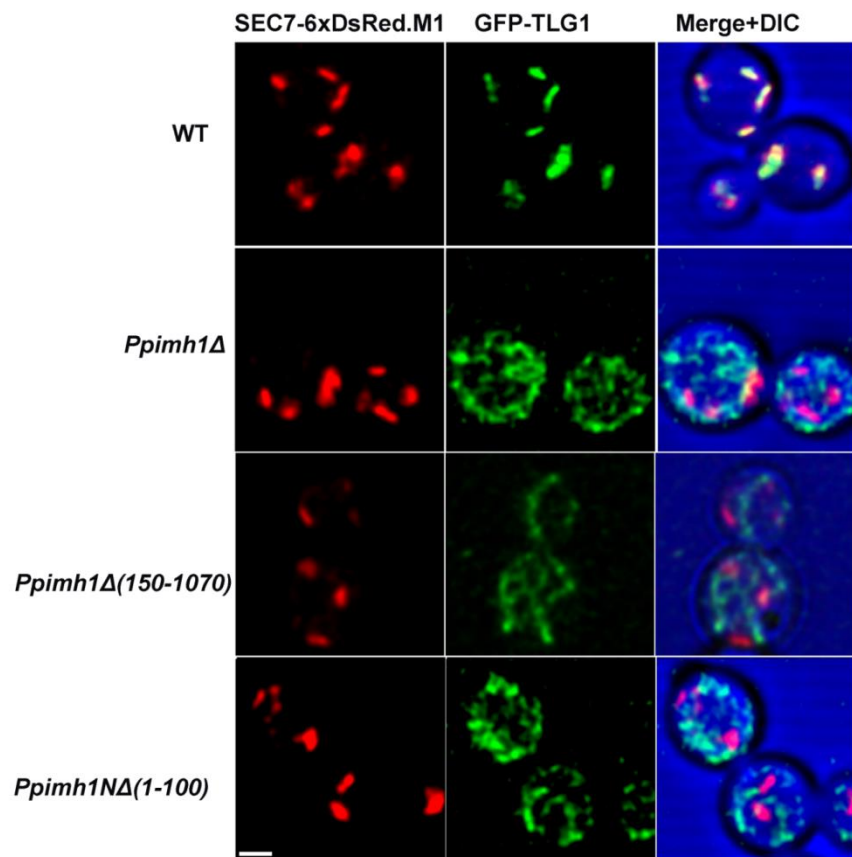


Figure 5.10 N terminal 100 amino acids region of *PpImh1* are essential for endosome to Golgi transport

Pichia pastoris cells expressing SEC7-DsRed.M1x6 and iGFP-TLG1 were knocked out with *Ppimh1Δ*, *Ppimh1Δ* (150-1070) and *Ppimh1NA* (1-100) domain. Cells were grown to log phase and images under Leica SP8 system. Optical sections of 200nm thickness were collected for the entire volume of cells. Image hyper stack were deconvoluted using Huygens Pro and further filtered and Z-projected using ImageJ. Representative cells are shown. Scale bar: 1 μm.

To validate whether the similar region of *PpImh1* is functionally conserved or not, we deleted the N terminal 100Amino acids residues of endogenous *PpImh1*. We observed that in such strain Tlg1 fails to localize in Golgi, suggesting that endosome to Golgi vesicle capturing function is compromised (Fig 5.11). These results further confirm that the deletion of only 1-100 amino acids residues of endogenous *PpImh1* is sufficient to abolish vesicle capture function of *PpImh1*. Coiled-coil domain deletion of endogenous *PpImh1* also has abolished the vesicle capture function (Fig 5.11). It suggests that N terminal 1-100 amino acids are necessary for vesicle capture along with the coiled-coil domain.

5.2.9: *PpImh1* N terminal is dispensable for cisternal stacking function of *PpImh1*

We also tested the effect of N terminal deletion (1-100AA) on cisternal stacking phenotype by electron microscopy and light microscopy. Surprisingly such experiment showed no change in inter-cisternal distance and other parameters (Fig 5.12A, B, C, D.)

This result suggests that the cisternal stacking function of *PpImh1* is not dependent on its vesicle capturing function. However, the vesicle capturing function may be dependent on its stacking function as the deletion coiled-coil domain (the essential domain for cisternal stacking function) abolishes the vesicle capture function as well.

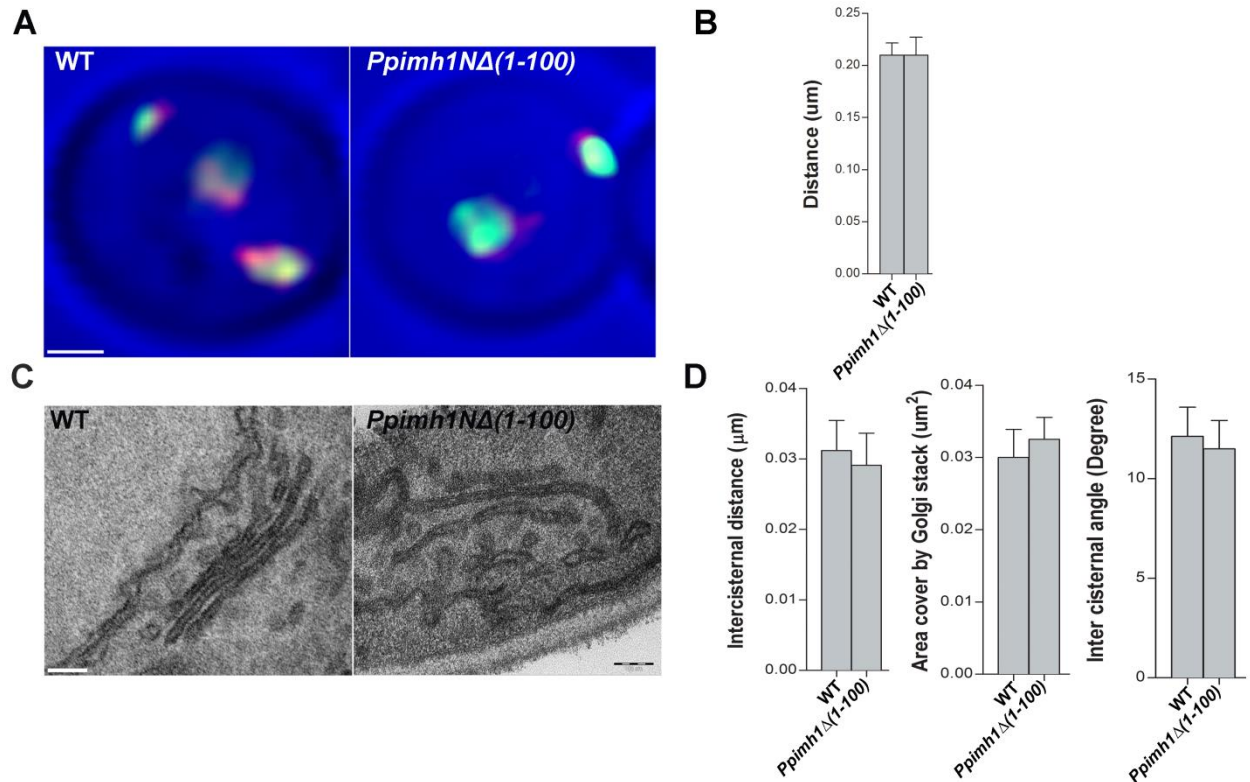


Figure 5.11 Deletion of N-terminal 100 amino acids region of PpImh1 has no effect on Golgi cisternal stacking.

(A). *PpImh1N* (1-100) domain was deleted in *Pichia pastoris* cells. WT cells and *Ppimh1Δ* (1-100) expressing msGFP-VIG4 and SEC7-DsRed.M1x6 were grown to log phase and images were captured under Leica SP8 system. Optical sections of 200nm thickness were collected for the entire volume of cells. Image hyper stack were deconvoluted using Huygens Pro and further filtered and Z-projected using ImageJ. Representative cells are shown. Scale bar: 1 μm. (B). The distance between the green and red spot was measured using Imaris Biplane. To quantitative the inter-cisternal distance, the distance between the green and red spot were measured. Values represent mean±SEM (60cells) student t-test ***P<0.0006). (C). Thin section electron micrograph of *Pichia pastoris* PPY12 wild-type, *Ppimh1 NΔ* (1-100) cells. *Pichia pastoris* WT and *Ppimh1 NΔ* (1-100) cells were grown until log phase. Cells were concentrated, fixed & stained. Sections were observed under an electron microscope (100 CXII; JEOL U.S.A. Inc.) The representative cell is shown. Scale bar –100nm (D). Quantitative data from thin section electrograph were measured using iTEM analysis software (i) Maximum inter-cisternal distance between two cisternae, (ii) Area covered by the entire Golgi stack (iii) Angle between two cisternae. Values represent mean±SEM (45cells) student t-test ***P<0.0002).

5.3: Discussion

The discovery of the Golgins coincided with the observation that Golgi membranes could be extracted with detergent to leave a proteinaceous matrix that retained the organization of Golgi cisternae. Golgins GM130, p115 and Golgin 95 were discovered as matrix proteins which can maintain the architecture of Golgi cisternae [140-142]. It was also observed that a single knockdown of Golgins results in Golgi fragmentation [82, 84], suggesting a role of Golgins in Golgi structure and maintenance.

Our results suggest that Golgin *PpImh1* knockout affect cisternal stacking between medial and trans-Golgi. We also showed that the coiled-coil domain of Golgin *PpImh1* shown to be essential for cisternal stacking. The GRASPs contains PDZs domain which can mediate lateral linking of cisternae by oligomerization, suggesting oligomerization a mode of cisternal stacking[26, 28, 33]. The Golgin *PpImh1* forms parallel homodimer where the central coiled-coil domain remains in the dimeric state[136], suggesting that the coiled-coil domain of Golgin *PpImh1* dimerizes and hold cisternae together.

Our results support our hypothesis that the long coiled-coil domain could potentially mediate dimerization of Golgin molecules residing on two different Golgi Cisterna and multiple such dimerized Golgin pairs can bring two Golgi cisternae together to form a stack. Our data suggest that *PpImh1* mediates the cisternal stacking of TGN and medial Golgi.

The established function of Golgins is to capture vesicle coming from the different region of the cells. GRIP domain Golgins GCC185, Golgin 97, Golgin 245 captures the vesicle coming from the endosome and transfers it to trans Golgi [82, 84, 139]. Our results support that Golgin *PpImh1* mediates transport between endosome to TGN.

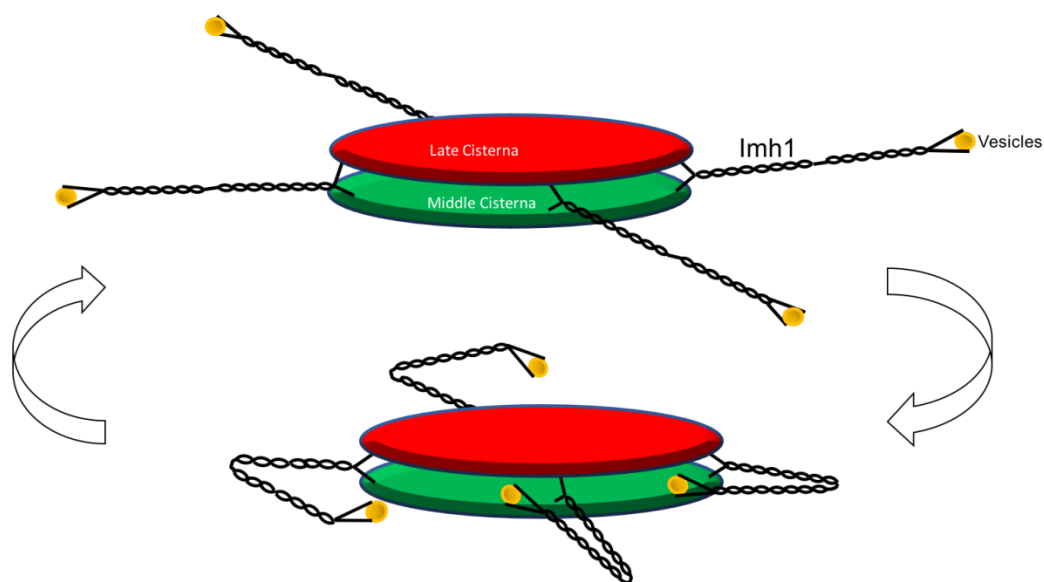


Figure 5.12 Model depicting the dual function of *PpImh1*

GRIP domain Golgins GCC185 forms a Y shaped structure where N terminal domain form splayed end and shown to be essential for vesicle capture [81, 130]. Golgin *PpImh1* forms a parallel homodimer with splayed N terminus[136]. Our data further support that N terminal domain of *PpImh1* is essential for vesicle capture function of Golgin *PpImh1*.

It appears that its cisternal stacking function is independent of the vesicle capturing function since deletion of vesicle capture domain (*PpImh1* (1-100) has no effect on cisternal stacking. But the deletion of the coiled-coil domain which is essential for cisternal stacking affect vesicle capture functions. That further suggests that stacking is indispensable for vesicle capture. We hypothesize that cisternal stacking is independent of vesicle capturing functions, but the efficacy of the latter may be dependent on the former, which possibly enhance the robustness of the secretory function of the Golgi apparatus.

However, a natural question arises about how *PpImh1* accommodate these two separate functions simultaneously. To address that, we have hypothesized a potential model (Fig 5.13). For vesicle capturing function Y-shaped N terminal dimers of Golgins are a favored structure in which splayed N-terminal of dimers are proposed to get hold of the vesicles[81, 130]. We have shown that N terminal domain of *PpImh1* is essential for vesicle capture. The C terminal domain of Golgin dimers anchors to the Golgi membrane through Arl1 interaction. The coiled-coil region of *PpImh1* contains certain breaks region which possible form the hinge region which can provide flexibility to Golgin molecule to transport vesicle to the Golgi membrane [81, 136]

For cisternal stacking function, the dimers anchor its two GRIP domain C-terminal tail into two different neighboring cisternae and dimerization of coiled-coil domain bring two cisternae together and mediate cisternal stacking.

Our results suggest the possible role of Golgins in Golgi structure maintenance and vesicle capture. Golgins could mediate cisternal stacking in lower eukaryotes and organisms lacking GRASPs. Golgin potentially could be stacking factor as they are conserved in all the organisms.

6. Summary and conclusion

6.1: Summary and conclusion

Budding yeast *Pichia pastoris* has highly advanced secretory pathways resembling mammalian systems, an advantage that makes it a suitable model system to study vesicular trafficking. Golgins are large Golgi resident proteins, primarily reported to play role in cargo vesicle capture, but details of such mechanisms are yet to be deciphered. Golgins that localize to the Golgi via their GRIP domain, a C-terminal Golgi anchoring domain, are known as GRIP domain Golgins. We have identified and a functionally characterized homolog of one such GRIP domain Golgin protein, Imh1, from the budding yeast *Pichia pastoris*. We have demonstrated that the GRIP domain present at C-terminal of *Pichia pastoris* Imh1 (*PpImh1*) functions as its Golgi-targeting sequence. Using a combination of yeast two-hybrid analysis, Dynamic Light Scattering and Electron Microscopy, we have shown that *PpImh1* can self-associate and form a homodimer. Analysis of purified recombinant *PpImh1* by CD spectroscopy indicates the presence of 85% α -helical structure, a characteristic of high content alpha helical coiled-coil sequences normally present in other Golgin family proteins. Two-hybrid analysis indicated self-interaction between C-terminal fragments, yet N terminal fragments do not mediate any such form of self-interaction, suggesting that *PpImh1* may form a parallel dimer. Electron Microscopy data indicates *PpImh1* forms extended rod-like homo-dimeric molecules with splayed N terminal end which can act as a tether for capturing vesicles. Our study, provide the first evidence in support of the dimeric Y shaped structure for any Golgin in the budding yeast.

Shape regulation of dynamic organelles is a basic cell biological problem. Moreover, the mechanism that regulates cisternal stacking of Golgi apparatus is still not completely understood primarily due to the lack of any cross-species universal factors that may mediate such function. Although (GRASPs) has been implicated in cisternal stacking in metazoans, the lack of functional

GRASP homolog in budding yeast and plants raises the possibilities of the existence of other potential universal factors with similar functions. Golgins represent such likely class of molecules that may mediate the adhesive role for cisternal stacking. With their long coiled-coil domains, Golgins could potentially mediate dimerization with other Golgin molecules residing on different Golgi cisterna and multiple such dimerization events collectively may bring neighboring Golgi cisternae together to form a stack. In our present study, we observed that deletion of *Pichia pastoris* Golgin *PpIMH1* causes an increase in inter-cisternal distance between medial and late Golgi compartment. Although a full-length *PpImh1* can rescue such phenotype, but *PpImh1* lacking coiled-coil region failed to rescue the unstacking phenotype. This result suggests that *PpImh1* may indeed play a role in cisternal stacking through coiled-coil domain dimerization as hypothesized. Such a conclusion further strengthened by the fact that an overexpression of only the *PpImh1* GRIP domain can cause a similar cisternal unstacking. Deletion of the N terminal (1-100) amino acid domain abolishes the vesicle capture function of *PpImh1*, but such deletion does not affect cisternal stacking. Our results suggest that *PpImh1* mediate the dual function of cisternal stacking and vesicle capture via its two different functional domains. We hypothesize that cisternal stacking is independent of vesicle capturing functions, but the efficacy of the latter may be dependent on the former, which possibly enhance the robustness of the secretory function of the Golgi apparatus.

Following are salient features of this research:

- a. *PpImh1* deletion strains display cisternal unstacking between medial and trans-Golgi
- b. Coiled-coil domain of *PpImh1* is essential for cisternal stacking
- c. *Arl1* and *Arl3* deletion strains result in a cisternal unstacking phenotype
- d. *PpImh1* co-localize with both early and late Golgi marker.

- e. *PpImh1* knockout strain affects transport between endosome and TGN
- f. GRIP domain of *PpImh1* is important for Golgi localization
- g. *PpImh1* comprised of a high degree of alpha-helical coiled-coil domain
- h. *PpImh1* form parallel homodimer and has splayed N terminus.

6.2: Future Perspectives

Our study suggests that Golgin *PpImh1* perform the dual function of cisternal stacking and vesicle capture. We have shown that Golgin *PpImh1* contains coiled-coil domain which has the ability to form a dimer. For cisternal stacking function, it possibly holds Golgi cisternae by means of Golgi localizing GRIP domain and brings two cisternae together by dimerization of coiled-coil domain. Furthermore, it would be interesting to understand the force behind the dimerization of the coiled-coil domain. It will enable us to strengthen the fact that Golgin can mediate cisternal stacking. Since the dimerization is a crucial step for cisternal stacking it would be interesting to identify the minimal region of Golgin *PpImh1* required for cisternal stacking.

With respect to vesicle capture function, we have shown that *PpImh1* contain long coiled-coil domain which provides an extended arm to capture the upcoming vesicle. The coiled-coil region also contains a certain region which has a very low probability of coiled coil. The possible function of these regions may be to provide sufficient physical flexibility to the *PpImh1* molecule in order to capture vesicle from the distance and bring it to the Golgi cisternae. It would be fascinating to study whether these regions function as a hinge to allow the bending of Golgins? What are the other factors or forces that are involved in this bending of Golgins? A variety of Rab's has been known to bind the Golgins throughout their length. Probably the ability of Golgins to bind multiple

Rabs may serve a role in allowing their bending. Hence, we need to know what are the specific Rabs responsible for binding to different regions of Golgins and allowing their bending?

Also, what are the other candidate factors responsible for cisternal stacking? There are 4 different Golgins known in *P. pastoris*. Out of these 4 Golgins, we have shown that Rud3 is not involved in cisternal stacking while Imh1 is involved in medial and TGN stacking. There are 2 other Golgins that are remained to study, namely Coy1 and Sgm1. Do these Golgins play a similar role in cisternal stacking? If yes then how exactly do they perform this function? Is their mechanism of stacking similar to that of PpImh1? Is there any functional redundancy among these Golgins? All these questions may help us to further explore the mechanism of cisternal stacking.

7. Bibliography

1. Chan, Y.H. and W.F. Marshall, *How cells know the size of their organelles*. Science, 2012. **337**(6099): p. 1186-9.
2. Glick, B.S. and A. Nakano, *Membrane traffic within the Golgi apparatus*. Annu Rev Cell Dev Biol, 2009. **25**: p. 113-32.
3. Nakamura, N., J.H. Wei, and J. Seemann, *Modular organization of the mammalian Golgi apparatus*. Curr Opin Cell Biol, 2012. **24**(4): p. 467-74.
4. Lowe, M., *Structural organization of the Golgi apparatus*. Curr Opin Cell Biol, 2011. **23**(1): p. 85-93.
5. Liu, S. and B. Storrie, *Are Rab proteins the link between Golgi organization and membrane trafficking?* Cell Mol Life Sci, 2012. **69**(24): p. 4093-106.
6. Joshi, G., et al., *Abeta-induced Golgi fragmentation in Alzheimer's disease enhances Abeta production*. Proc Natl Acad Sci U S A, 2014. **111**(13): p. E1230-9.
7. Stieber, A., Z. Mourelatos, and N.K. Gonatas, *In Alzheimer's disease the Golgi apparatus of a population of neurons without neurofibrillary tangles is fragmented and atrophic*. Am J Pathol, 1996. **148**(2): p. 415-26.
8. Petrosyan, A., *Onco-Golgi: Is Fragmentation a Gate to Cancer Progression?* Biochem Mol Biol J, 2015. **1**(1).
9. Marshall, W.F., *Organelle size control systems: from cell geometry to organelle-directed medicine*. Bioessays, 2012. **34**(9): p. 721-4.
10. Chan, Y.H. and W.F. Marshall, *Scaling properties of cell and organelle size*. Organogenesis, 2010. **6**(2): p. 88-96.
11. Palade, G., *Intracellular aspects of the process of protein synthesis*. Science, 1975. **189**(4200): p. 347-58.

12. Bannykh, S.I., T. Rowe, and W.E. Balch, *The organization of endoplasmic reticulum export complexes*. J Cell Biol, 1996. **135**(1): p. 19-35.
13. Droscher, A., *The history of the Golgi apparatus in neurones from its discovery in 1898 to electron microscopy*. Brain Res Bull, 1998. **47**(3): p. 199-203.
14. Farquhar, M.G. and G.E. Palade, *The Golgi apparatus: 100 years of progress and controversy*. Trends in Cell Biology, 1998. **8**(1): p. 2-10.
15. Losev, E., et al., *Golgi maturation visualized in living yeast*. Nature, 2006. **441**(7096): p. 1002-6.
16. Matsuura-Tokita, K., et al., *Live imaging of yeast Golgi cisternal maturation*. Nature, 2006. **441**(7096): p. 1007-10.
17. Ito, Y., T. Uemura, and A. Nakano, *Formation and maintenance of the Golgi apparatus in plant cells*. Int Rev Cell Mol Biol, 2014. **310**: p. 221-87.
18. Glick, B.S. and A. Luini, *Models for Golgi traffic: a critical assessment*. Cold Spring Harb Perspect Biol, 2011. **3**(11): p. a005215.
19. Cluett, E.B. and W.J. Brown, *Adhesion of Golgi cisternae by proteinaceous interactions: intercisternal bridges as putative adhesive structures*. J Cell Sci, 1992. **103** (Pt 3): p. 773-84.
20. Shorter, J., et al., *GRASP55, a second mammalian GRASP protein involved in the stacking of Golgi cisternae in a cell-free system*. EMBO J, 1999. **18**(18): p. 4949-60.
21. Levi, S.K., et al., *The yeast GRASP Grh1 colocalizes with COPII and is dispensable for organizing the secretory pathway*. Traffic, 2010. **11**(9): p. 1168-79.
22. Barr, F.A., et al., *GRASP65, a protein involved in the stacking of Golgi cisternae*. Cell, 1997. **91**(2): p. 253-62.

23. Feinstein, T.N. and A.D. Linstedt, *GRASP55 regulates Golgi ribbon formation*. Mol Biol Cell, 2008. **19**(7): p. 2696-707.
24. Bekier, M.E., 2nd, et al., *Knockout of the Golgi stacking proteins GRASP55 and GRASP65 impairs Golgi structure and function*. Mol Biol Cell, 2017. **28**(21): p. 2833-2842.
25. Xiang, Y. and Y. Wang, *GRASP55 and GRASP65 play complementary and essential roles in Golgi cisternal stacking*. J Cell Biol, 2010. **188**(2): p. 237-51.
26. Truschel, S.T., et al., *Structure of the membrane-tethering GRASP domain reveals a unique PDZ ligand interaction that mediates Golgi biogenesis*. J Biol Chem, 2011. **286**(23): p. 20125-9.
27. Feng, Y., et al., *Structural insight into Golgi membrane stacking by GRASP65 and GRASP55 proteins*. J Biol Chem, 2013. **288**(39): p. 28418-27.
28. Bachert, C. and A.D. Linstedt, *Dual anchoring of the GRASP membrane tether promotes trans pairing*. J Biol Chem, 2010. **285**(21): p. 16294-301.
29. Heinrich, F., et al., *Myristoylation restricts orientation of the GRASP domain on membranes and promotes membrane tethering*. J Biol Chem, 2014. **289**(14): p. 9683-91.
30. Short, B., et al., *A GRASP55-rab2 effector complex linking Golgi structure to membrane traffic*. J Cell Biol, 2001. **155**(6): p. 877-83.
31. Barr, F.A., N. Nakamura, and G. Warren, *Mapping the interaction between GRASP65 and GM130, components of a protein complex involved in the stacking of Golgi cisternae*. EMBO J, 1998. **17**(12): p. 3258-68.
32. Puthenveedu, M.A., et al., *GM130 and GRASP65-dependent lateral cisternal fusion allows uniform Golgi-enzyme distribution*. Nat Cell Biol, 2006. **8**(3): p. 238-48.

33. Sengupta, D., et al., *Organelle tethering by a homotypic PDZ interaction underlies formation of the Golgi membrane network*. J Cell Biol, 2009. **186**(1): p. 41-55.
34. Sengupta, D. and A.D. Linstedt, *Mitotic inhibition of GRASP65 organelle tethering involves Polo-like kinase 1 (PLK1) phosphorylation proximate to an internal PDZ ligand*. J Biol Chem, 2010. **285**(51): p. 39994-40003.
35. Kineth, M.A., et al., *The Golgi-associated protein GRASP is required for unconventional protein secretion during development*. Cell, 2007. **130**(3): p. 524-34.
36. Duran, J.M., et al., *Unconventional secretion of Acb1 is mediated by autophagosomes*. J Cell Biol, 2010. **188**(4): p. 527-36.
37. Manjithaya, R., et al., *Unconventional secretion of Pichia pastoris Acb1 is dependent on GRASP protein, peroxisomal functions, and autophagosome formation*. J Cell Biol, 2010. **188**(4): p. 537-46.
38. Bruns, C., et al., *Biogenesis of a novel compartment for autophagosome-mediated unconventional protein secretion*. J Cell Biol, 2011. **195**(6): p. 979-92.
39. Rabouille, C. and A.D. Linstedt, *GRASP: A Multitasking Tether*. Front Cell Dev Biol, 2016. **4**: p. 1.
40. Xiang, Y., et al., *Regulation of protein glycosylation and sorting by the Golgi matrix proteins GRASP55/65*. Nat Commun, 2013. **4**: p. 1659.
41. Wang, Z.H., C. Rabouille, and E.R. Geisbrecht, *Loss of a Clueless-dGRASP complex results in ER stress and blocks Integrin exit from the perinuclear endoplasmic reticulum in Drosophila larval muscle*. Biol Open, 2015. **4**(5): p. 636-48.
42. Goldfischer, S., *The internal reticular apparatus of Camillo Golgi: a complex, heterogeneous organelle, enriched in acid, neutral, and alkaline phosphatases, and*

- involved in glycosylation, secretion, membrane flow, lysosome formation, and intracellular digestion.* J Histochem Cytochem, 1982. **30**(7): p. 717-33.
43. Ohtsubo, K. and J.D. Marth, *Glycosylation in cellular mechanisms of health and disease.* Cell, 2006. **126**(5): p. 855-67.
44. Weisz, O.A. and E. Rodriguez-Boulan, *Apical trafficking in epithelial cells: signals, clusters and motors.* J Cell Sci, 2009. **122**(Pt 23): p. 4253-66.
45. Scheiffele, P. and J. Fullekrug, *Glycosylation and protein transport.* Essays Biochem, 2000. **36**: p. 27-35.
46. Kornfeld, R. and S. Kornfeld, *Assembly of asparagine-linked oligosaccharides.* Annu Rev Biochem, 1985. **54**: p. 631-64.
47. Varki, A., *Factors controlling the glycosylation potential of the Golgi apparatus.* Trends Cell Biol, 1998. **8**(1): p. 34-40.
48. Roth, J., *Protein N-glycosylation along the secretory pathway: relationship to organelle topography and function, protein quality control, and cell interactions.* Chem Rev, 2002. **102**(2): p. 285-303.
49. Wildt, S. and T.U. Gerngross, *The humanization of N-glycosylation pathways in yeast.* Nat Rev Microbiol, 2005. **3**(2): p. 119-28.
50. Moremen, K.W., M. Tiemeyer, and A.V. Nairn, *Vertebrate protein glycosylation: diversity, synthesis and function.* Nat Rev Mol Cell Biol, 2012. **13**(7): p. 448-62.
51. Dupuis, N., et al., *A novel RAB33B mutation in Smith-McCort dysplasia.* Hum Mutat, 2013. **34**(2): p. 283-6.

52. Syx, D., et al., *The RIN2 syndrome: a new autosomal recessive connective tissue disorder caused by deficiency of Ras and Rab interactor 2 (RIN2)*. Hum Genet, 2010. **128**(1): p. 79-88.
53. Basel-Vanagaite, L., et al., *RIN2 deficiency results in macrocephaly, alopecia, cutis laxa, and scoliosis: MACS syndrome*. Am J Hum Genet, 2009. **85**(2): p. 254-63.
54. Huse, J.T., et al., *Beta-secretase processing in the trans-Golgi network preferentially generates truncated amyloid species that accumulate in Alzheimer's disease brain*. J Biol Chem, 2002. **277**(18): p. 16278-84.
55. Mizuno, Y., et al., *Familial Parkinson's disease. Alpha-synuclein and parkin*. Adv Neurol, 2001. **86**: p. 13-21.
56. Hilditch-Maguire, P., et al., *Huntingtin: an iron-regulated protein essential for normal nuclear and perinuclear organelles*. Hum Mol Genet, 2000. **9**(19): p. 2789-97.
57. Fujita, Y. and K. Okamoto, *Golgi apparatus of the motor neurons in patients with amyotrophic lateral sclerosis and in mice models of amyotrophic lateral sclerosis*. Neuropathology, 2005. **25**(4): p. 388-94.
58. Mourelatos, Z., et al., *The Golgi apparatus of spinal cord motor neurons in transgenic mice expressing mutant Cu,Zn superoxide dismutase becomes fragmented in early, preclinical stages of the disease*. Proc Natl Acad Sci U S A, 1996. **93**(11): p. 5472-7.
59. Gonatas, N.K., J.O. Gonatas, and A. Stieber, *The involvement of the Golgi apparatus in the pathogenesis of amyotrophic lateral sclerosis, Alzheimer's disease, and ricin intoxication*. Histochem Cell Biol, 1998. **109**(5-6): p. 591-600.
60. Inoue, K., *PLP1-related inherited dysmyelinating disorders: Pelizaeus-Merzbacher disease and spastic paraplegia type 2*. Neurogenetics, 2005. **6**(1): p. 1-16.

61. Ting, C.H., et al., *The spinal muscular atrophy disease protein SMN is linked to the Golgi network*. PLoS One, 2012. **7**(12): p. e51826.
62. Zhang, C., et al., *Mutations in ABCB6 cause dyschromatosis universalis hereditaria*. J Invest Dermatol, 2013. **133**(9): p. 2221-8.
63. Condon, K.H., et al., *The Angelman syndrome protein Ube3a/E6AP is required for Golgi acidification and surface protein sialylation*. J Neurosci, 2013. **33**(9): p. 3799-814.
64. Kornak, U., et al., *Impaired glycosylation and cutis laxa caused by mutations in the vesicular H⁺-ATPase subunit ATP6V0A2*. Nat Genet, 2008. **40**(1): p. 32-4.
65. Fischer, B., et al., *Further characterization of ATP6V0A2-related autosomal recessive cutis laxa*. Hum Genet, 2012. **131**(11): p. 1761-73.
66. Ohtsubo, K., et al., *Dietary and genetic control of glucose transporter 2 glycosylation promotes insulin secretion in suppressing diabetes*. Cell, 2005. **123**(7): p. 1307-21.
67. Van Beek, W.P., L.A. Smets, and P. Emmelot, *Changed surface glycoprotein as a marker of malignancy in human leukaemic cells*. Nature, 1975. **253**(5491): p. 457-60.
68. Mitchell, E., et al., *Structural basis for oligosaccharide-mediated adhesion of Pseudomonas aeruginosa in the lungs of cystic fibrosis patients*. Nat Struct Biol, 2002. **9**(12): p. 918-21.
69. Schulz, B.L., et al., *Glycosylation of sputum mucins is altered in cystic fibrosis patients*. Glycobiology, 2007. **17**(7): p. 698-712.
70. Wang, Y., et al., *Golgi cisternal unstacking stimulates COPI vesicle budding and protein transport*. PLoS One, 2008. **3**(2): p. e1647.

71. Novick, P., C. Field, and R. Schekman, *Identification of 23 complementation groups required for post-translational events in the yeast secretory pathway*. Cell, 1980. **21**(1): p. 205-15.
72. Bevis, B.J., et al., *De novo formation of transitional ER sites and Golgi structures in Pichia pastoris*. Nat Cell Biol, 2002. **4**(10): p. 750-6.
73. Rossanese, O.W., et al., *Golgi structure correlates with transitional endoplasmic reticulum organization in Pichia pastoris and Saccharomyces cerevisiae*. J Cell Biol, 1999. **145**(1): p. 69-81.
74. Papanikou, E. and B.S. Glick, *The yeast Golgi apparatus: insights and mysteries*. FEBS Lett, 2009. **583**(23): p. 3746-51.
75. Munro, S., *The golgin coiled-coil proteins of the Golgi apparatus*. Cold Spring Harb Perspect Biol, 2011. **3**(6).
76. Nozawa, K., M.J. Fritzler, and E.K. Chan, *Unique and shared features of Golgi complex autoantigens*. Autoimmun Rev, 2005. **4**(1): p. 35-41.
77. Gillingham, A.K. and S. Munro, *Finding the Golgi: Golgin Coiled-Coil Proteins Show the Way*. Trends Cell Biol, 2016. **26**(6): p. 399-408.
78. Sinka, R., et al., *Golgi coiled-coil proteins contain multiple binding sites for Rab family G proteins*. The Journal of Cell Biology, 2008. **183**(4): p. 607-615.
79. Hayes, G.L., et al., *Multiple Rab GTPase Binding Sites in GCC185 Suggest a Model for Vesicle Tethering at the Trans-Golgi*. Molecular Biology of the Cell, 2009. **20**(1): p. 209-217.
80. Luke, M.R., et al., *The trans-Golgi network GRIP-domain proteins form alpha-helical homodimers*. Biochem J, 2005. **388**(Pt 3): p. 835-41.

81. Cheung, P.Y., et al., *Protein flexibility is required for vesicle tethering at the Golgi*. Elife, 2015. **4**.
82. Derby, M.C., et al., *The trans-Golgi network golgin, GCC185, is required for endosome-to-Golgi transport and maintenance of Golgi structure*. Traffic, 2007. **8**(6): p. 758-73.
83. Reddy, J.V., et al., *A functional role for the GCC185 golgin in mannose 6-phosphate receptor recycling*. Mol Biol Cell, 2006. **17**(10): p. 4353-63.
84. Lu, L., G. Tai, and W. Hong, *Autoantigen Golgin-97, an effector of Arl1 GTPase, participates in traffic from the endosome to the trans-golgi network*. Mol Biol Cell, 2004. **15**(10): p. 4426-43.
85. Lee, I., et al., *Membrane adhesion dictates Golgi stacking and cisternal morphology*. Proc Natl Acad Sci U S A, 2014. **111**(5): p. 1849-54.
86. Dean, N., Y.B. Zhang, and J.B. Poster, *The VRG4 gene is required for GDP-mannose transport into the lumen of the Golgi in the yeast, Saccharomyces cerevisiae*. J Biol Chem, 1997. **272**(50): p. 31908-14.
87. Poster, J.B. and N. Dean, *The yeast VRG4 gene is required for normal Golgi functions and defines a new family of related genes*. J Biol Chem, 1996. **271**(7): p. 3837-45.
88. Gao, X.D. and N. Dean, *Distinct protein domains of the yeast Golgi GDP-mannose transporter mediate oligomer assembly and export from the endoplasmic reticulum*. J Biol Chem, 2000. **275**(23): p. 17718-27.
89. Bhave, M., et al., *Golgi enlargement in Arf-depleted yeast cells is due to altered dynamics of cisternal maturation*. J Cell Sci, 2014. **127**(Pt 1): p. 250-7.

90. Arakawa, K., et al., *Molecular cloning and characterization of a Pichia pastoris ortholog of the yeast Golgi GDP-mannose transporter gene*. J Gen Appl Microbiol, 2006. **52**(3): p. 137-45.
91. Sata, M., et al., *Brefeldin A-inhibited guanine nucleotide-exchange activity of Sec7 domain from yeast Sec7 with yeast and mammalian ADP ribosylation factors*. Proc Natl Acad Sci U S A, 1998. **95**(8): p. 4204-8.
92. Beraud-Dufour, S., et al., *A glutamic finger in the guanine nucleotide exchange factor ARNO displaces Mg²⁺ and the beta-phosphate to destabilize GDP on ARF1*. EMBO J, 1998. **17**(13): p. 3651-9.
93. Richardson, B.C. and J.C. Fromme, *Autoregulation of Sec7 Arf-GEF activity and localization by positive feedback*. Small GTPases, 2012. **3**(4): p. 240-3.
94. McDonold, C.M. and J.C. Fromme, *Four GTPases differentially regulate the Sec7 Arf-GEF to direct traffic at the trans-golgi network*. Dev Cell, 2014. **30**(6): p. 759-67.
95. Franzusoff, A., et al., *Localization of components involved in protein transport and processing through the yeast Golgi apparatus*. J Cell Biol, 1991. **112**(1): p. 27-37.
96. Rossanese, O.W., et al., *A role for actin, Cdc1p, and Myo2p in the inheritance of late Golgi elements in Saccharomyces cerevisiae*. J Cell Biol, 2001. **153**(1): p. 47-62.
97. Li, B. and J.R. Warner, *Mutation of the Rab6 homologue of Saccharomyces cerevisiae, YPT6, inhibits both early Golgi function and ribosome biosynthesis*. J Biol Chem, 1996. **271**(28): p. 16813-9.
98. Kjer-Nielsen, L., et al., *A novel Golgi-localisation domain shared by a class of coiled-coil peripheral membrane proteins*. Curr Biol, 1999. **9**(7): p. 385-8.

99. Munro, S. and B.J. Nichols, *The GRIP domain - a novel Golgi-targeting domain found in several coiled-coil proteins*. Curr Biol, 1999. **9**(7): p. 377-80.
100. Setty, S.R., et al., *Golgi recruitment of GRIP domain proteins by Arf-like GTPase 1 is regulated by Arf-like GTPase 3*. Curr Biol, 2003. **13**(5): p. 401-4.
101. Lee, F.J., et al., *Characterization of an ADP-ribosylation factor-like 1 protein in Saccharomyces cerevisiae*. J Biol Chem, 1997. **272**(49): p. 30998-1005.
102. Behnia, R., et al., *Targeting of the Arf-like GTPase Arl3p to the Golgi requires N-terminal acetylation and the membrane protein Sys1p*. Nat Cell Biol, 2004. **6**(5): p. 405-13.
103. Gillingham, A.K., A.C. Pfeifer, and S. Munro, *CASP, the alternatively spliced product of the gene encoding the CCAAT-displacement protein transcription factor, is a Golgi membrane protein related to giantin*. Mol Biol Cell, 2002. **13**(11): p. 3761-74.
104. Anderson, N.S., et al., *The Golgin protein Coy1 functions in intra-Golgi retrograde transport and interacts with the COG complex and Golgi SNAREs*. Mol Biol Cell, 2017.
105. Siniosoglou, S. and H.R. Pelham, *An effector of Ypt6p binds the SNARE Tlg1p and mediates selective fusion of vesicles with late Golgi membranes*. EMBO J, 2001. **20**(21): p. 5991-8.
106. Fridmann-Sirkis, Y., S. Siniosoglou, and H.R. Pelham, *TMF is a golgin that binds Rab6 and influences Golgi morphology*. BMC Cell Biol, 2004. **5**: p. 18.
107. VanRheenen, S.M., et al., *Sec34p, a protein required for vesicle tethering to the yeast Golgi apparatus, is in a complex with Sec35p*. J Cell Biol, 1999. **147**(4): p. 729-42.
108. Gillingham, A.K., et al., *The GTPase Arf1p and the ER to Golgi cargo receptor Erv14p cooperate to recruit the golgin Rud3p to the cis-Golgi*. J Cell Biol, 2004. **167**(2): p. 281-92.

109. Inoue, H., H. Nojima, and H. Okayama, *High efficiency transformation of Escherichia coli with plasmids*. Gene, 1990. **96**(1): p. 23-8.
110. Liu, H. and J.H. Naismith, *An efficient one-step site-directed deletion, insertion, single and multiple-site plasmid mutagenesis protocol*. BMC Biotechnol, 2008. **8**: p. 91.
111. Higuchi, R., et al., *A general method for cloning eukaryotic structural gene sequences*. Proc Natl Acad Sci U S A, 1976. **73**(9): p. 3146-50.
112. Day, K.J., et al., *Improved deconvolution of very weak confocal signals*. F1000Res, 2017. **6**: p. 787.
113. Sherman, F., *Getting started with yeast*. Methods Enzymol, 2002. **350**: p. 3-41.
114. Becker, D.M. and L. Guarente, *High-efficiency transformation of yeast by electroporation*. Methods Enzymol, 1991. **194**: p. 182-7.
115. Looke, M., K. Kristjuhan, and A. Kristjuhan, *Extraction of genomic DNA from yeasts for PCR-based applications*. Biotechniques, 2011. **50**(5): p. 325-8.
116. Harju, S., H. Fedosyuk, and K.R. Peterson, *Rapid isolation of yeast genomic DNA: Bust n' Grab*. BMC Biotechnol, 2004. **4**: p. 8.
117. Jagilinki, B.P., et al., *Functional Basis and Biophysical Approaches to Characterize the C-Terminal Domain of Human-Ribosomal S6 Kinases-3*. Cell Biochem Biophys, 2016. **74**(3): p. 317-25.
118. Siddiqui, M.Q., et al., *Structural and biophysical properties of h-FANCI ARM repeat protein*. J Biomol Struct Dyn, 2017. **35**(14): p. 3032-3042.
119. Ishida, R., et al., *GM130 is a parallel tetramer with a flexible rod-like structure and N-terminally open (Y-shaped) and closed (I-shaped) conformations*. FEBS J, 2015. **282**(11): p. 2232-44.

120. Sambrook, J. and D.W. Russell, *SDS-Polyacrylamide Gel Electrophoresis of Proteins*. CSH Protoc, 2006. **2006**(4).
121. Mahmood, T. and P.C. Yang, *Western blot: technique, theory, and trouble shooting*. N Am J Med Sci, 2012. **4**(9): p. 429-34.
122. James, P., *Yeast two-hybrid vectors and strains*. Methods Mol Biol, 2001. **177**: p. 41-84.
123. Brandizzi, F. and C. Barlowe, *Organization of the ER-Golgi interface for membrane traffic control*. Nat Rev Mol Cell Biol, 2013. **14**(6): p. 382-92.
124. Papanikou, E. and B.S. Glick, *Golgi compartmentation and identity*. Curr Opin Cell Biol, 2014. **29**: p. 74-81.
125. Yu, I.-M. and F.M. Hughson, *Tethering Factors as Organizers of Intracellular Vesicular Traffic*. Annual Review of Cell and Developmental Biology, 2010. **26**(1): p. 137-156.
126. Goud, B. and P.A. Gleeson, *TGN golgins, Rab and cytoskeleton: regulating the Golgi trafficking highways*. Trends in Cell Biology. **20**(6): p. 329-336.
127. Cheung, P.Y. and S.R. Pfeffer, *Transport Vesicle Tethering at the Trans Golgi Network: Coiled Coil Proteins in Action*. Front Cell Dev Biol, 2016. **4**: p. 18.
128. Lu, L. and W. Hong, *Interaction of Arl1-GTP with GRIP domains recruits autoantigens Golgin-97 and Golgin-245/p230 onto the Golgi*. Mol Biol Cell, 2003. **14**(9): p. 3767-81.
129. Lupas, A., M. Van Dyke, and J. Stock, *Predicting coiled coils from protein sequences*. Science, 1991. **252**(5009): p. 1162-1164.
130. Wong, M., A.K. Gillingham, and S. Munro, *The golgin coiled-coil proteins capture different types of transport carriers via distinct N-terminal motifs*. BMC Biol, 2017. **15**(1): p. 3.

131. Klumperman, J., *Architecture of the mammalian Golgi*. Cold Spring Harb Perspect Biol, 2011. **3**(7).
132. Wang, Y. and J. Seemann, *Golgi biogenesis*. Cold Spring Harb Perspect Biol, 2011. **3**(10): p. a005330.
133. Zhang, X. and Y. Wang, *GRASPs in Golgi Structure and Function*. Front Cell Dev Biol, 2015. **3**: p. 84.
134. Ramirez, I.B. and M. Lowe, *Golgins and GRASPs: holding the Golgi together*. Semin Cell Dev Biol, 2009. **20**(7): p. 770-9.
135. Alzhanova, D. and D.E. Hruby, *A trans-Golgi network resident protein, golgin-97, accumulates in viral factories and incorporates into virions during poxvirus infection*. J Virol, 2006. **80**(23): p. 11520-7.
136. Jain, B.K., et al., *Identification and characterization of GRIP domain Golgin PpImh1 from Pichia pastoris*. Yeast, 2018.
137. Panic, B., et al., *Structural basis for Arl1-dependent targeting of homodimeric GRIP domains to the Golgi apparatus*. Mol Cell, 2003. **12**(4): p. 863-74.
138. Yoshino, A., et al., *tGolgin-1 (p230, golgin-245) modulates Shiga-toxin transport to the Golgi and Golgi motility towards the microtubule-organizing centre*. J Cell Sci, 2005. **118**(Pt 10): p. 2279-93.
139. Lieu, Z.Z., et al., *The golgin GCC88 is required for efficient retrograde transport of cargo from the early endosomes to the trans-Golgi network*. Mol Biol Cell, 2007. **18**(12): p. 4979-91.
140. Nakamura, N., et al., *Characterization of a cis-Golgi matrix protein, GM130*. J Cell Biol, 1995. **131**(6 Pt 2): p. 1715-26.

141. Slusarewicz, P., et al., *Isolation of a matrix that binds medial Golgi enzymes*. J Cell Biol, 1994. **124**(4): p. 405-13.
142. Waters, M.G., D.O. Clary, and J.E. Rothman, *A novel 115-kD peripheral membrane protein is required for intercisternal transport in the Golgi stack*. J Cell Biol, 1992. **118**(5): p. 1015-26.

Appendix

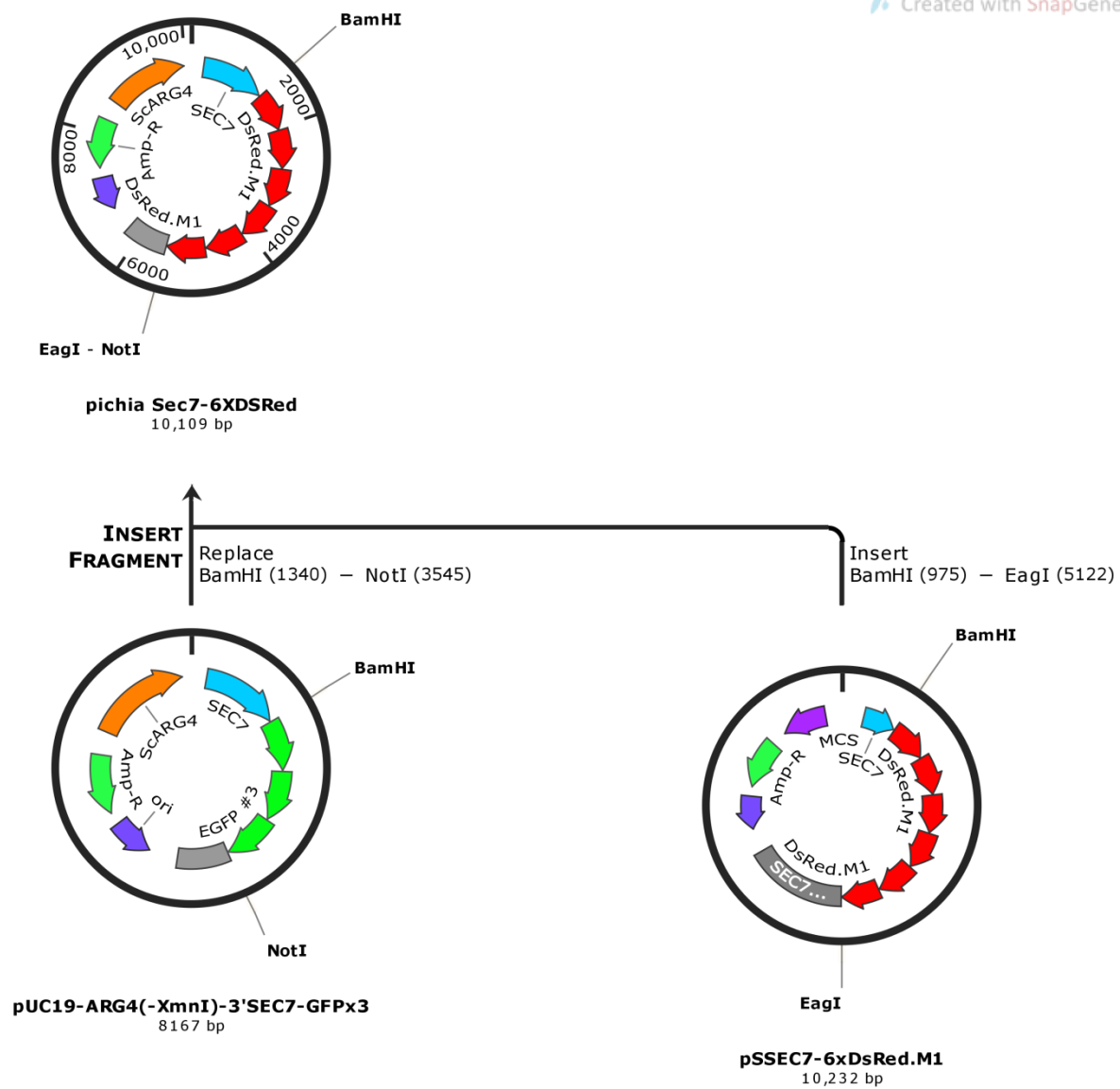
Appendix 1

1.1 msGFP-VIG4pIB1

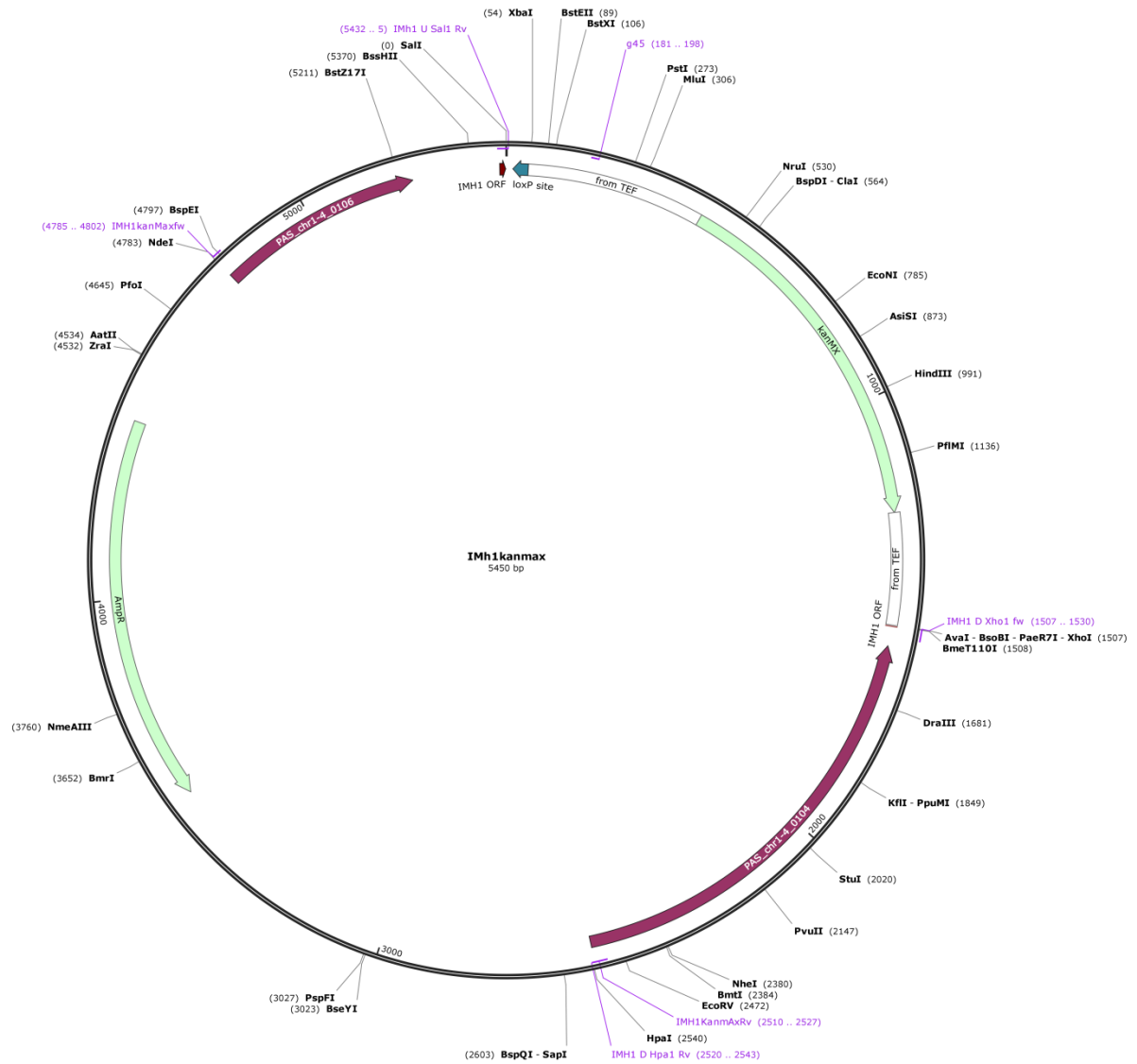


1.2 Cloning strategy for SEC7-6xDsRed.M1

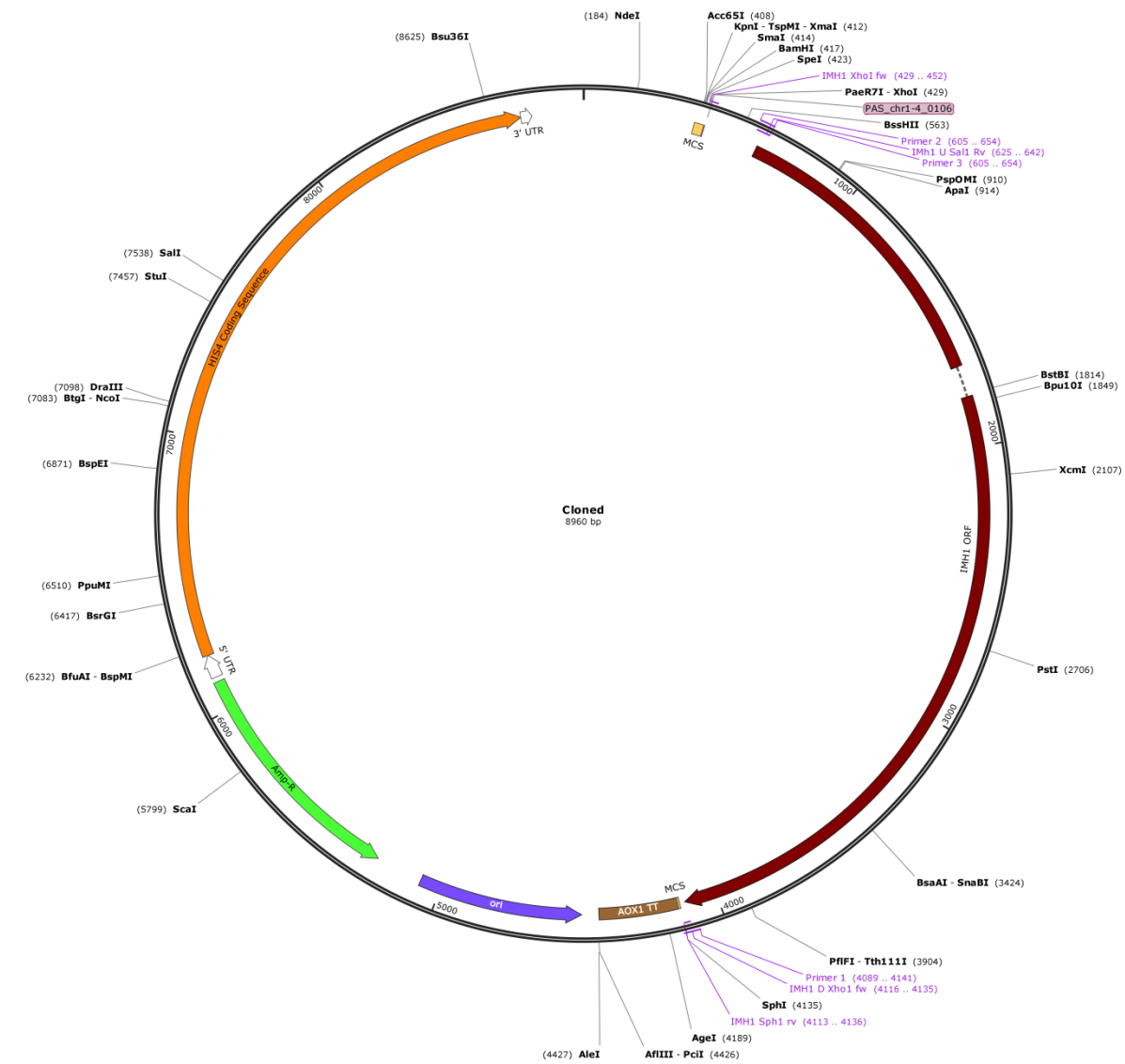
Created with SnapGene®



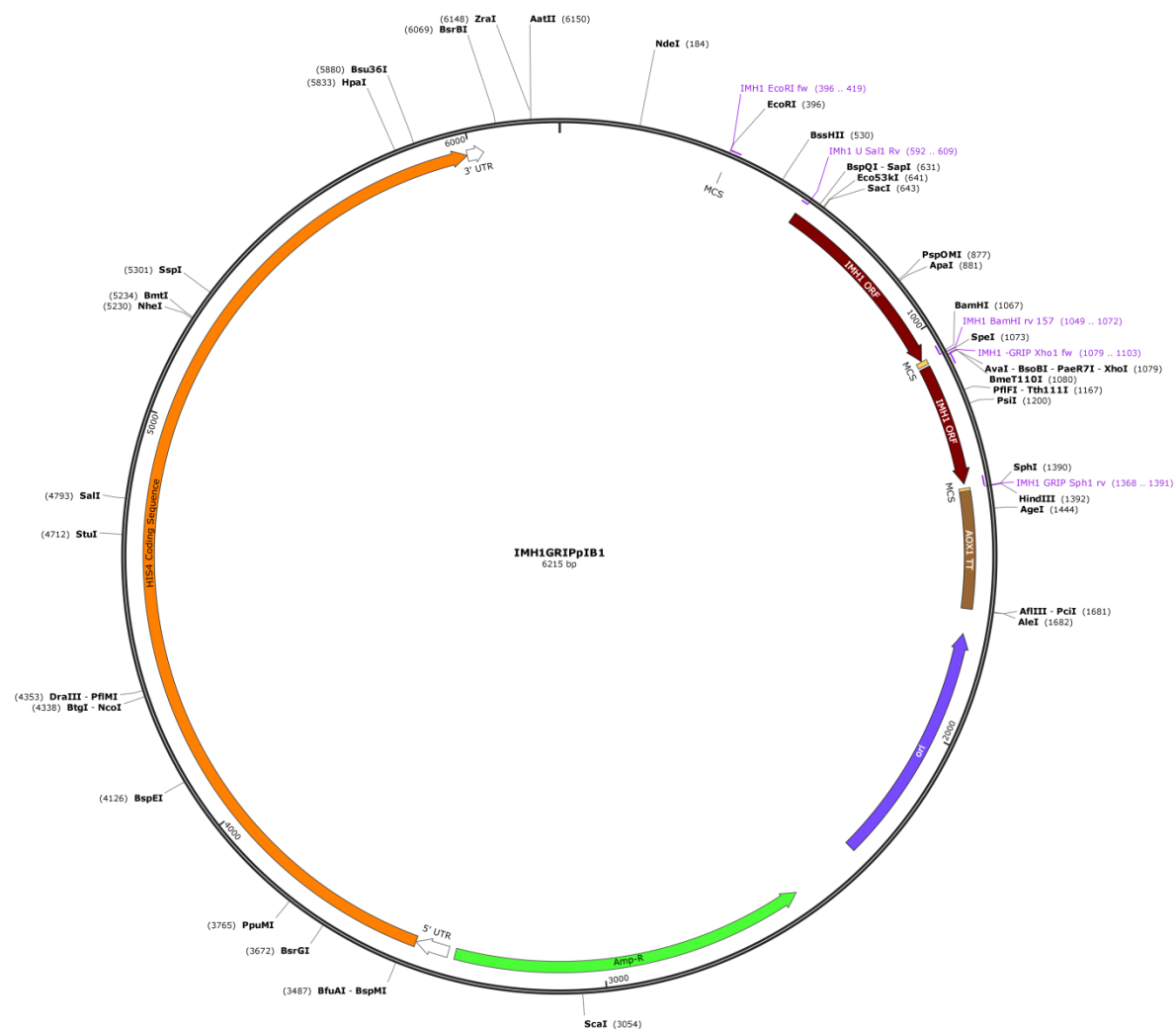
1.3 IMH1pUG6



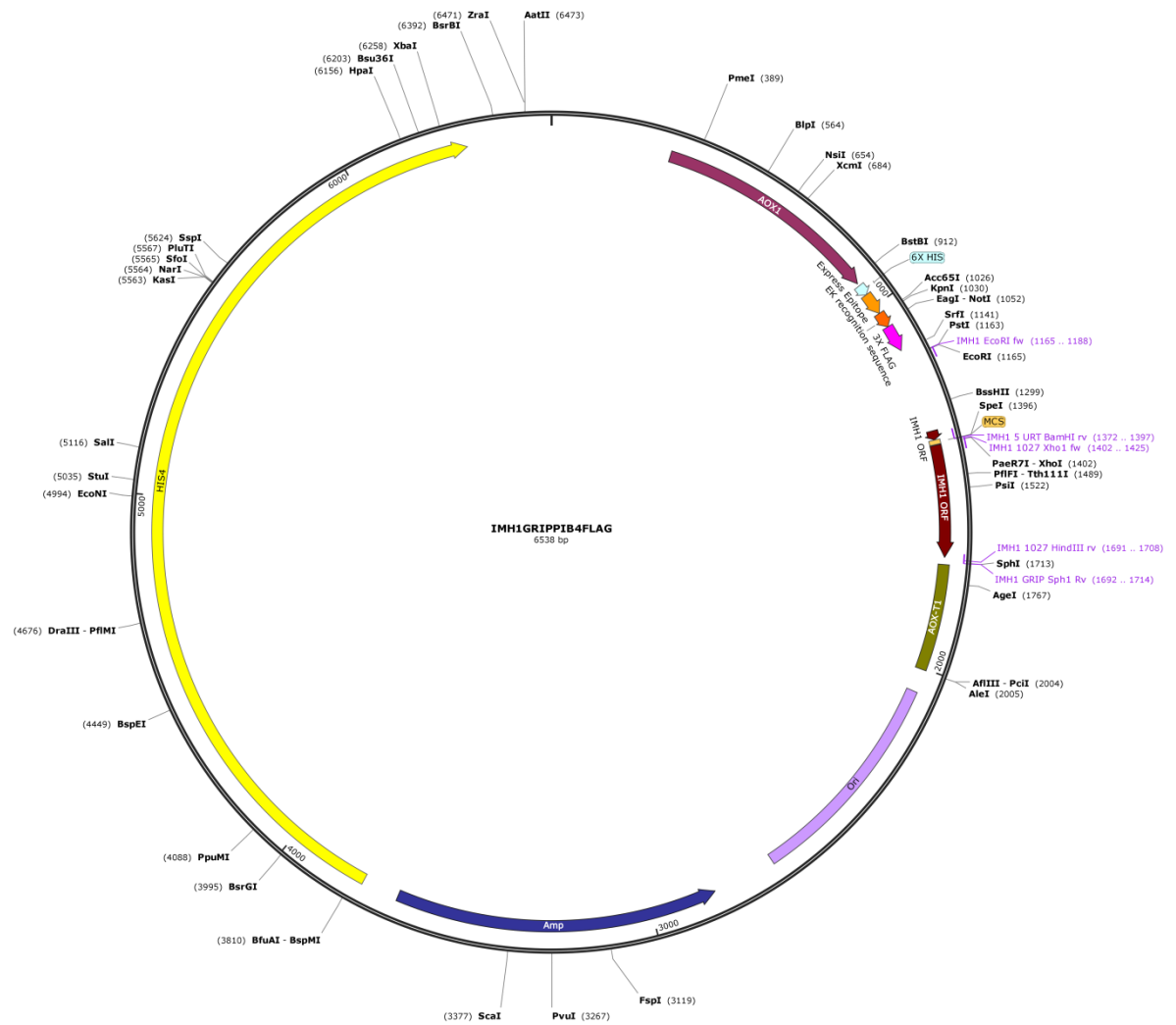
1.4 IMH1pIB1



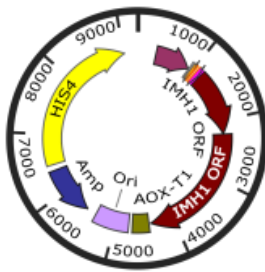
1.5 IMH1GRIPpIB1



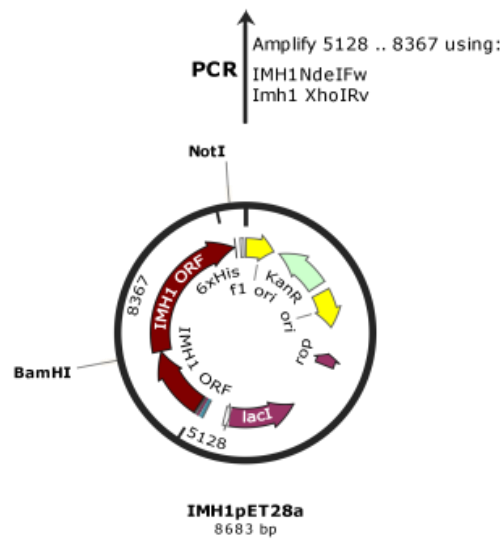
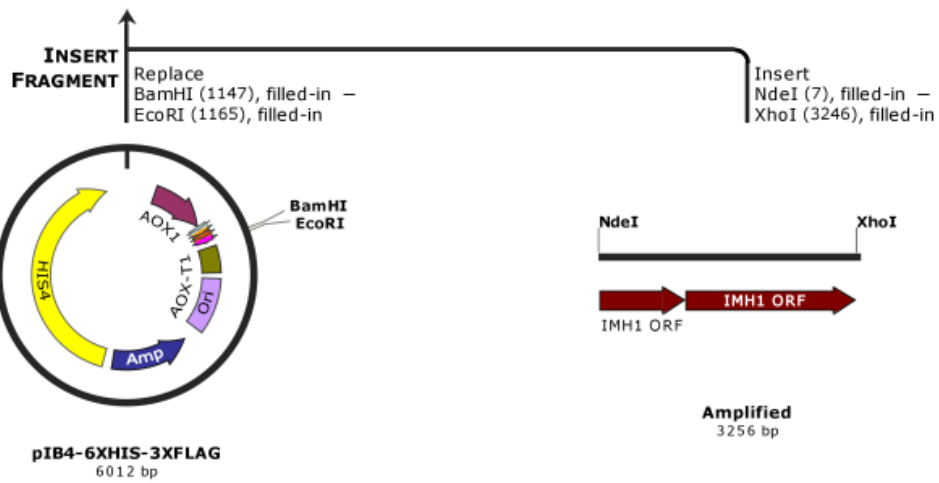
1.6 IMH1GRIP-pIB4



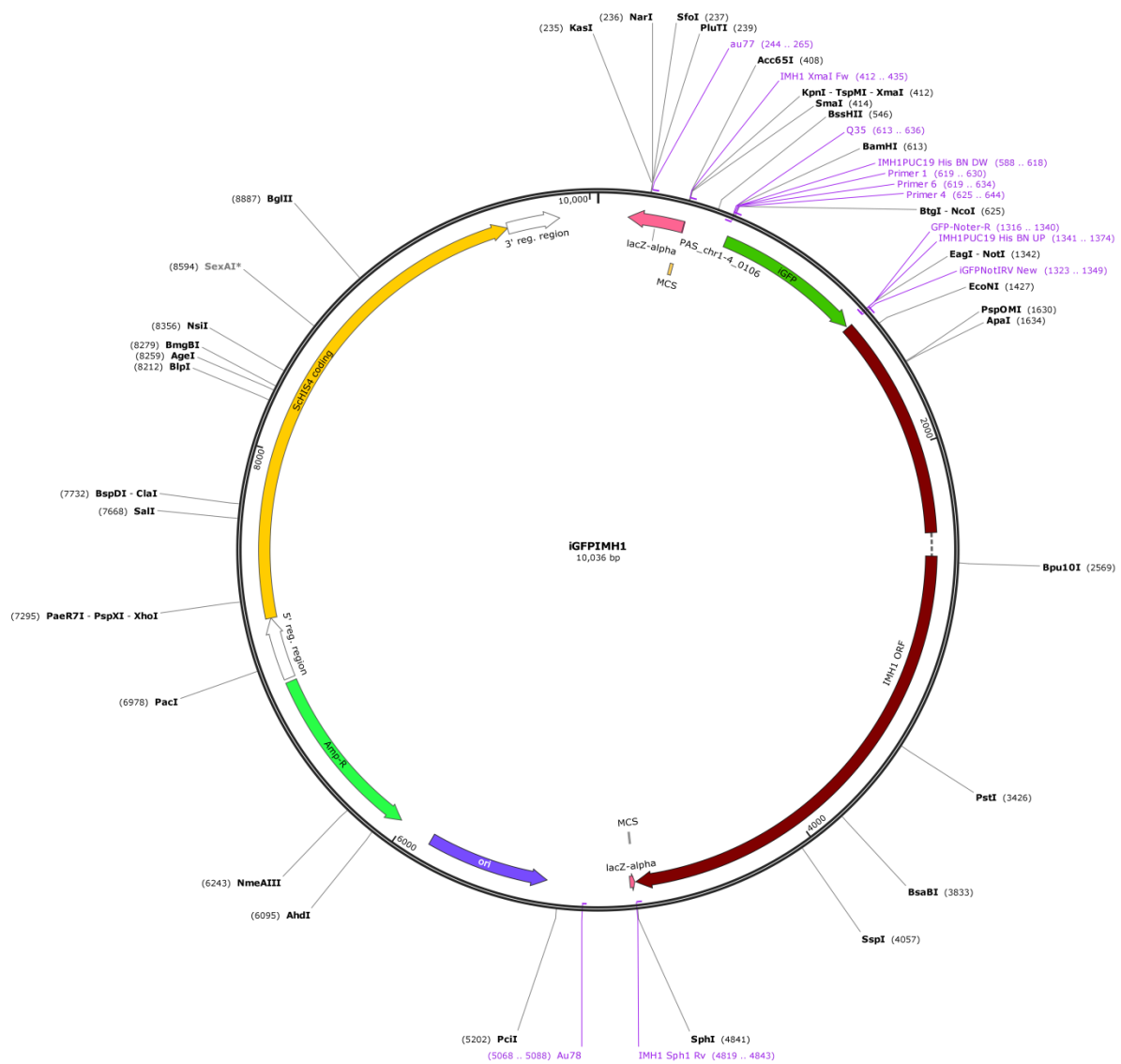
1.7 Cloning strategy for IMH1CC-pIB4



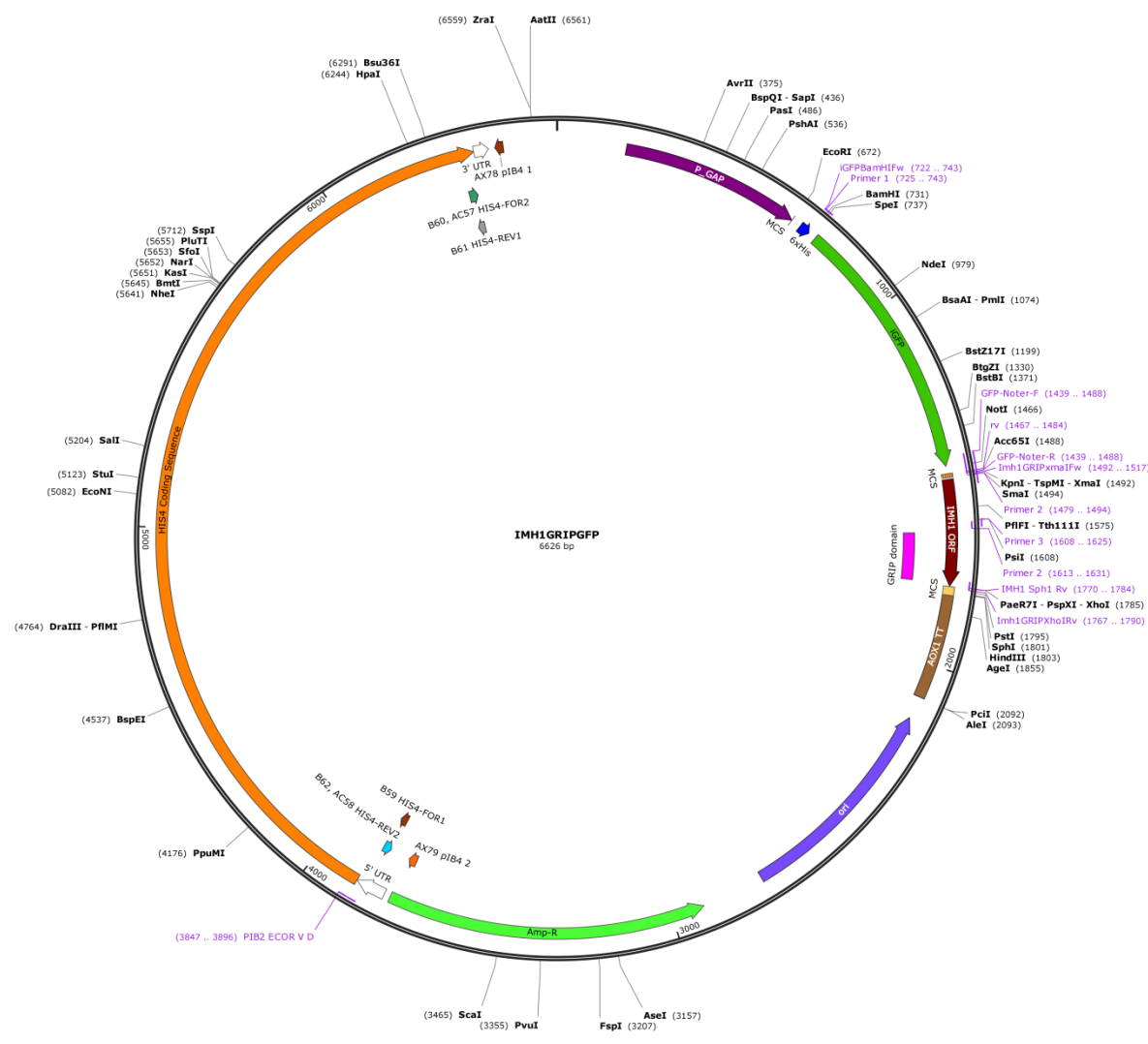
Cloned
9241 bp



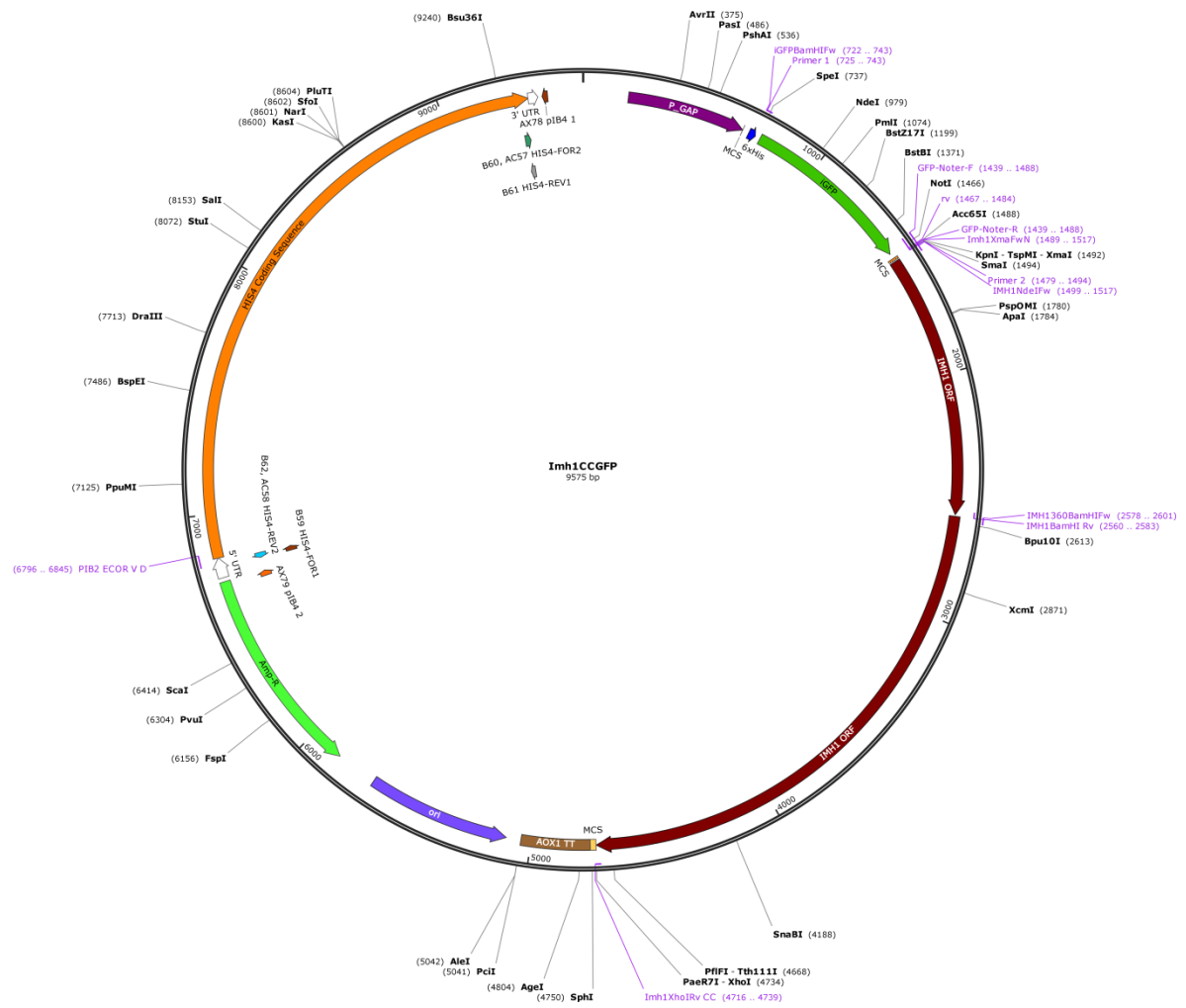
1.8 GFP-IMH1



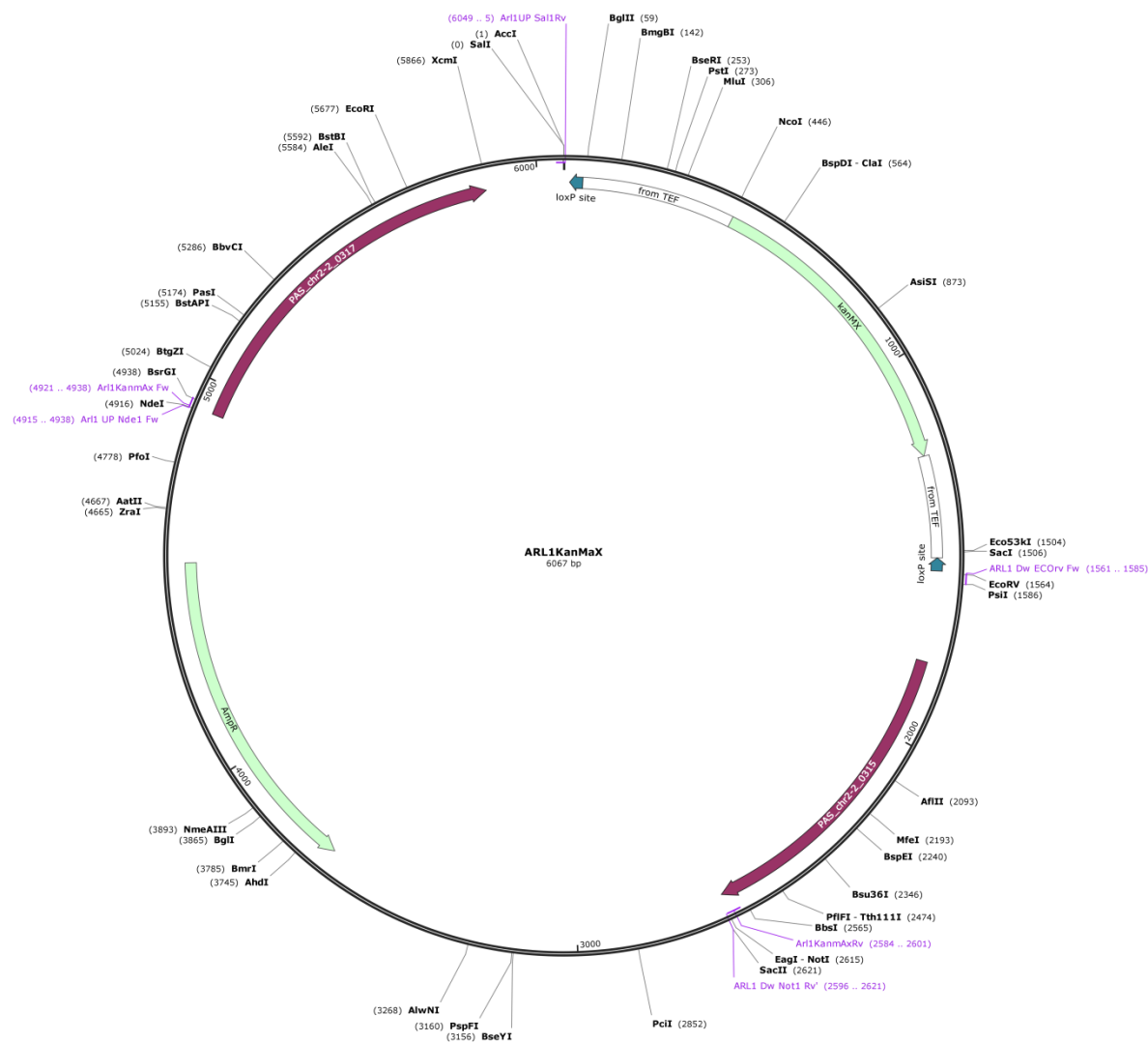
1.9 GFP-GRIP



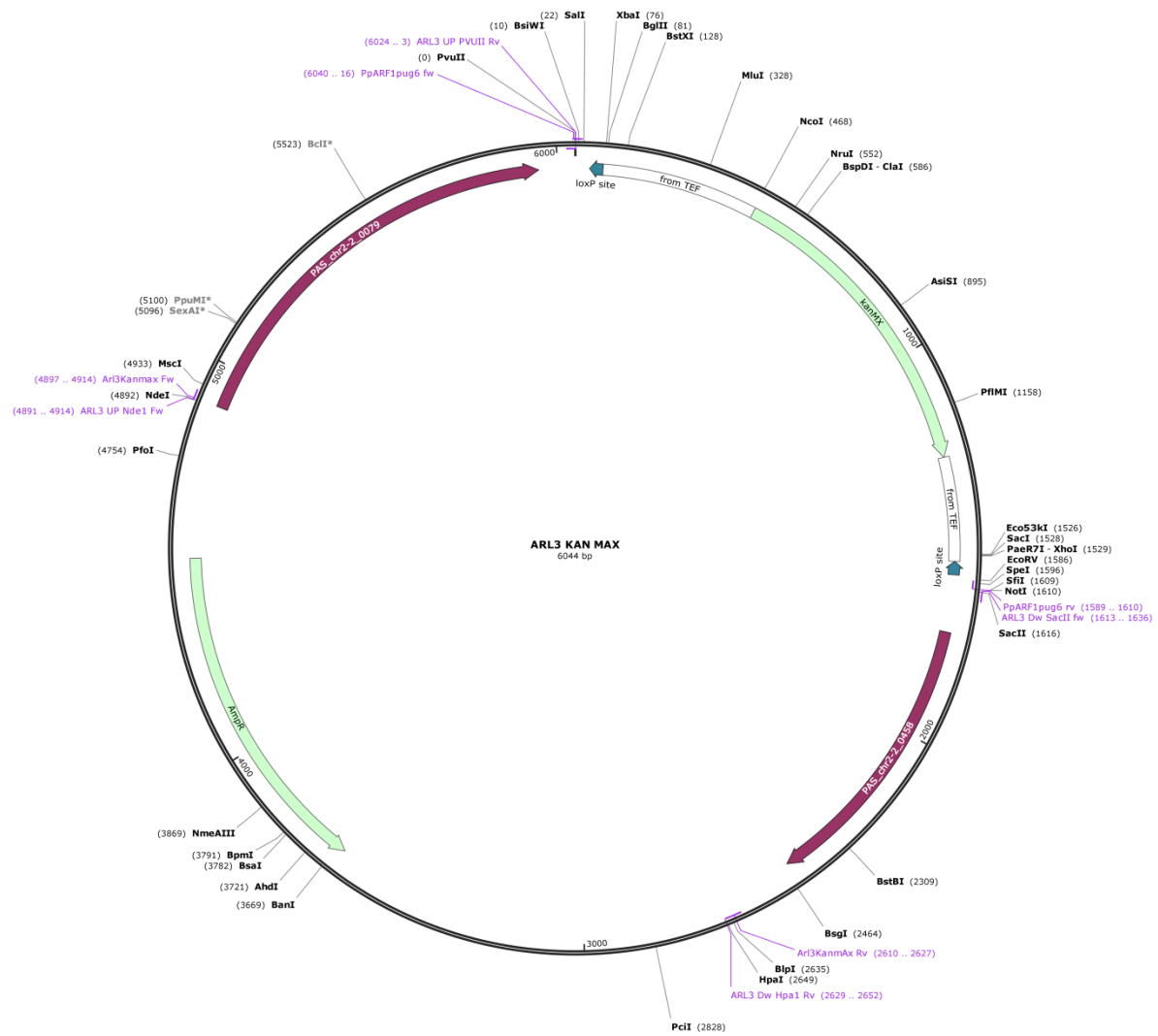
1.10 GFP-IMH1CC



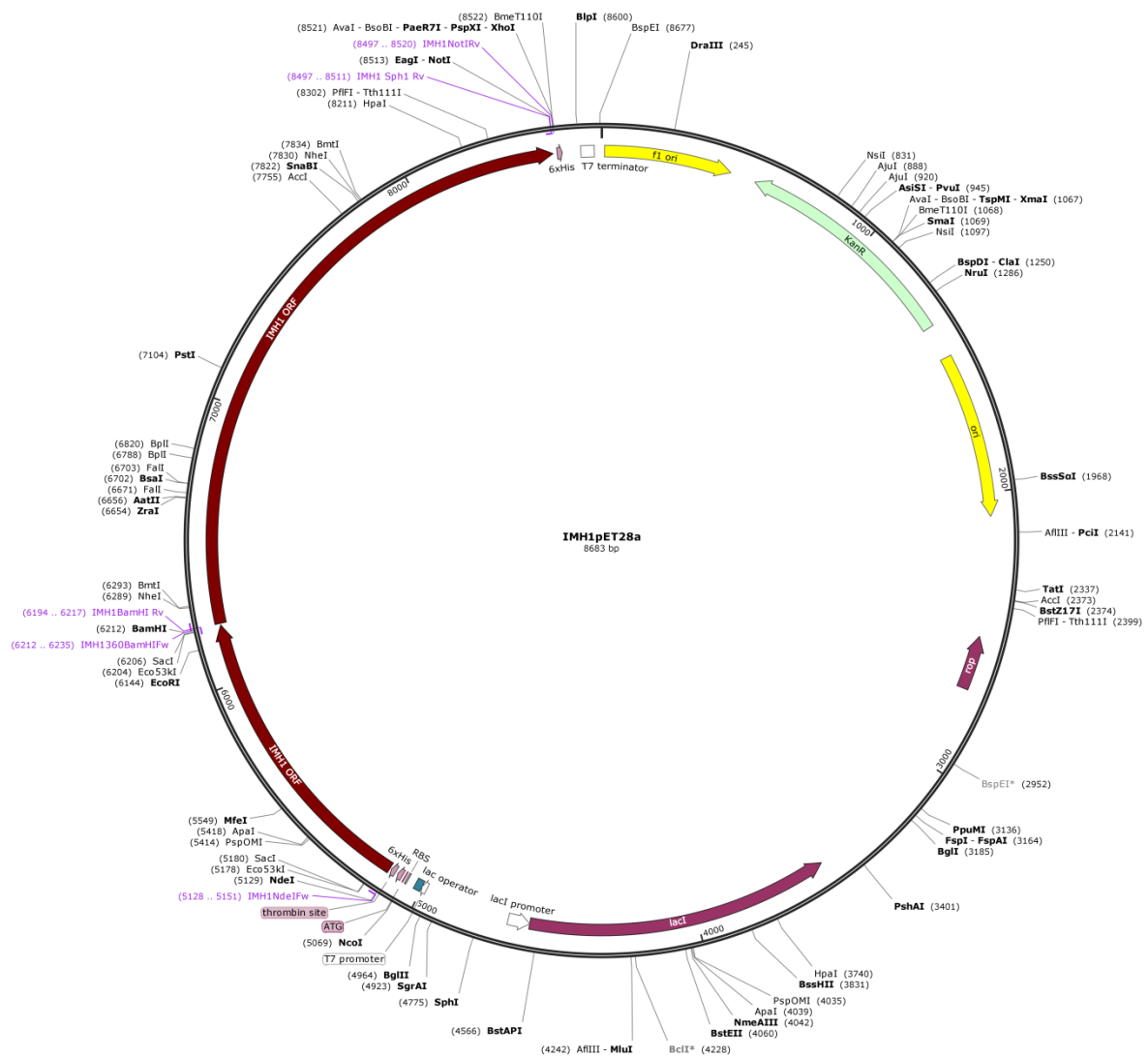
1.11 Arl1pUG



1.12 Arl3pUG6



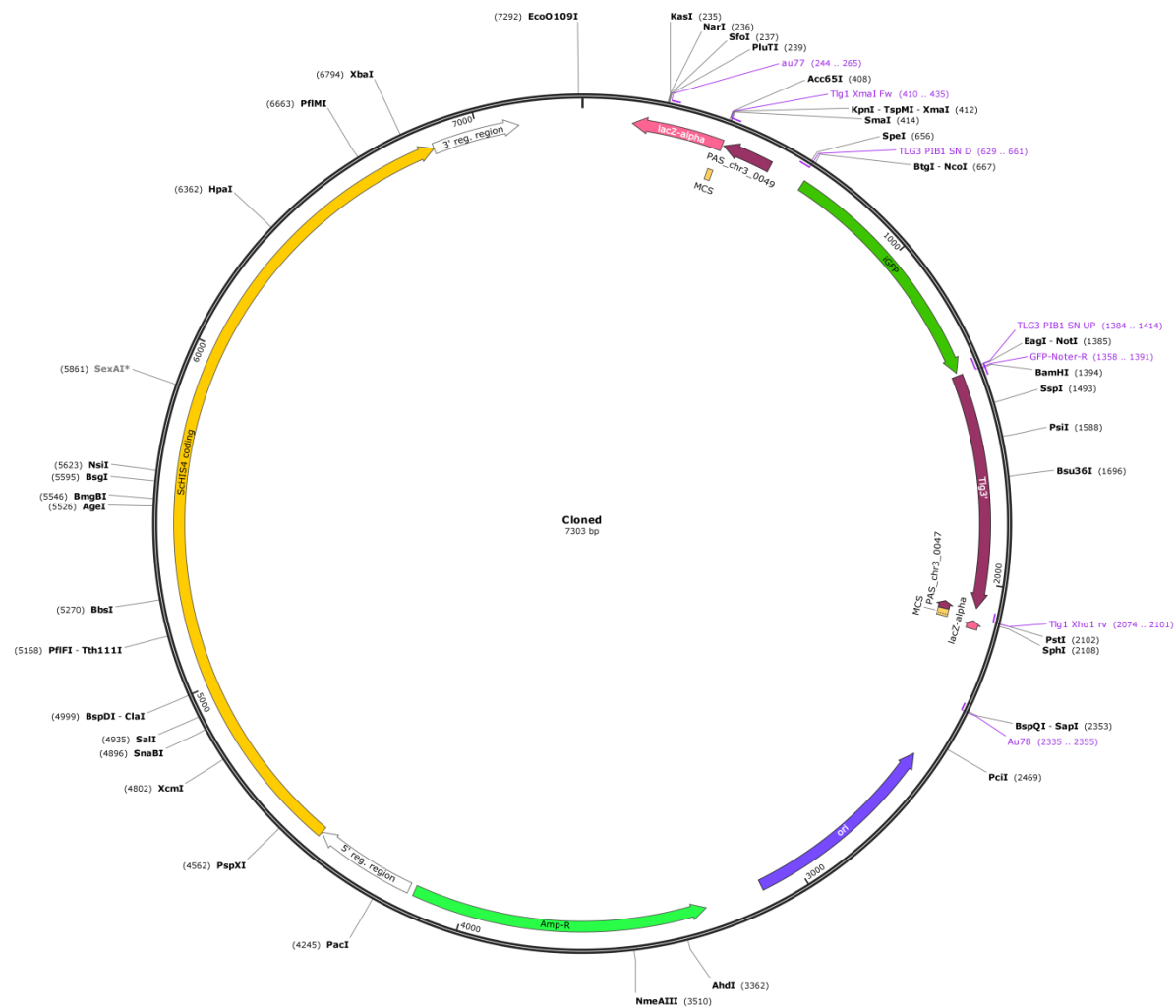
1.13 IMH1pET28a



1.14 IMH1N(1-100)ΔpUC19His



1.15 GFP-TLG1pUC19His



Appendix 2 List of yeast strains used in the study

Sr.No	Strain Name	Genotype
1	PPY12	his4 arg4
2	PPY12 msGFP-VIG4 SEC7-DsRed.M1x6	msGFP-VIG4His4::his4SEC7-DsRed.M1x6 pUC19Arg::ARG4
3	PPY12 msGFP-VIG4 SEC7-DsRed.M1x6 <i>imh1</i> Δ	msGFP-VIG4His4::his4SEC7-DsRed.M1x6 pUC19Arg::ARG4 IMH1::IMH1 Kanmax
4	PPY12 msGFP-VIG4 SEC7-DsRed.M1x6 <i>imh1</i> Δ-IMH-PIB1	msGFP-VIG4::hygroSEC7-DsRed.M1x6 pUC19Arg::ARG4 IMH1::IMH1 Kanmax /IMH1-pIB1
5	PPY12 msGFP-VIG4 SEC7-DsRed.M1x6 <i>imh1</i> Δ-IMHGRIP-PIB1	msGFP-VIG4::hygroSEC7-DsRed.M1x6 pUC19Arg::ARG4 IMH1::IMH1 Kanmax /GRIPIMH1-pIB1
6	PPY12 msGFP-VIG4 SEC7-DsRed.M1x6 <i>imh1</i> CCA	msGFP-VIG4His4::his4SEC7-DsRed.M1x6 pUC19Arg::ARG4 IMH1::IMH1 CCKanmax
7	PPY12 msGFPVIG4 SEC7DsRed.M1x6 <i>arl1</i> Δ	msGFP-VIG4His4::his4SEC7-DsRed.M1x6 pUC19Arg::ARG4 ARL1::ARL1 Kanmax
8	PPY12 msGFPVIG4 SEC7DsRed.M1x6 <i>arl3</i> Δ	msGFP-VIG4His4::his4SEC7-DsRed.M1x6 pUC19Arg::ARG4 ARL3::ARL3 Kanmax
9	PPY12 iGFP-IMH1	iGFP-IMH1His4::his4
10	PPY12 iGFP-IMH1 SEC7-DsRed.M1x6	iGFP-IMH1His4::his4SEC7-DsRed.M1x6 pUC19Arg::ARG4
11	PPY12 iGFP-IMH1 mcherry-VIG4-bAG32	iGFP-IMH1His4::his4 mcherry-VIG4-

		bAG32 Hygro
12	PPY12 iGFP-IMH1GRIP-PIB4	GFP-IMH1GRIPpIB4HIS4:: his4
13	PPY12 iGFP-IMH1CC-PIB4	GFP-IMH1CCpIB4HIS4:: his4
14	PPY12 iGFP-IMH1 arl1Δ	iGFP-IMH1HIS4::his4 ARL1::arl1Kanmax
15	PPY12 iGFP-IMH1 arl3Δ	iGFP-IMH1HIS4::his4 ARL3::arl3Kanmax
16	PPY12 iGFP-TLG1 SEC7DsRed.M1x6	GFP-TLG1HIS4::his4 SEC7-DsRed.M1x6Arg4::arg4
17	PPY12 iGFP-TLG1 SEC7DsRed.M1x6 imh1Δ	GFP- TLG1HIS4::his4SEC7-DsRed.M1x6 M1x6Arg4::arg4IMH1::imh1Kanmax
18	PPY12 iGFP-TLG1 SEC7DsRed.M1x6 imh1CCAΔ	GFP- TLG1HIS4::his4SEC7-DsRed.M1x6 M1x6Arg4::arg4IMH1::imh1CCKanmax
19	PPY12 iGFP-TLG1 SEC7DsRed.M1x6 imh1(1-100)Δ	GFP- TLG1HIS4::his4SEC7-DsRed.M1x6 M1x6Arg4::arg4IMH1::imh1(1-100)Kanmax
20	PPY12 msGFPVIG4 SEC7DsRed.M1x6 <i>imh1(1-100)Δ</i>	msGFP- VIG4His4::his4SEC7-DsRed.M1x6 pUC19Arg::ARG4 IMH1::IMH1(1-100)Kanmax
21	PPY12 GFPGRIPpIB2	his4 arg4 GFP-GRIPpIB2::HIS4
22	PPY12 GFPGRIP(T-A)pIB2	his4 arg4 GFP-GRIP(Y-A)pIB2::HIS4
23	PPY12 GFPGRIPpIB2 PpSEC7-DsRed.M1x6	his4 arg4 GFPGRIP:: HIS4 SEC7-DsRed.M1x6 pUC19Arg::ARG4
24	PPY12 iGFPImh1 arl1Δ	his4 arg4 GFP- <i>PpImh1</i> - pUC19His::HIS4 <i>PpArl1</i> ::Kanmax

Appendix 3 List of Constructs used in the study

Sr.No	Construct Name
1	msGFP-VIG4-pIB1
2	SEC7DsRed.M1x6
3	pUG6- <i>PpIMH1</i> ::KanMAX
4	IMH1-pIB1
5	GRIPIMH1-pIB1
6	GFP-GRIPIMH1-pIB4
7	GFP-CCIMH1-pIB4
8	pUG6- <i>PpARL3</i> :: KanMAX
9	pUG6- <i>PpARL1</i> :: KanMAX
10	iGFP-IMH1-pUC19His
11	pUG6- <i>PpIMH1CC</i> ::KanMAX
12	iGFP-TLG1-pIB1
13	IMH1(1-100) Δ -pUC19His
14	mCherry-VIG4-bAG32
15	GFP-GRIPpIB2
16	GFP-GRIP(Y-A)pIB2
17	SEC7-DsRed.M1x6 pUC19Arg
18	<i>PpImh</i> -pET28a
19	<i>PpImh1</i> -pGAD
20	<i>PpImh1</i> -pGBDU
21	<i>PpImh1</i> (725-1124)-pGAD
22	<i>PpImh1</i> (725-1124)-pGBDU
23	<i>PpImh1</i> (1-355)-pGAD
24	<i>PpImh1</i> (1-355)-pGBDU
25	pGAD
26	pGBDU
27	pUG6- <i>PpArl1</i> ::KanMAX

Appendix 4 List of primers used in the study

Sr.No	Name of Primer	Sequence (5-3)
1	VIG4EcoRIFw	CTATAGAATTCATCTCGTACCTATTCTG
2	VIG4SphIRv	CAATTGCATGCGctagctctgtcagttgcta
3	VIG4BamHI-NotIUP	atacttatcatcaagcaagacatCCGCGGCCGcATTACGGATCCatggctgacaaagatcggtacggg
4	VIG4BamHI-NotIDw	ccgctaccgatcctttgtcagccatGGATCCGTAATgCGGCCGCGGatgtcttgctttgatataagtat
5	msGFPVig4SacIFw	tctacGAGCTCCATCTCGTACCTATTCTG
6	msGFPVig4SpeIRv	cgtacACTAGTCATGCGctagctctgtca
7	IMH1 U Nde1 Fw	cgcggCATATGttattgaagatgaaagt
8	IMH1 U Sal1 Rv	gttcgGTCGACgttttgagaacatctacc
9	IMH1 D Xho1 fw	tagtaCTCGAGctgtttcctcgggatg
10	IMH1 D Hpa1 Rv	ttagtGTTAACTgattcatcctctgttt
11	Kamaxintcheckfw	ggatgtatgggctaaatg
12	IMH1GRIP Xho1 fw	gtgacCTCGAGcagttgctgaagttcgag
13	IMH1GRIP HindIIIrv	gccggAAGCTTaaccagcttattttaatg
14	IMH1 XmaIFw	ctggcCCCGGGctttaatgttaatagaca
15	IMH1Nterm100AABamHIRv	GctacGGATCCcatctaccttcaaaagaa
16	IMH1Nterm100AABamHIfw	gagcgGGATCCgcgaatatgacgagaaa
17	IMH1 Sph1 Rv	gtcgtGCATGCTtattttaatgagctggc
18	IMH1 Sph1 Rv	gtcgtGCATGCTtattttaatgagctggc
19	IMH1 XmaIFw	ctggcCCCGGGctttaatgttaatagaca
20	IMH1 BamHI fw	gcggcGGATCCctttaatgttaatagaca
21	IMH1 Coiled coil Sph1 Rv	catctGCATGCTctacttctctgattgac
22	TLg1 XmaIFw	aactaCCCGGGgtcgaatatgactgtcgc
23	TLg1 Xho1 rv	ggctgCTCGAGataagtgtttgtttacat
24	TLG3 PIB1 SN UP	actcagaaaccttaagaacaacatCgactagttgactGCGGCCGcatggatccatttaagatgttta
25	TLG3 PIB1 SN D	taaacatcattaaatggatccatgCGGCCCGcagtaactagtcGatgtttgtcttaaggtttctgagt
26	ARL3 UP Nde1 Fw	tattgCATATGgttatcgtgggaagcgggt
27	ARL3 UP Sal1 Rv	gaaggGTCGACggaagagaacaggtgaag
28	ARL3 Dw SacIIfw	gtttaCCGCGGatgttggtgacgttcgct
29	ARL3 Dw Hpa1 Rv	tatgtGTTAACTgtatggctgagcaaggt
30	Arl1 UP Nde1 Fw	tgtagCATATGgagtgaggagataatcagt
31	Arl1UP Sal1Rv	agaggGTCGACggagaattgattgaagat
32	ARL1 Dw ECOrvFw	tcgatGATATCtatatgaaacgggtatgtt
33	ARL1 Dw Not1 Rv'	agtcgGCGGCCGCgctgaccttaactcttg
34	Imh1CCXmaFw	ctgtaCCCGGGGgatgttctcaaaacttcc
35	Imh1CCXhoIRv	cgttaCTCGAGattttcatcactccccgc
36	Imh1GRIPxmaIFw	gtccgCCCGGGGCctgaagttcgagagactg
37	Imh1GRIPXhoIRv	gcattCTCGAGttttaatgagctggctaa
38	PpImh1NdeIFw	GTGTACATATGatgttctcaaaacttcc
39	PpImh1NotIRv	GttttGCGGCCGCttttaatgagctggc
40	PpImh1GRIPXmaIFw	gtccgCCCGGGGCctgaagttcgagagactg
41	PpImh1GRIPXhoIRv	gcattCTCGAGttttaatgagctggctaa
42	GRIP(Y-A)Up	aaaatgagagagataaagttgccGCAattaagaacgtccttctaggtatt
43	GRIP(Y-A)Dw	aaatcctagaaggagcttcttaattGCGgcaactttatctctctcattttc
44	PpImh1NtermBamHIFw	GCGGATCCGGCAGCTatgttctcaaaacttcc
45	PpImh1 NtermSal1Rv	cctatGTCGACtatctgtgacttttctcc
46	PpImh1CtermBamHI	GCGGATCCGGCAGCTattgccgaagaaaaagcc
47	PpImh1CtermSal1Rv	gctgtGTCGACttttaatgagctggctaa
48	PpImh1XmaIFw	GTGTACCCGGGatgttctcaaaacttcc
49	PpImh1Sal1Rv	gtgctGTCGACttttaatgagctggctaa

Publication

Identification and characterization of GRIP domain Golgin *PpImh1* from *Pichia pastoris*

Bhawik Kumar Jain^{1,2} | Pankaj Singh Thapa^{1,2} | Ashok Varma^{1,2} |
Dibyendu Bhattacharyya^{1,2} 

¹Advanced Centre for Treatment Research and Education in Cancer, Tata Memorial Centre, Kharghar, Navi Mumbai 410210 MH, India

²Training School Complex, Homi Bhabha National Institute, Anushakti Nagar, Mumbai, MH 400085, India

Correspondence

Dibyendu Bhattacharyya, Advanced Centre for Treatment Research and Education in Cancer, Tata Memorial Centre, Kharghar, Navi Mumbai 410210 MH, India.
Email: dbhattacharyya@actrec.gov.in

Funding information

Department of Biotechnology, Govt. of India, Grant/Award Number: 102/IFD/SAN/2282/2012-2013

Abstract

Budding yeast *Pichia pastoris* has highly advanced secretory pathways resembling mammalian systems, an advantage that makes it a suitable model system to study vesicular trafficking. Golgins are large Golgi-resident proteins, primarily reported to play role in cargo vesicle capture, but details of such mechanisms are yet to be deciphered. Golgins that localize to the Golgi via their GRIP domain, a C-terminal Golgi anchoring domain, are known as GRIP domain Golgins. In this present study, we have identified and functionally characterized a homologue of one such GRIP domain Golgin protein, Imh1, from the budding yeast *P. pastoris*. We have demonstrated that the GRIP domain present at the C-terminal of *P. pastoris* Imh1 (*PpImh1*) functions as its Golgi-targeting sequence. Using a combination of yeast two-hybrid analysis, dynamic light scattering and electron microscopy, we have shown that *PpImh1* can self-associate and form a homodimer. Analysis of purified recombinant *PpImh1* by CD spectroscopy indicates the presence of an 85% α -helical structure, a characteristic of high-content α -helical coiled-coil sequences normally present in other Golgin family proteins. Two-hybrid analysis indicated self-interaction between C-terminal fragments, yet N-terminal fragments do not mediate any such form of self-interaction, suggesting that *PpImh1* may form a parallel dimer. Electron microscopy data indicates that *PpImh1* forms extended rod-like homo-dimeric molecules with splayed N-terminal end which can act as a tether for capturing vesicles. Our study provides the first evidence in support of the dimeric Y-shaped structure for any Golgin in the budding yeast.

KEYWORDS

Golgi, GRIP domain, *Pichia pastoris*, *PpImh1*

1 | INTRODUCTION

The Golgi apparatus, being present in almost all eukaryotic systems, plays a central role in the secretory pathway (Lowe, 2011). Proteins are synthesized in the endoplasmic reticulum (ER), folded properly and finally packaged into transport vesicles, which then delivers them to the Golgi (Brandizzi & Barlowe, 2013). There are various types of vesicles that participate in the secretory pathways. COPII vesicles or clathrin-coated vesicles usually carry the cargo proteins that are to

be transported via the anterograde pathway. Some ER-resident proteins are brought back to ER in the retrograde pathway via COPI vesicles (Papanikou & Glick, 2014). Golgins are reported to mediate the upstream 'tethering' of any incoming vesicle to Golgi, before their fusion with the Golgi membrane, to form initial contacts (Yu & Hughson, 2010). Usually Golgins are large α -helical coiled-coil domain proteins present at different Golgi locations. GM130, p115 and GMAP-210 localize to the *cis*-Golgi, the GRIP domain Golgins (Golgin-97, Golgin-245, GCC88 and GCC185) to the *trans*-Golgi,

and TMF, CASP, Golgin-84 and Giantin on Golgi rims (Goud & Gleeson, 2010). Such precise localization of specific Golgins helps to capture the specific class of vesicles. For example, different ER-born vesicles are usually captured by GM130, p115 and GMAP-210, intra Golgi vesicles by TMF, CASP and Golgin-84, and vesicles from endosomes by Golgin-97, Golgin-245, GCC88 and GCC185 (Gillingham & Munro, 2016).

This last class, which captures the vesicles coming from endosomes, is a family of Golgins that are targeted to the *trans*-Golgi by their C-terminal GRIP domains (Munro & Nichols, 1999; Setty, Shin, Yoshino, Marks, & Burd, 2003). In mammalian cells, four such GRIP domain Golgins have been reported, namely Golgin97, Golgin245, GCC185 and GCC88. GRIP domain sequences have been identified in mammals, flies, plants, yeast (Imh1) and parasites (Munro, 2011). The GRIP domain functions majorly as a TGN targeting signal. TGN Golgins contain a high percentage (75–85%) of α -helical coiled coils. Golgins such as GCC185 and Golgin97 form parallel homodimer. Recent studies utilizing atomic force microscopy suggested that the GCC185 N terminus end forms a splayed end or Y-shaped structure, which has an affinity for vesicles coming from endosomes (Cheung & Pfeffer, 2016).

Pichia pastoris shares structural and molecular similarities in secretory pathways with mammalian systems. Unlike *Saccharomyces cerevisiae*, *Pichia* is well known for its highly efficient extracellular protein secretion, while it displays a stacked Golgi apparatus (Rossanese et al., 1999). Moreover, most of the powerful yeast genetic manipulation tools are well established in *Pichia*. For all the above reasons, we decided to study the functions of Golgins in *P. pastoris*.

In the present study, we identified and characterized the GRIP domain Golgin of *P. pastoris*, *Pplmh1*. We demonstrated that *Pplmh1* contains the conserved GRIP domain. Biophysical studies and electron microscopy results suggest that *Pplmh1* forms a parallel homodimer and a Y-shaped structure.

2 | MATERIALS AND METHODS

All of the plasmids and constructs used in this studies are listed in Table 1. Experiments with *P. pastoris* were carried out using the

TABLE 1 List of plasmids used in study

Sample no.	Construct name
1	GFP-GRIPpIB2
2	GFP-GRIP(Y-A)pIB2
3	SEC7-DsRed.M1x6 pUC19Arg
4	<i>Pplmh1</i> -pET28a
5	<i>Pplmh1</i> -pGAD
6	<i>Pplmh1</i> -pGBDU
7	<i>Pplmh1</i> (725–1124)-pGAD
8	<i>Pplmh1</i> (725–1124)-pGBDU
9	<i>Pplmh1</i> (1–355)-pGAD
10	<i>Pplmh1</i> (1–355)-pGBDU
11	pGAD
12	pGBDU
13	pUG6- <i>PpArl1</i> ::KanMAX

prototrophic wild-type strain PPY12 and its derivatives (Table 2). General methods for the growth and transformation of *P. pastoris* have been described previously (Sears, O'Connor, Rossanese, & Glick, 1998). Yeast cells were grown at 30°C at 200 rpm. *Pichia pastoris* transformation was performed using electroporation method. Gene sequences for GCC185, GCC88, Golgin97, Golgin245, *S. cerevisiae* Imh1, and *P. pastoris* Imh1, *Arl1* were obtained from NCBI database.

2.1 | Construction of GFP-GRIP and GFP-GRIP(Y-A) strain

GRIP domain of *Pplmh1* was tagged with Green Fluorescent Protein (GFP). GRIP domain (1030–1125 residues) of *Pplmh1* was PCR amplified using primers, *Pplmh1*GRIPsmaIFw and *Pplmh1*GRIPXhoIRv (Table 3). The amplified fragment was digested with SmaI and XhoI and ligated into pIB2, which was also digested with the same enzymes. In the resulting plasmid, GFP was cloned between EcoRI and KpnI sites, to get GFP-GRIP-pIB2 construct. This construct was linearized with StuI to integrate at the His4 locus of *P. pastoris*. Using primers, GRIP (Y-A) Up and GRIP (Y-A) Dw, GFP-GRIP-pIB2 plasmid was mutagenized in the position of tyrosine (1083). Resulting plasmids were sequenced to confirm the (Y-A) mutation. This construct was linearized with StuI to integrate at the His4 locus of *P. pastoris*.

2.2 | Construction of SEC7-DsRed.M1 × 6 strain

Golgi marker protein Sec7 was tagged with a hexa-DsRed.M1 cassette by pop-in gene replacement using the same general strategy as described above for GRIP. The plasmid pUC19-ARG4-Sec7-DsRed.M1 × 6 was linearized with XmnI to integrate at the Arg4 locus of *P. pastoris*.

2.3 | Cloning, expression and purification of *Pplmh1*

Full-length *Pplmh1* was amplified using primers *Pplmh1*NdeIFw and *Pplmh1*NotIRv. The amplified fragment was cloned in pET28a between NdeI and NotI sites. The resultant plasmid was then transformed into the Rosetta2DE3 strain for expression. Transformed cells were grown in LB media containing kanamycin (50 µg/mL) and chloramphenicol (34 µg/mL). When the culture OD₆₀₀ reached 0.6, it was induced with 0.4 mM IPTG and grown overnight at 22°C, 180 rpm. The pellet from a 2 L culture was re-suspended in 30 mL of buffer A (10 mM HEPES, 300 mM NaCl, 5% glycerol, 0.1% Triton X-100, pH 8.5) and sonicated six times (60% amplitude, 1 min, 50% pulse) until a clear suspension was obtained. This suspension was centrifuged at 14,000 rpm for 40 min and the supernatant was allowed to bind the Ni-NTA beads (4 mL, pre-equilibrated with buffer A) for 1 h followed by washing with 10-bed volumes of wash buffer (10 mM imidazole + buffer A). The bound protein was eluted (3 mL) using elution buffer (200 mM imidazole + buffer A). Elution fractions from affinity purification were loaded on 8% SDS gel. The affinity eluted fraction was then concentrated to 1 mL using 30 kDa cutoff centricon (Amicon Ultra-15 Centrifugal Filter Units) and injected into a gel filtration column to obtain pure protein fraction.

TABLE 2 List of yeast strains

Sample no.	Strain name	Genotype
1	PPY12	his4 arg4
2	PPY12 GFPGRIPpIB2	his4 arg4 GFP-GRIPpIB2::HIS4
3	PPY12 GFPGRIP(T-A)pIB2	his4 arg4 GFP-GRIP(Y-A)pIB2::HIS4
4	PPY12 GFPGRIPpIB2 PpSEC7-DsRed.M1 × 6	his4 arg4 GFPGRIP::HIS4 SEC7-DsRed.M1 × 6 pUC19Arg::ARG4
5	PPY12 GFPImh1 arl1Δ	his4 arg4 GFP-Pplmh1-pUC19His::HIS4 PpArl1::Kanmax

TABLE 3 List of primers used in study

Sample no.	Name of the primer	Sequence (5'–3')
1	Pplmh1NdelFw	GTGTACATATGatgttctcaaaactttcc
2	Pplmh1NotIRv	GttttGCGGCCGCttttaatgagctggc
3	Pplmh1GRIPXmalFw	gtccgCCCCGGGCGctgaagttcgagagactg
4	Pplmh1GRIPXholRv	gcattCTCGAGttttaatgagctggctaa
5	GRIP(Y-A)Up	aaaatgagagataaaagtgtccGCAattaagaacgtccttctaggattt
6	GRIP(Y-A)Dw	aaatcctaagaaggactgttctaatTGCggcaactttatctctctatttc
7	Pplmh1NtermBamHIFw	GCGGATCCGGCAGCTatgttctcaaaactttcc
8	Pplmh1 NtermSal1Rv	cctatGTCGACTatctgtgacttttctcc
9	Pplmh1CtermBamHI	GCGGATCCGGCAGCTattgccgaagaaaagcc
10	Pplmh1CtermSal1Rv	gctgtGTCGACTttaatgagctggctaa
11	Pplmh1XmalFw	GTGTACCCGGGatgttctcaaaactttcc
12	Pplmh1Sal1Rv	gtgctGTCGACTttaatgagctggctaa

2.4 | Circular dichroism spectroscopy

The secondary structure of purified Pplmh1 protein was characterized using a Jasco J-810 (Japan), circular dichroism (CD) polarimeter. A far-UV CD scan of protein (30 μM Pplmh1 in 2.5 mM HEPES pH 8.5, 50 mM NaCl buffer) was collected in the 200–240 nm wavelength range at 20°C.

2.5 | Dynamic light scattering

Dynamic light scattering (DLS) was performed using 70 μL of FPLC-purified fraction. The hydrodynamic radius of Pplmh1 protein was calculated using DynaProNanoStar, Wyatt Technology. Before the DLS experiment, all of the samples were filtered using a 0.45 μm filter.

2.6 | Fluorescence microscopy

Live-cell confocal imaging was performed for PPY12GFP-GRIP-pIB2, PPY12GFP-GRIP(Y-A)-pIB2 and PPY12GFP-GRIP-pIB2, SEC7-DsRed.M1 × 6 strains. Cells were attached to the glass cover dish surface, washed and covered with minimal SD medium. Image capture was performed using a Leica SP8 confocal microscope. GFP fluorescence was visualized using 488 nm excitation and 495–550 nm bandpass emission and DsRed fluorescence was visualized using 561 nm excitation and 580–750 nm bandpass emission. The pixel size was 65 nm, the pinhole size was 1.2 Airy units, and the interval between optical sections was 0.3 μm. Twenty optical sections were captured every 1.2 s to span the entire cell thickness. The red and green fluorescence images were processed by hybrid median filtering followed by average projection and then merged with blue images of the cells.

2.7 | Yeast two-hybrid interaction assays

Protein–protein interactions were tested using the yeast two-hybrid system (James, 2001). Interactions were tested between the proteins fused to the Gal4 DNA-binding domain and the Gal4 activation domain. Pplmh1 (full length), Pplmh1 (1–300), Pplmh1 (400–765) and Pplmh1 (725–1124) were PCR amplified from *P. pastoris* genomic DNA, with XmaI and SalI as the restriction sites. The digested amplified fragments were inserted into pGBDU ('bait') and pGAD ('prey') vectors digested with the same restriction enzymes. Plasmids were transformed into *S. cerevisiae* strain PJ694A using the lithium acetate method (Gietz & Woods, 2002). Transformants were selected on SD Leu–Ura plates. Interactions were tested by plating the transformants on SD–Leu–Ura–His plates.

2.8 | Negative staining to visualize purified Pplmh1

Purified native Pplmh1 was diluted to 10 μM using distilled water, adsorbed to a 400-mesh Formvar-coated copper grid (Nisshin EM Co. Ltd, Tokyo, Japan) and placed in 1% uranyl acetate solution for 10 s. After drying, the samples were observed using a transmission electron microscope (JEM- 1400Plus; Jeol Ltd, Tokyo, Japan) at an acceleration voltage of 120 kV (Bhattacharya, Kumar, & Panda, 2017; Ishida et al., 2015).

2.9 | Deletion of Arl1 in *P. pastoris* cells

Sequences of 1 kb flanking the Arl1 coding sequence were amplified from genomic DNA using the upstream or downstream primers. The amplified fragments were digested with NdeI and SalI (for the upstream fragment) and EcoRV and NotI (for the downstream

fragment). The upstream fragment was ligated with the pUC19kanmax vector that had been digested with NdeI and SalI. The resulting plasmid was cut with EcoRV and NotI to ligate the downstream fragment that results in pUC19-Arl1::Kanmax. Finally, a 3.2 kb NdeI–NotI fragment was excised from this plasmid and transformed into PPY12 cells. G418-positive transformants were screened by PCR to confirm that Arl1 had been deleted.

3 | RESULTS

3.1 | Sequence alignment and characterization of GRIP domain of Pplmh1

The GRIP domain, whether expressed in mammalian cells or in budding yeast *S. cerevisiae*, always localizes to the Golgi. Also, overexpression of GRIP domain saturates the binding sites of endogenous GRIP domain proteins on the Golgi. These data suggest that the GRIP domain helps the Golgin to localize to Golgi. *S. cerevisiae* encodes a single GRIP domain-containing protein, Imh1 which localizes to the Golgi (Munro & Nichols, 1999; Setty et al., 2003). With sequence alignment studies of *P. pastoris* using PSI-BLAST, we identified the single GRIP domain-containing protein in *P. pastoris*, Pplmh1. We compared the sequence of the C-terminal domain of different GRIP domain-containing proteins (Human GCC185, Human GCC88, Human Golgin97, Human Golgin245, *S. cerevisiae* Imh1 and *P. pastoris* Imh1) using PSI-BLAST (Figure 1a).

To examine whether or not the Pplmh1 GRIP domain is capable of localizing to the Golgi, we tagged the GRIP domain with mGFP and expressed it in *P. pastoris* cells. We found that Pplmh1 forms a punctate pattern which mostly corresponds to the Golgi (Figure 1b). When co-expressed along-with Sec7-DsRed, a *trans*-Golgi marker protein, mGFP tagged Pplmh1 GRIP domain co-localized with Sec7-DsRed (Figure 1c). These results display agreement with previous studies that showed that GRIP domain-containing protein localizes to the *trans*-Golgi/TGN. The conserved tyrosine residue of GRIP domain is essential for Golgi targeting (Panic, Perisic, Veprintsev, Williams, & Munro, 2003). Our studies conform that mutation of this conserved tyrosine aborts the Golgi targeting of Pplmh1 (Figure S1 in the Supporting Information). It has been reported that Arl1 binds to the GRIP domain Golgins and recruits them to the TGN (Lu & Hong, 2003). In order to check its role in recruitment of Pplmh1 to the Golgi, we deleted Arl1 from a *P. pastoris* strain expressing GFP-Pplmh1. We observed that GFP-Pplmh1 fails to localize to the Golgi and remains cytosolic in this strain which lacks Arl1 (Figure S3).

3.2 | Expression, purification and analysis of purified His6-tagged Pplmh1

To understand the structural properties of Pplmh1, we overexpressed His-tagged Pplmh1 in Rosetta2DE3 cells and purified it using nickel affinity chromatography (Figure 2a) and gel filtration (Figure 2b). We confirmed the purified protein using mass spectrometry analysis (Table 4) and western blot against His-tagged Pplmh1 (Figure 2c).

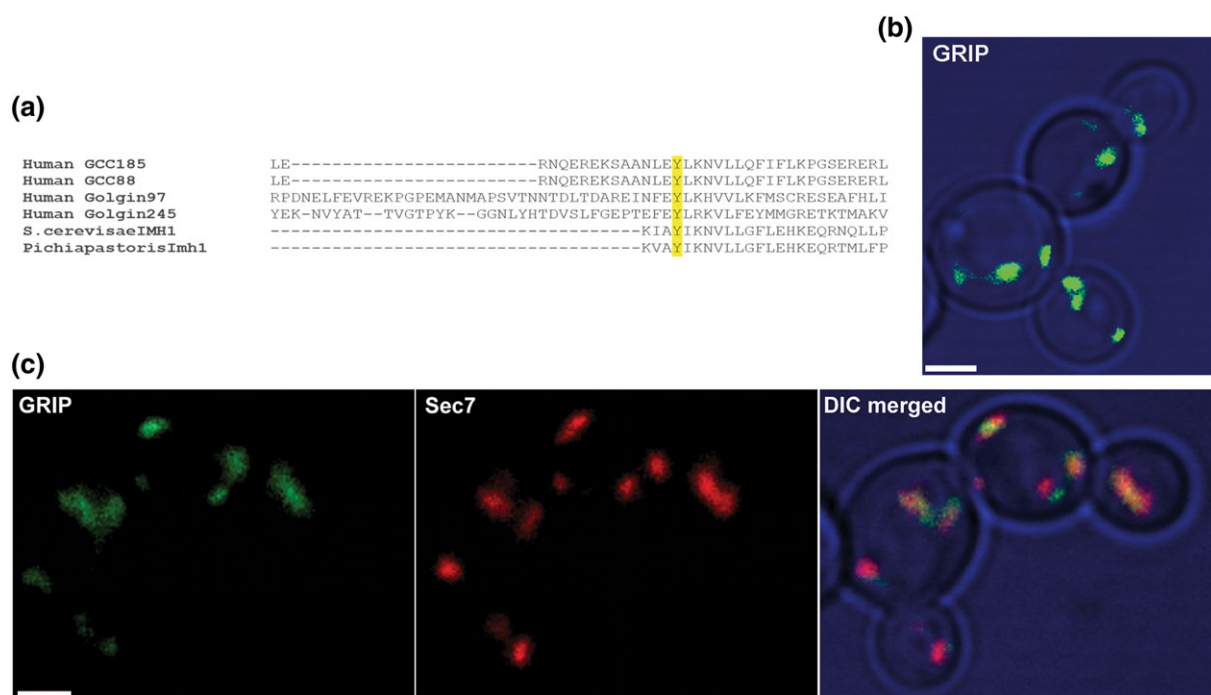


FIGURE 1 GRIP domain of Pplmh1 is important for Golgi targeting. (a) Alignment of the carboxy-terminal portions of the indicated proteins. C-terminal domain of Golgins was aligned using PSI-BLAST Tool (Human GCC185, Human GCC88, Human Golgin 97, Human Golgin 245, *Saccharomyces cerevisiae* Imh1, *Pichia pastoris* Imh1). The tyrosine conserved residues that are identical (yellow) sequences are shaded. (b) Fluorescence confocal image of live *P. pastoris* cells expressing GFP fused to the GRIP domain of the Pplmh1 protein. The fusions contained the carboxy-terminal (1030–1125) residues of Pplmh1. Scale bar 1 μ m. (c) Green fluorescent protein (GFP)–Pplmh1p–GRIP fusion (encoding amino acids 1030–1125) was expressed in wild-type strains PPY12 expressing Sec7-6XDsRed which localize to Golgi compartments. Colocalization can be observed as yellow in the panels. Scale bar 1 μ m [Colour figure can be viewed at wileyonlinelibrary.com]

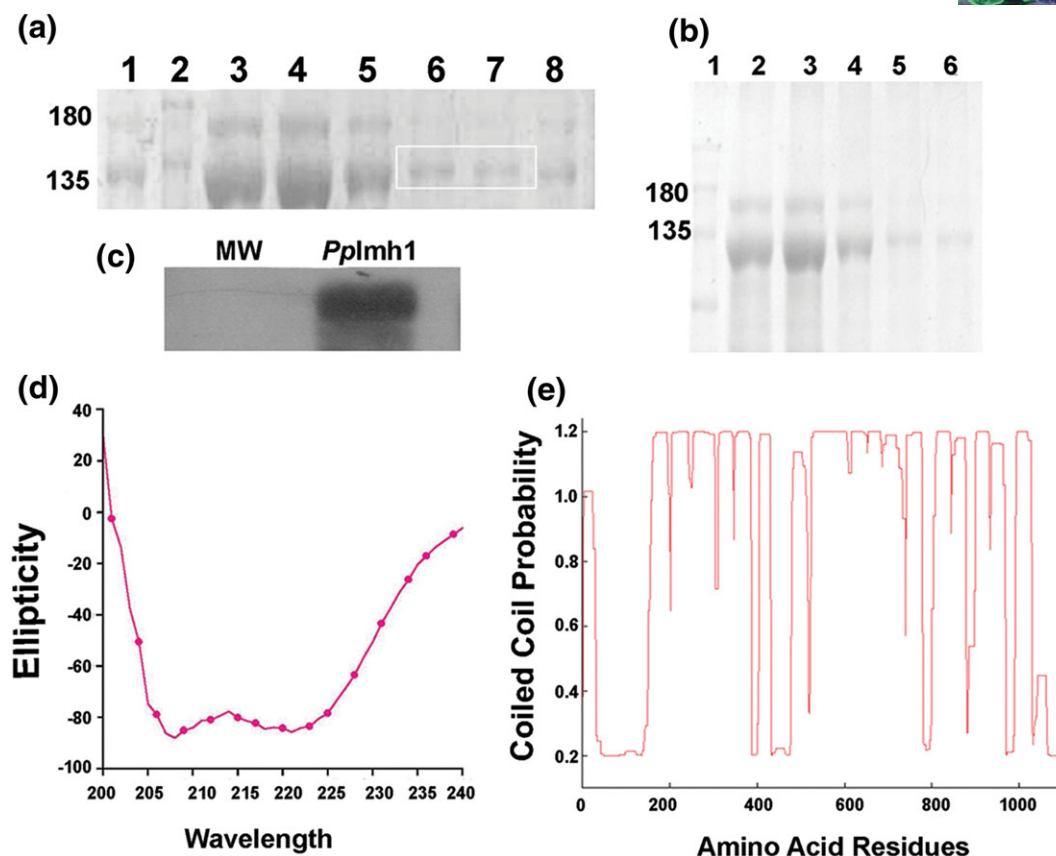


FIGURE 2 Biophysical characterization of *Pplmh1*. (a) Purified His6-tagged Imh1 analysed by SDS/PAGE (8%) and stained with Coomassie Blue. Fractions obtained after affinity purification were loaded. Gel A: 1, beads after washing; 2, protein marker; 3–7, affinity elution fraction. Marked protein band at 130 kDa was excised from the gel and processed for in-gel digestion and mass spectrometry (Q-TOF 5600 Triple TOF AbSciex). The raw data was processed using Protein Pilot 4.5 and was aligned to FASTA of *P.pastoris* (taxon ID- 4922, as on 21 June 2017) from UniProt (Table 1). All of the molecular weights (MW) are shown in kilodaltons. (b) The elution fraction was concentrated to 1 mL and resolved for further purity using a Sephadex 200 FPLC column. Gel: 1, concentrated affinity fraction; 2, protein marker; 3–6, FPLC elution. (c) Immunoblot using Anti-His antibody against His-tagged *Pplmh1*. (d) CD spectrum of purified His6-tagged *Pplmh1* (30 μM). Ellipticity is plotted as a function of wavelength (nm) for *Pplmh1* (30 μM). The data are superimposed with the nonlinear best fit using the K2D2 program, yielding 85% α -helix, 1.24% β -strand. (e) Predicted probability of each amino acid in the sequences of the *Pplmh1* to form coiled-coil using structure secondary structure prediction tool Coils [Colour figure can be viewed at wileyonlinelibrary.com]

TABLE 4 Mass spectrometry analysis

N	Unused	Total	Coverage (%)	Accession No.	Name	Species	Peptides (95%)
1	290.64	290.64	91.8	trIF2QN57I F2QN57_KOMPC	Vesicular transport protein OS = <i>Komagataella phaffii</i> (strain ATCC 76273/CBS 7435/CECT11047/NRRL Y-11430/Wegner 21-1), GN = IMH1, PE = 4, SV = 1	KOMPC	526

Protein Group 1 Vesicular transport protein OS = *Komagataella phaffii* (strain ATCC 76273/CBS 7435 /CECT11047/NRRL Y-11430/Wegner 21-1), GN = IMH1, PE = 4, SV = 1. Protein sequence coverage - vesicular transport protein OS = *Komagataella phaffii* (strain ATCC 76273/CBS 7435 /CECT11047/NRRL Y-11430/Wegner 21-1), GN = IMH1, PE = 4, SV = 1.

We also performed CD spectroscopy of purified recombinant His-tagged *Pplmh1* to determine the nature of the secondary structure. The data plotted as ellipticity vs. wavelength is shown in Figure 2(d). The CD spectrum of Golgin *Pplmh1* shows double minima at ~210 and 220 nm, which is a characteristic of the α -helical structure. This result was confirmed by non-linear least-squares analysis using the program K2D2, which yielded a best fit to 85% α -helical structure.

To further understand the nature of the α -helical structure, coil analysis (Lupas, Van Dyke, & Stock, 1991) showed the probability of coiled-coil formation (Figure 2e). This prediction asserts that *Pplmh1* has a domain that comprises a coiled-coil structure.

3.3 | Yeast two-hybrid and DLS analysis indicate that *Pplmh1* forms parallel homodimer

To determine whether *Pplmh1* forms an oligomer or not, we performed yeast two-hybrid assay in which full-length *Pplmh1* was cloned into bait and prey vectors. The two-hybrid assay strain PJ694A was transformed with bait and prey constructs, and grown on selective medium as described in the 'Materials and methods' section. Interactions between *Pplmh1* proteins were monitored by the ability of the transformed yeast cells to grow in a medium lacking histidine. A strong interaction was observed between the full-length

Pplmh1 constructs, *Pplmh1*-pGAD and *Pplmh1*-pGBDU, confirming that *Pplmh1* forms an oligomer (Figure 3a).

To investigate the oligomeric nature further, we analysed the behaviour of *Pplmh1* using DLS. The correlation graph and fast decay time suggest that the mean radius of the particles is within the expected range for proteins, which is usually between 1 and 100 μ s. It showed the estimated molecular weight of the *Pplmh1* dimer to be ~260 kDa, which is precisely double the molecular weight of its monomeric form, i.e. 130 kDa (Figure 3c). We observed that polydispersity is high, which can be attributed to the multiple oligomeric states present in the protein sample. Such a native dimeric state was also confirmed through native gel followed by western blot using antibody against the His-tagged *Pplmh1*, where it showed a band around 260 kDa (Figure S2).

According to the results obtained through the above experiments, it can be concluded that *Pplmh1* probably forms a homodimer. However, a dimer may be orientated in a parallel (head-to-head) or anti-parallel (head-to-tail) fashion. To distinguish between these possibilities, we utilized the yeast two-hybrid assay to analyse interactions between various N- and C-terminal truncated constructs. Strong self-interaction was observed between the coiled-coil regions and C-terminal [GAD-*Pplmh1* (725–1124) with GBDU-*Pplmh1* (725–1124) and GAD-*Pplmh1* (400–765) and GBDU-*Pplmh1* (400–765) (Figure 3b)].

However, no self-interaction was detected between N-terminal (1–300) regions. Neither was any interaction detected between C-terminal (725–1124) and N-terminal regions (1–300). This result indicates that *Pplmh1* probably dimerizes through the self-interactive central coiled-coil regions and C-terminal regions. However, the N-terminal domain does not mediate such dimerization either through self-interaction or through interaction with the C-terminal region. All of these results together suggest that *Pplmh1* forms parallel homodimers.

3.4 | Electron Microscopy (EM) data suggests that *Pplmh1* forms parallel homodimer with splayed N terminus

To further elucidate the nature of the dimer, we visualized purified *Pplmh1* under transmission electron microscope. We observed that the *Pplmh1* particles exhibit two profiles: either a Y-shaped or a clustered form (Figure 4a). The majority of individual *Pplmh1* particles seemed to form a Y-shaped structure which appeared at a significant frequency of 24% (Table 5). The clustered or network-like profiles may represent assemblies of the Y-shaped forms of *Pplmh1* or other differently folded forms of *Pplmh1*. Some particles had no head or a short head, which may be because of proteolysis or restricted conformation. The most biologically accepted form as per the function of Golgins would be a Y-shaped conformation as it favours the capture

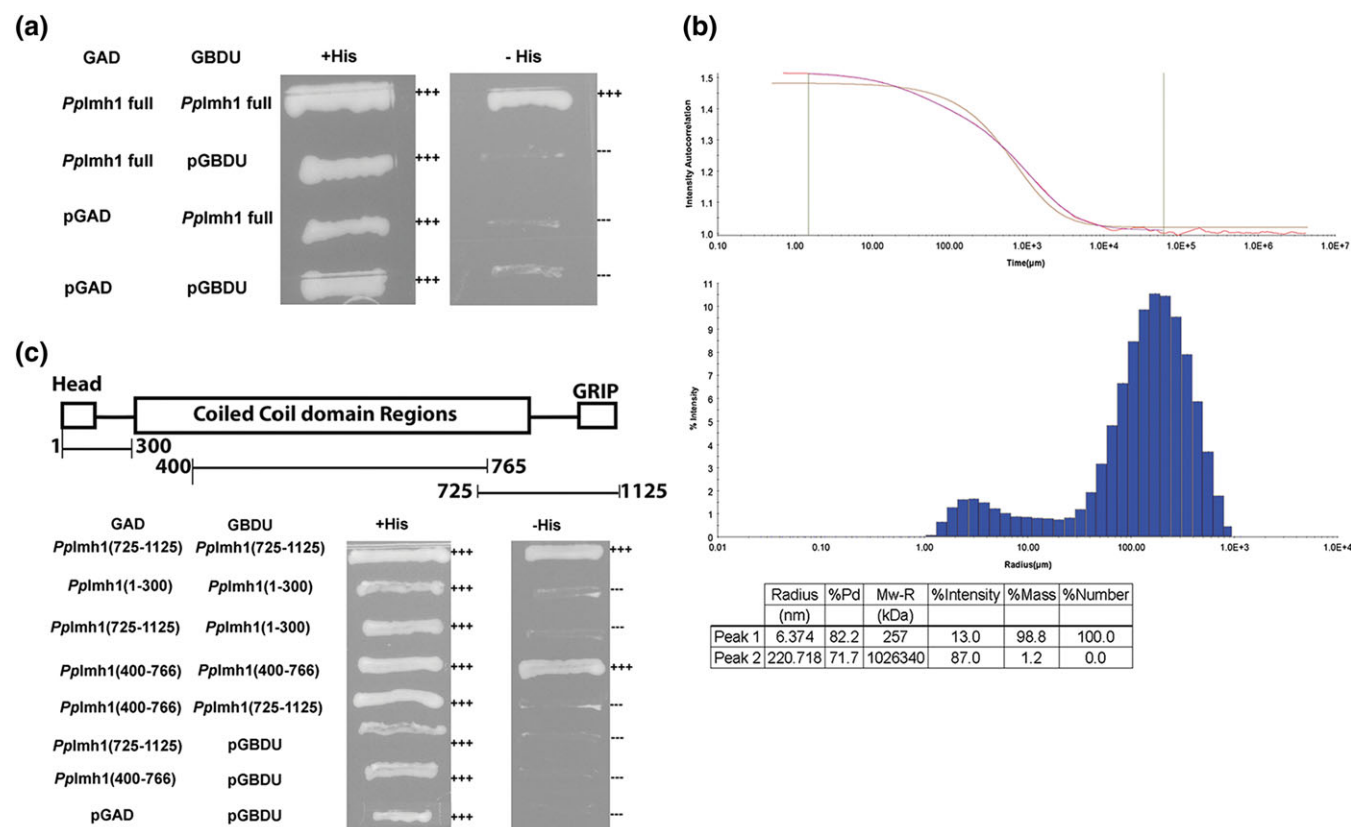


FIGURE 3 *Pplmh1* forms parallel dimer. (a) To test whether *Pplmh1* forms dimers or monomers we used yeast two-hybrid analysis. The 'prey' vector encoded the full length of *Pplmh1*, and the 'bait' vector encoded the full-length *Pplmh1* protein. Both vectors were transformed into *S. cerevisiae* tester strain. Growth on plates lacking histidine reflects an interaction. (b) DLS Data 1. Correlation function plot, 2. Intensity (%) vs. radius (nm). Plot showing multimodal polydisperse population with ~99% mass contributed by molecules estimated to have molecular weight ~260 kDa. (c) To test whether *Pplmh1* form parallel or antiparallel dimers, we cloned *Pplmh1* (1–300), *Pplmh1* (400–765) and *Pplmh1* (725–1125) fragments in bait and prey vector. Both the constructs were transformed into *S. cerevisiae* tester strain. Growth on plates lacking histidine reflects an interaction [Colour figure can be viewed at wileyonlinelibrary.com]

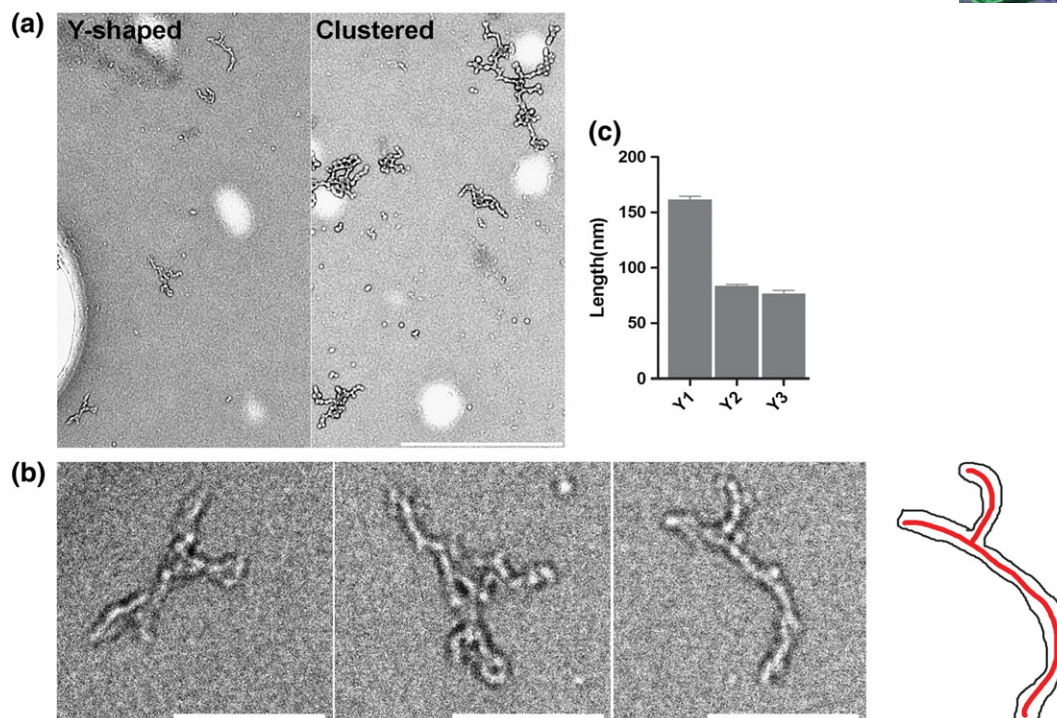


FIGURE 4 Negative-stain Electron Microscopy (EM) of purified *Pplmh1*. (a) Purified *Pplmh1* and control buffer sample were absorbed on the grid and stained with 1% uranyl acetate and observed using TEM (Jeol 1400 plus 120 kV, USA) transmission electron microscopy at magnification 5000 \times . Representative images are shown. Y-shaped profile is marked. Scale bar 500 nm. (b) Magnified representative images of Y-shaped profiles of *Pplmh1* and outline of predicted *Pplmh1* structure. Scale bar 100 nm. (c) Measurement of length of each branch of Y-shaped conformation of *Pplmh1* using iTEM analysis software. The branch lengths were classified as Y1 (rod) and branches Y2 and Y3. The values are statically significant ($p < 0.0001$, paired t -test) [Colour figure can be viewed at wileyonlinelibrary.com]

TABLE 5 Quantification of *Pplmh1* profiles by electron microscopy

Profile	Number	Ratio (%)
Y-shaped	48	24
Cluster	154	76
Total	200	100

of the vesicle by the *N*-terminal splayed end. Yeast two-hybrid results indicate that the *N*-terminal region of *Pplmh1* is monomeric and that the C-terminal region is dimeric (Figure 3c). It is most probable that the Y-shaped profile represents a parallel dimer with two branched monomeric *N*-terminal regions and a single dimeric C-terminal region. In the Y-shaped structure, the stalk represents the self-interacting coiled-coil domain. The splayed end represents *N*-terminal domain which does not appear to self-interact or form a dimer. The length of each branch of the Y-shaped profile was measured. The branch lengths were categorized as lower rods (Y1) and upper arms (Y2 and Y3) (Figure 4b). The average lengths were 76, 86 and 161 nm for Y3, Y2 and Y1 respectively. Therefore, we observed that the difference in the length between C-terminal rod structures and *N*-terminal arm structures, such as between Y1 and Y2, or Y1 and Y3, was significant, suggesting that one branch is significantly longer than the other two branches. However, no significant length differences were found between the *N*-terminal arm structures, such as Y2 and Y3 themselves. The minor difference in length that was observed could be due to the uneven spreading of two branches of *Pplmh1* on EM Grid. It is also possible that different parts of the *Pplmh1* molecules were adsorbed on the membrane with different angles.

Therefore, it might be possible that the lengths of two branches appeared different (Ishida et al., 2015; Figure 4c). It is to be noted that the combined size of self-interacting central and C-terminal domains of *Pplmh1* is almost double that of its non-interacting *N*-terminal domains. This quantification strengthens the fact that the Y-shaped structure represents a dimer of *Pplmh1*. Lack of splayed structure on both sides of the dimer further emphasizes the fact that *Pplmh1* indeed forms parallel dimers, but not the anti-parallel dimers.

4 | DISCUSSION

We have identified the sole GRIP domain Golgin of *P. pastoris*. Arl1 binds to the GRIP domain and recruits Golgins to TGN. A conserved tyrosine residue of GRIP domain is essential for Arl1 interaction and subsequent Golgi targeting (Lu & Hong, 2003; Munro & Nichols, 1999). In case of mammalian cells, mutation of this tyrosine residue to alanine affects the localization of Golgin 97 and Golgin 245 (Kjer-Nielsen et al., 1999). *Pplmh1* fails to localize to the Golgi when this corresponding tyrosine of its GRIP domain is mutated to alanine. This result indicates that sequence-specific interaction of GRIP domain is essential for Golgi targeting of GRIP domain protein.

Apart from GRIP domain, TGN Golgins have a long coiled-coil domain and an *N*-terminal head domain. TGN Golgins capture the vesicles of recycling endosomes through the *N*-terminal head domain (Wong et al., 2017). Their long coiled-coil domain possibly functions as a spacer to extend the vesicle capture domain (Cheung & Pfeffer,

2016). We have demonstrated that Pplmh1 also contains a higher-grade α -helical coiled coil domain which possibly performs a similar function.

Mammalian TGN Golgins such as GCC185 and Golgin97 have been shown to form a parallel homodimer. Moreover, GCC185 has also been shown to form a Y-shaped dimeric structure with its N terminus forming a splayed end that has an affinity to bind vesicles (Cheung & Pfeffer, 2016). No such study has been reported yet on the abilities of yeast Golgins to form such structures. Our yeast two-hybrid analysis suggests that Pplmh1 possibly forms a parallel homodimer. In addition, EM data confirms that Pplmh1 displays such Y-shaped structures. Golgin97, the mammalian homologue of Pplmh1, captures the vesicles which shuttle between endosomes and TGN. However, whether Pplmh1 exhibits the same function requires further investigation.

COMPETING FINANCIAL INTERESTS

The authors have no conflict of interest.

ACKNOWLEDGEMENTS

This work was supported by funding from DBT (Government of India; DBT grant 102/IFD/SAN/2282/2012-2013 to D.B.) and an ACTREC doctoral fellowship through HBNI to B.K.J. We thank Bhattacharyya laboratory members for carefully reviewing the manuscript.

ORCID

Dibyendu Bhattacharyya  <http://orcid.org/0000-0003-3252-7440>

REFERENCES

- Bhattacharyya, D., Kumar, A., & Panda, D. (2017). WhmD promotes the assembly of *Mycobacterium smegmatis* FtsZ: A possible role of WhmD in bacterial cell division. *International Journal of Biological Macromolecules*, 95, 582–591. <https://doi.org/10.1016/j.ijbiomac.2016.11.056>
- Brandizzi, F., & Barlowe, C. (2013). Organization of the ER-Golgi interface for membrane traffic control. *Nature Reviews. Molecular Cell Biology*, 14(6), 382–392. <https://doi.org/10.1038/nrm3588>
- Cheung, P. Y., & Pfeffer, S. R. (2016). Transport vesicle tethering at the trans Golgi network: Coiled coil proteins in action. *Frontiers in Cell and Developmental Biology*, 4, 18. <https://doi.org/10.3389/fcell.2016.00018>
- Gietz, R. D., & Woods, R. A. (2002). Transformation of yeast by lithium acetate/single-stranded carrier DNA/polyethylene glycol method. *Methods in Enzymology*, 350, 87–96.
- Gillingham, A. K., & Munro, S. (2016). Finding the Golgi: Golgin coiled-coil proteins show the way. *Trends in Cell Biology*, 26(6), 399–408. <https://doi.org/10.1016/j.tcb.2016.02.005>
- Goud, B., & Gleeson, P. A. (2010). TGN golgins, Rabs and cytoskeleton: Regulating the Golgi trafficking highways. *Trends in Cell Biology*, 20(6), 329–336. <https://doi.org/10.1016/j.tcb.2010.02.006>
- Ishida, R., Yamamoto, A., Nakayama, K., Sohda, M., Misumi, Y., Yasunaga, T., & Nakamura, N. (2015). GM130 is a parallel tetramer with a flexible rod-like structure and N-terminally open (Y-shaped) and closed (I-shaped) conformations. *The FEBS Journal*, 282(11), 2232–2244. <https://doi.org/10.1111/febs.13271>

- James, P. (2001). Yeast two-hybrid vectors and strains. *Methods in Molecular Biology*, 177, 41–84. <https://doi.org/10.1385/1-59259-210-4:041>
- Kjer-Nielsen, L., Teasdale, R. D., van Vliet, C., & Gleeson, P. A. (1999). A novel Golgi-localisation domain shared by a class of coiled-coil peripheral membrane proteins. *Current Biology*, 9, 385–388.
- Lowe, M. (2011). Structural organization of the Golgi apparatus. *Current Opinion in Cell Biology*, 23(1), 85–93. <https://doi.org/10.1016/j.ceb.2010.10.004>
- Lu, L., & Hong, W. (2003). Interaction of Arl1-GTP with GRIP domains recruits autoantigens Golgin-97 and Golgin-245/p230 onto the Golgi. *Molecular Biology of the Cell*, 14(9), 3767–3781. <https://doi.org/10.1091/mbc.E03-01-0864>
- Lupas, A., Van Dyke, M., & Stock, J. (1991). Predicting coiled coils from protein sequences. *Science*, 252(5009), 1162–1164. <https://doi.org/10.1126/science.252.5009.1162>
- Munro, S. (2011). The golgin coiled-coil proteins of the Golgi apparatus. *Cold Spring Harbor Perspectives in Biology*, 3(6). <https://doi.org/10.1101/cshperspect.a005256>
- Munro, S., & Nichols, B. J. (1999). The GRIP domain – A novel Golgi-targeting domain found in several coiled-coil proteins. *Current Biology*, 9(7), 377–380.
- Panic, B., Perisic, O., Veprintsev, D. B., Williams, R. L., & Munro, S. (2003). Structural basis for Arl1-dependent targeting of homodimeric GRIP domains to the Golgi apparatus. *Molecular Cell*, 12(4), 863–874.
- Papanikou, E., & Glick, B. S. (2014). Golgi compartmentation and identity. *Current Opinion in Cell Biology*, 29, 74–81. <https://doi.org/10.1016/j.ceb.2014.04.010>
- Rossanese, O. W., Soderholm, J., Bevis, B. J., Sears, I. B., O'Connor, J., Williamson, E. K., & Glick, B. S. (1999). Golgi structure correlates with transitional endoplasmic reticulum organization in *Pichia pastoris* and *Saccharomyces cerevisiae*. *The Journal of Cell Biology*, 145(1), 69–81.
- Sears, I. B., O'Connor, J., Rossanese, O. W., & Glick, B. S. (1998). A versatile set of vectors for constitutive and regulated gene expression in *Pichia pastoris*. *Yeast*, 14(8), 783–790. [https://doi.org/10.1002/\(SICI\)1097-0061\(19980615\)14:8%3C783::AID-YEA272%3E3.0.CO;2-Y](https://doi.org/10.1002/(SICI)1097-0061(19980615)14:8%3C783::AID-YEA272%3E3.0.CO;2-Y)
- Setty, S. R., Shin, M. E., Yoshino, A., Marks, M. S., & Burd, C. G. (2003). Golgi recruitment of GRIP domain proteins by Arf-like GTPase 1 is regulated by Arf-like GTPase 3. *Current Biology*, 13(5), 401–404.
- Wong, M., Gillingham, A. K., & Munro, S. (2017). The golgin coiled-coil proteins capture different types of transport carriers via distinct N-terminal motifs. *BMC Biology*, 15, 3.
- Yu, I.-M., & Hughson, F. M. (2010). Tethering factors as organizers of intracellular vesicular traffic. *Annual Review of Cell and Developmental Biology*, 26(1), 137–156. <https://doi.org/10.1146/annurev.cellbio.042308.113327>

SUPPORTING INFORMATION

Additional supporting information may be found online in the Supporting Information section at the end of the article.

How to cite this article: Jain BK, Thapa PS, Varma A, Bhattacharyya D. Identification and characterization of GRIP domain Golgin Pplmh1 from *Pichia pastoris*. *Yeast*. 2018;1–8. <https://doi.org/10.1002/yea.3317>